REAL OPTIONS VALUATION IN ENERGY MARKETS

A Thesis
Presented to
The Academic Faculty

by

Jieyun Zhou

In Partial Fulfillment
of the Requirements for the Degree
Doctor of Philosophy in the
H. Milton Stewart School of Industrial and Systems Engineering

Georgia Institute of Technology
May 2010

REAL OPTIONS VALUATION IN ENERGY MARKETS

Approved by:

Professor Shi-Jie Deng, Advisor
H. Milton Stewart School of Industrial and Systems Engineering
Georgia Institute of Technology

Professor Minqiang Li
College of Management
Georgia Institute of Technology

Professor Jiangang (Jim) Dai
H. Milton Stewart School of Industrial and Systems Engineering
Georgia Institute of Technology

Professor Steve Hackman
H. Milton Stewart School of Industrial and Systems Engineering
Georgia Institute of Technology

Professor David M. Goldsman
H. Milton Stewart School of Industrial and Systems Engineering
Georgia Institute of Technology

Date Approved: April 1st, 2010

ACKNOWLEDGEMENTS

I am so grateful to all the people who have cared about me and helped me through my process of growth in all these years.

First, I would like to express my gratitude to my advisor Professor Shi-jie Deng. He gave me the valuable opportunity to study at Georgia Tech and introduced me to such an interesting research field. His guidance and support are essential to both my academic and my career growth. Special thanks goes to Professor Minqiang Li, who has given me invaluable guidance and help through two research projects. I also would like to thank Professor Jim Dai for his guidance in a research project and rigorous suggestions to my thesis. I also thank Professor Steve Hackman and David M. Goldsman for serving as my thesis committee members.

I am grateful to Professor Jiazhong Yang in Peking University, for his encouragement, generous help, and faith in me.

I also thank Aram at Constellation Energy, Sandeep and Warren at UBS AG for giving me the precious intern opportunities. I learned a lot and enjoyed the experience working with these great colleagues. I'm also thankful to Alexander Eydeland at Morgan Stanley, Zimin Lu at BP, Michael Ludkovski at UCSB, Cyriel de Jong and Alexander Boogert for their insightful comments and help in my research process.

In addition, I want to thank my friends Jie Chen, Yi He, Lulu Kang, Guanghui Lan, Yaxian Li, Yun Li, Xuyuan Liu, Adaora Okwo, Haibin Sun, Zhaohui Tong, Zhengang Xia, Li Xu and Na Zhu. Their companionship has brought so much fun and precious memory.

Finally, I would like to thank my dear husband, my parents, my sister, and my parents in-law for their unconditional love, encouragement, and support.

TABLE OF CONTENTS

LIST OF TABLES

LIST OF FIGURES

SUMMARY

Real options have been widely applied to analyze investment planning and asset valuation under uncertainty in many industries, especially energy markets. Because of their close analogy to financial options, real options can be valued using the classical financial option pricing theories and their extensions. However, as real options valuation often involves complex payoff structures and operational constraints of the underlying real assets or projects, accurate and flexible methods for solving the valuation problem are essential. This thesis investigates three different approaches to real options valuation and contributes to aspects of modeling realism and computational efficiency. The contributions are illustrated through two important applications of real options in energy markets: natural gas storage and power plant valuation.

Because spread options are commonly used in basic real options valuation techniques, the first part of the thesis addresses the problems of spread option pricing and hedging. We develop a new closed-form approximation method for pricing two-asset spread options. Numerical analysis shows that our method is more accurate than existing analytical approximations. Our method is also extremely fast, with computing time more than two orders of magnitude shorter than one-dimensional numerical integration. Closed-form approximations for the Greeks of spread options are also developed. In addition, we analyze the price sensitivities of spread options and provide lower and upper bounds for digital spread options.

We then further generalize the above results to multi-asset spread options on an arbitrary number of assets. We provide two new closed-form approximation methods for pricing spread options on a basket of risky assets: the extended Kirk approximation and the second-order boundary approximation. Numerical analysis shows that both methods are extremely

fast and accurate, with the latter method being more accurate than the former. Closed-form approximations for important Greeks are also derived. Because our approximation methods enable the accurate pricing of a bulk volume of spread options on two or more assets in real time, it offers traders a potential edge in a dynamic market environment.

In the third part of this thesis, we propose a market-based valuation framework for valuing natural gas storage facility with realistic operational characteristics. The operational process is modeled as a multi-stage stochastic optimization problem. We develop a Gaussian quadrature scheme to solve for the dynamically optimal spot trading strategy and show that the computational efficiency of this method exceeds existing approaches in about two orders of magnitude. Furthermore, with this flexible quadrature scheme, we propose to value a gas storage based on a novel hybrid trading strategy that successfully incorporates both spot and forward trading, thus improving the storage valuation significantly by accounting for both the inter-month and intra-month operational flexibilities and price volatility.

In the fourth part of this work, we develop a continuous-time formulation for power plant valuation in infinite time horizon. We propose a real-option-based model for a power plant to account for the embedded operational flexibility. This model incorporates start-up and shut-down costs as two major operational constraints. Under this continuous valuation model, spark spread is modeled directly as a continuous stochastic process to take account of the long term co-integration relationship between electricity and fuel prices. Instead of discretizing the stochastic process, we preserve continuity of the stochastic spark spread process and work directly with the value function. Closed-form of value function under threshold policy is obtained. The corresponding optimal operational strategy can then be solved. The advantage of this approach is that it reduces computational complexity while incorporates major operation characteristics. It enables fast computation of a power plant value that approximates the real market value and sensitivity analysis of the asset value with respect to the cost parameters of a power plant and the distribution parameters of

spark spread.

CHAPTER I

OVERVIEW

1.1 Real options

A real option is a right, but not an obligation, to take actions regarding a real asset or investment project. Real options are closely analogous to financial options. A real option valuation framework borrows the ideas from classical financial option pricing theories and views the real asset or investment project as an option on the underlying cash flows. This option value and the optimal exercise decisions are derived by methods developed from financial options pricing problems. Usually, more effort is needed to solve a real options valuation problem than a financial option, as real-options-based modeling must incorporate physical characteristics of the underlying real asset or project and be subject to various operational constraints.

Unlike traditional discounted cash flow analysis, which measures a project value by net present value, real options valuation takes into account the embedded options value, such as the operational flexibility of a power plant. Thus, real options valuation gives more accurate valuation results.

Real options valuation has been widely applied to analyze investment planning or asset valuation under uncertainty in many industries. The classical book by Dixit and Pindyck (1994) provides the first detailed introduction of real options approach to investigating investment decisions problems of firms. Schwartz and Trigeorgis (2004) introduce more recent contributions and applications of real options. With deregulation of the energy markets, interest in real options-based valuation for energy assets has grown. Natural gas storage and power plant valuation are two important application areas of real options. At each operation time, the operator of a natural gas storage facility operator has the options

to choose between different operation decisions: store, inject, or withdraw. Similarly, the owner of a power plant has the right, but not the obligation, to operate the plant in response to market changes of the spread between electricity price and fuel cost. We will see more details about these two applications in Chapter 4 and Chapter 5, respectively. Other applications of real options in energy markets include biomass energy in Obersteiner et al. (2002), emissions allowances in Insley (2003), and oil fields development decision in Dias (2004), among others.

1.2 Valuation methods

1.2.1 Contingent claims analysis

Contingent claims analysis is one major approach to real options valuation. It assumes that the cash flows of the real options object being priced can be replicated by a portfolio of tradable assets. By no-arbitrage condition, the portfolio value should equal the real options value. In contingent claims analysis, cash flows of the portfolio are discounted by risk-free interest rate. Accordingly, distribution of stochastic price process is under risk-neutral measure, with risk-neutral drift that usually incorporates convenience yield. Convenience yield measures the benefit of holding the physical underlying commodity rather than the financial product.

Spread options approach

One basic contingent claim analysis is the spread options approach. Many complex real options valuation problems can be approximated as the sum of a portfolio of spread options by ignoring physical operational constraints. Spread option is the most commonly seen option in energy markets. It is defined as an option that allows investors to simultaneously take positions in two or more assets and profit from their price difference over some spread. The spread option approach is widely used by practitioners because it is more intuitive for pricing and hedging. For instance, as in Deng, Johnson, and Sogomonian (1998) and Deng (2005), a thermal power plant can be modeled as a series of spark spread options, which

exchanges a specific fuel for electricity. Though a replicating portfolio is not applicable in power market because electricity is non-storable, contingent claim analysis can still be applied as there are tradable electricity futures or forward contracts. Eydeland and Wolyniec (2003) offer the example of a natural gas storage facility that is modeled as a combination of calendar spread options written on the same underlying and strike prices but different expiration months.

Many studies have focused on spread options applications in energy markets, such as Girma and Paulson (1998, 1999) and Deng et al. (2001). However, even under setups in which the asset returns are jointly normally distributed, it is a challenge to compute spread option prices efficiently and accurately, as no exact closed-form formula exists for spread options with general nonzero spread. Existing numerical methods and analytical approximations have their own weaknesses. Thus, we are motivated to design a method for spread option pricing and hedging that is both accurate and fast. This method is presented in Chapter 2.

In Chapter 3, we generalize our method to tackle a much more challenging problem of pricing spread options with more than two underlying assets. Multi-asset spread options are in great demand in many real options applications in the both the financial and energy industries. For example, spark spread option and its variants designed for exchanging one or several types of fuel for electricity are commonly used in hedging both short-term and long-term cross-commodity risks. Moreover, demand for pricing spread options involving three, four and even more commodities in bulk quantity with contract parameters spanning a large range is growing. In such applications, developing a numerical algorithm that is capable of quickly and accurately pricing large quantities of spread options on multiple assets with varying parameters is critical.

1.2.2 Dynamic programming

Though valuing a complex real option as the sum of a series of spread options is intuitive and efficient in computation, it overlooks the physical operational constraints, which set real options in the energy market apart from pure financial options. This oversimplification will lead to the overvaluation of the real options. Incorporating realistic operational characteristics in modeling will usually lead to a stochastic dynamic programming problem. Under such a problem, sequential decisions are made. At each time step, decisions are divided into an immediate decision and a subsequent decision. One can solve a sequence of optimal operation strategy by considering both the present payoff and the expected continue value. In contrast to the contingent claims method, which assumes a risk-neutral measure, dynamic programming analysis uses an exogenous risk-adjusted discount rate to discount cash flows. Due to the complicated nature of solving the dynamic programming problem for real options, no closed-form solutions exist. Sophisticated numerical methods must be applied. Below are some commonly used numerical methods:

Lattice method

One important approach is lattice or tree method. Binomial lattice is a basic approach for financial options pricing. By modeling the underlying financial instrument as discrete-time binary state variables, option values are solved by a recursive induction process. Binomial lattice is easy to implement and flexible, but can not deal with options with multiple underlying or other more exotic features. Other lattice methods, such as trinomial lattice and adaptive mesh models, have been developed for financial options, such as trinomial lattice and adaptive mesh models. When applied to real options valuation, more sophisticated lattice needs to be developed, as operational constraints and multiple sources of uncertainty complicate the problem. For instance: Deng and Oren (2003) propose a stochastic dynamic programming model for power generation capacity and solve it by constructing discrete-time multinomial lattice processes. Jaillet et al. (2004) design multi-layered trinomial trees to value swing option, which is one kind of real options with the embedded

flexibility of delivery options. Ghiuvea et al. (2003), Manoliu (2004), Parsons (2005) and Barrera-Esteve et al. (2006) extend this tree-building technique to the problem of natural gas storage valuation.

Monte Carlo simulation

Monte Carlo simulation has been one major pricing method for financial options. In simulation approach, sample paths of underlying energy prices are simulated. Starting from the known payoff on maturity date, this algorithm solves the problem by backward induction. With the payoff and expected holding value computed, optimal decision policies are determined along the simulated paths. One example is valuing natural gas storage by simulation, as in de Jong and Walet (2003), Barrera-Esteve et al. (2006), and Boogert and de Jong (2008).

This approach has great flexibility in incorporating operational constraints, more than one stochastic driver and exotic payoffs. For instance, Tseng and Barz (2002) tackle the short-term generation asset valuation problem by simulating power prices and taking account of physical constraints such as start-up and shut-down costs, minimum run time, and maximum ramp rate.

One major disadvantage of the simulation approach is its slow computation speed. A more efficient scheme is needed, especially for real time valuation of a bulk volume of real options or under a flexible trading strategy that takes positions in multiple financial instruments. This need motivates us to develop a novel numerical algorithm called Gaussian quadrature method to solve the multi-stage stochastic optimization problem. We illustrate it with a real-options-based valuation of gas storage facility in Chapter 4.

In summary, contingent claims and dynamic programming are two major valuation methods for real options. Dixit and Pindyck (1994) give examples in which these two methods are equivalent. Insley and Wirjanto (2006) further show that when discount rates are constant, some restrictions must be met to have the same valuation result. These two

methods have strengths and weaknesses. Unlike the dynamic programming method, contingent claim analysis does not need an exogenous, risk-adjusted discount rate. However, the risk-neutral assumption of contingent claims requires that the uncertainty of the investment or project under valuation be fully replicated by tradable assets. In addition, convenience yield is often not easy to estimate. Which analysis is preferable depends on specific application and model setup. We will present examples of each method in the following chapters of this thesis.

Many other methods of solving the stochastic dynamic programming problem are discussed in the literature. Some researchers, such as Ahn et al. (2002), Weston (2002), Chen and Forsyth (2007), Thompson et al. (2009) translate the Bellman equations into quasi-variational partial differential equations, which are solved by finite difference methods.

Most of the numerical methods need to discretize the underlying price process. In Chapter 5, we propose a continuous-time formulation for power plant valuation. We preserve continuity of the stochastic spark spread process and work directly with the value function.

1.3 Outline and main results of the thesis

This thesis is organized as follows. First, because decomposing a complex real option into the sum of a portfolio of spread options is a widely applied approach, the efficient valuation scheme for spread option pricing and hedging is important. In Chapter 2, we develop a new closed-form approximation method for pricing two-asset spread options. Numerical analysis shows that our method is more accurate than existing analytical approximations and also extremely fast. Closed-form approximations for the Greeks of spread options are developed. We then further generalize the above results for multi-asset spread options in Chapter 3. Two new closed-form approximation methods are developed: the extended Kirk approximation and the second-order boundary approximation. Closed-form approximations for important Greeks are also derived.

In Chapter 4, we apply the real options approach to value a natural gas storage facility. A market-based valuation framework with realistic operational characteristics is proposed. The operational process is modeled as a multi-stage stochastic optimization problem. We develop a Gaussian quadrature scheme to solve for the dynamically optimal spot trading strategy and propose a novel hybrid trading strategy that successfully incorporates both spot and forward trading.

In Chapter 5, we investigate the power plant valuation problem as another important application of real options. Two important operational characteristics, start-up and shutdown cost structures, are considered in the model. We develop a continuous-time formulation for power plant valuation in infinite time horizon. Spark spread is modeled directly as a mean-reverting process. Instead of discretizing the stochastic process, we preserve continuity of the stochastic spark spread process and work directly with the value function. Closed form of value function under threshold policy is obtained. The corresponding optimal operational strategy and sensitivity analysis of the asset value with respect to the cost parameters of a power plant and the distribution parameters of spark spread can then be solved.

CHAPTER II

SPREAD OPTIONS PRICING AND HEDGING

2.1 Introduction

Spread options allow investors to simultaneously take positions in two or more assets and profit from their price difference over some spread. Spread options are prevalent in equity, fixed income, foreign exchange and commodity markets. For instance, in the fixed income markets, various instruments are traded on exchanging securities with different maturities (such as Treasury Notes and Bonds), with different quality levels (such as the Treasury Bills and Eurodollars), and with different issuers (such as French and German bonds, or Municipal bonds and Treasury Bonds). In the agricultural markets, the CBOT trades the so-called crush spread which exchanges raw soybeans with a combination of soybean oil and soybean meal. In the energy markets, crack spread options, which either exchange crude oil and unleaded gasoline or exchange crude oil and heating oil, are traded on the NYMEX. Electricity spark spread options are also traded over the counter for exchanging a specific fuel for electricity. Many studies have focused on spread options in these markets. For example, Arak et al. (1987), Jones (1991), and Easterwood and Senchack (1986) study spread options in the fixed income markets. Johnson et al. (1991) study spread options in the agricultural markets. Girma and Paulson (1998, 1999) and Deng et al. (2001) study spread options in the energy markets.

In this chapter, we first obtain lower and upper bounds for digital spread options by analyzing the exercise boundary. We then develop a new closed-form approximation for pricing spread options. Numerical analysis demonstrates that our method is more accurate than existing analytical approximations. It is also extremely fast, capable of computing one million spread options within 10 seconds. Thus, our method enables the accurate pricing

of a bulk volume of spread options with different specifications in real time which offers traders a potential edge in financial markets. The availability of a closed-form formula for spread options also helps us design and analyze real and financial contracts with embedded spread-option-like features.

We also derive closed-form approximations for the Greeks of spread options. The closed-form approximations of Greeks serve as valuable tools in financial applications. For instance, they can be used for calculating Value-at-Risk for a portfolio containing spread options. As byproducts, we analyze the price sensitivities of spread options. In particular, we point out the signs of vegas when the correlation is negative and when the correlation is positive and large. The analysis of the price sensitivities leads to improved understanding of the price behavior of spread options and is useful in formulating effective dynamic-hedging strategies.. The risk-neutral valuation of the two-asset spread option price involves a two-dimensional integration. We introduce a key concept called the exercise boundary. It is defined as the minimal log price of asset one, as a function of the log price of asset two, for the option to expire in the money. For convenience, we also standardize these two log prices. Under setups in which the asset returns are jointly normally distributed, closed-form formula (Margrabe 1978) exists for pricing exchange options, which are spread options with zero spreads. The critical reason why such a closed-form formula can be obtained for exchange options is that the exercise boundary of a spread option is linear when the spread is zero, which allows the double integration to be evaluated in closed form. However, for general spread options where the spread is not zero, the exercise boundary becomes non-linear, which prevents people from obtaining a closed-form formula. Thus, it is a challenge to compute spread option prices efficiently and accurately as no exact closed-form formula exists for spread options with general nonzero spread.

Existing methods for pricing spread options can be roughly divided into two groups: numerical methods and analytical approximations. Numerical methods include numerical

integration, Monte Carlo simulation, and fast Fourier transform. Analytical methods generally seek to obtain closed-form formula to approximate the spread option price. Various analytical methods have been proposed. In the Bachelier approximation (Wilcox 1990, Shimko 1994, Poitras 1998), one approximates the price difference of the two assets directly as a normal random variable and then uses the Bachelier formula for plain-vanilla options to approximate the spread option price. Unfortunately, the Bachelier approximation is found to be rather crude. Some attempts (Mbanefo (1997)) have been made to improve the accuracy of the Bachelier approximation, usually by including high-order moments of the price difference or using a Gram-Charlier density function pioneered in finance by Jarrow and Rudd (1982). Kirk (1995) uses the Margrabe formula to price spread options by combining the second asset and the fixed spread into a single asset which is then treated as lognormally distributed. His method is equivalent to a linearization of the nonlinear exercise boundary. This method is found to be relatively accurate and thus currently relatively popular among practitioners. Carmona and Durrleman (2003a, 2003b) design a new method to approximate the spread option price by giving the lower and upper price bounds. The Carmona-Durrleman method is generally more accurate than other analytical methods. However, a critical shortcoming is that in this method one needs to solve a nonlinear system of equations which is computationally costly and not completely trivial. Thus, unlike other analytical methods, the Carmona-Durrleman method does not give a closed-form formula for the spread option price.

However, there are weaknesses in the existing methods of both approaches. In general, while numerical methods are often accurate, their computing times are usually much longer than desirable. On the other hand, analytical approximation methods are generally faster than numerical methods but often lack accuracy and robustness. Thus, it is desirable to have a method that combines the strengths of existing methods while avoiding their weaknesses, namely, a method that is both accurate and fast.

The purpose of this chapter is to derive closed-form approximations for the spread

option price and Greeks which are more accurate and faster than existing methods. We make several important contributions. First, we propose a new closed-form approximation for pricing spread-options-based on a quadratic approximation of the exercise boundary. Our approximation is extremely accurate, often resulting in relative pricing errors smaller than 10^{-4}. Second, our approach differs from existing analytical approximations in that we approximate each term in the spread option price separately. Approximating individual terms allows us to compute digital-type spread options very accurately. More importantly, it also leads to extremely accurate approximations for the Greeks, which are of significant importance in practical applications such as dynamic hedging and Value-at-Risk calculations. Third, we develop lower and upper bounds for digital spread options. Finally, we provide an analytical study on the price sensitivities of the spread options. In particular, we characterize the signs of the vegas when the correlation coefficient between the two underlyings is negative or positive and large.

Our closed-form approximation formula for spread option prices can offer insights on the designing and analyzing of real options embedded in financial and real contracts. Spread options with zero spread, a.k.a. exchange options, have been employed extensively by researchers to model real options, partly because of the availability of the Margrabe formula. For example, McDonald and Siegel (1985) use the Margrabe formula to study the investment and valuation of firms when there is an option to shut down. Shevlin (1991) investigates the valuation of R&D firms with R&D limited partnerships. Albizzati and Geman (1994) value the surrender option in life insurance polices by extending the Margrabe formula to a Heath-Jarrow-Morton stochastic interest rate framework. Grinblatt and Titman (1989), and Johnson and Tian (2000) apply the Margrabe formula to study the design and effectiveness of performance-based contracts and executive stock options. However, in many of these applications, it is more natural to assume that we have a spread option instead of an exchange option. The spread K may correspond to the cost or salvage value of shutting down a firm, the cost or salvage value of terminating an R&D partnership, the

monetary penalty of surrendering the life insurance policy prematurely, a minimal level ($K > 0$) of performance difference that a manager has to achieve over a benchmark, or a cushion ($K < 0$) to insure the manager that he will not be unfairly penalized because of pure bad luck. The extra degree of freedom arising from a nonzero K could be extremely important in designing and analyzing these real options.

The chapter is organized as follows. Section 2.2 discusses the general framework we use; that is, asset returns are jointly-normally distributed. We reduce the spread option pricing problem to a one-dimensional problem in Proposition 2.2.1, show that it reduces to the Margrabe formula when the exercise boundary is linear in Proposition 2.2.2, and discuss the properties of the exercise boundary for general spread options in Proposition 2.2.3. Section 2.3 develops lower and upper bounds for the digital spread option in Proposition 2.3.1 and Proposition 2.3.2 based on a tangent line approximation and a chord approximation of the exercise boundary, respectively. Section 2.4 develops a closed-form approximation for spread options in Proposition 2.4.1 based on a quadratic approximation of the exercise boundary. Proposition 2.4.1 is the central result of this chapter. We also analyze the price sensitivities of spread options in our general framework in Proposition 2.4.2 and the special geometric Brownian motions case in Proposition 2.4.3. We then give closed-form approximations in Proposition 2.4.4 for the spread option Greeks. Section 2.5 compares our method with existing analytical approximations and numerical integration in terms of speed and accuracy and shows that our method is both very accurate and fast. Section 2.6 concludes. Proofs are in the Appendix.

2.2 The model setup

The main purpose of this chapter is to derive an efficient and accurate method for computing spread option prices. Under the general assumption of jointly-normal returns, closed-form formula exists for exchange options, that is, spread options with the spread K being zero. However, for general spread options with nonzero K, exact closed-form formula is not

available. In this chapter, we develop an extremely accurate analytical approximation for spread option prices with general values of K. The relative errors of our approximation are usually smaller than 10^{-4}, well within the observed bid-ask spreads of these options.

We first describe the setup we will use for pricing spread options, that is, the returns of the two assets are jointly normally distributed. Specifically, consider two assets whose prices at time t are denoted by $S_1(t)$ and $S_2(t)$. We are interested in options whose final payoffs are nonnegative only when $S_1(T) - S_2(T) - K \geq 0$ at some future time T, where the spread K is a constant. We focus on cash-or-nothing digital spread options with time-T payoff given by $1_{S_1(T) \geq S_2(T)+K}$, and spread options with time-T payoff $[S_1(T) - S_2(T) - K]^+$, where we use f^+ to denote the positive part of the function f. By the martingale pricing approach, the prices of a digital spread option Π^{D} and a spread option Π are given by

$$\Pi^{\mathrm{D}} = e^{-rT}\mathbb{E}^{\mathbb{Q}}[1_{\{S_1(T) \geq S_2(T)+K\}}], \quad \Pi = e^{-rT}\mathbb{E}^{\mathbb{Q}}[S_1(T) - S_2(T) - K]^+, \tag{2.2.1}$$

where $\mathbb{Q}$ is the risk-neutral measure under which discounted security prices are martingales, r is the risk-free interest rate.

To compute these option prices, distributional assumptions on $S_1(T)$ and $S_2(T)$ need to be made. We assume that $\log S_1(T)$ and $\log S_2(T)$ are jointly normally distributed. Specifically, let the initial prices of the two assets be $S_1(0) = S_1$, $S_2(0) = S_2$, and

$$\mathbb{E}^{\mathbb{Q}}[\log S_i(T)] = \mu_i, \quad \mathrm{var}^{\mathbb{Q}}[\log S_i(T)] = \nu_i^2, \quad (i = 1, 2) \tag{2.2.2}$$

where the means μ_i's and the variances ν_i's are all deterministic quantities. Next, we define

$$X = \frac{\log S_1(T) - \mu_1}{\nu_1}, \quad Y = \frac{\log S_2(T) - \mu_2}{\nu_2}. \tag{2.2.3}$$

Notice that X and Y are the standardized log prices of asset one and two, respectively. In our setup, we will assume that X and Y are jointly normal with correlation coefficient ρ and with standard normal marginal densities under $\mathbb{Q}$.

This general setup incorporates two important cases, namely, the geometric Brownian motions (GBMs) case and the mean-reverting log-Ornstein-Uhlenbeck (log-OU) case.

Specifically, let $W_1(t)$ and $W_2(t)$ be two Brownian motions with correlation ϱ. In the GBMs case, we have

$$\mathrm{d}S_i(t) = (r - q_i)S_i(t)\mathrm{d}t + \sigma_i S_i(t)\mathrm{d}W_i(t), \tag{2.2.4}$$

where r is the risk-free interest rate, σ_i's are the volatilities, and q_i's are the dividend rates. A simple application of Ito's lemma tells us that $\log S_1(T)$ and $\log S_2(T)$ are jointly normally distributed, with the μ_i's and ν_i's in equation (2.2.2) given by

$$\mu_i = \log S_i + (r - q_i - \sigma_i^2/2)T, \quad \nu_i = \sigma_i\sqrt{T}, \quad \rho = \varrho, \tag{2.2.5}$$

The GBMs case can be easily generalized to incorporate seasonality in parameters by allowing σ_i's, q_i's and ρ be to deterministic functions of the calendar time t. This is useful since for some spread options, their underlying assets exhibit strong seasonality in price volatilities and in their return correlations. Our general framework incorporates this generalized GBMs case.

In the log-OU case, we have

$$\mathrm{d}S_i(t) = -\lambda_i(\log S_i(t) - \eta_i)S_i(t)\mathrm{d}t + \sigma_i S_i(t)\mathrm{d}W_i(t), \tag{2.2.6}$$

where λ_i's are the mean-reverting strengths and η_i's are parameters controlling the long-run means. With some algebra, it can be shown that $S_1(T)$ and $S_2(T)$ are jointly normally distributed, with the μ_i's and ν_i's in equation (2.2.2) given by

$$\mu_i = \eta_i - \frac{\sigma_i^2}{2\lambda_i} + e^{-\lambda_i T}\left(\log S_i - \eta_i + \frac{\sigma_i^2}{2\lambda_i}\right), \quad \nu_i = \sigma_i\sqrt{\frac{1 - e^{-2\lambda_i T}}{2\lambda_i}}, \tag{2.2.7}$$

$$\rho = 2\varrho\frac{\sqrt{\lambda_1\lambda_2}}{\lambda_1 + \lambda_2}\frac{1 - e^{-(\lambda_1+\lambda_2)T}}{\sqrt{1 - e^{-2\lambda_1 T}}\sqrt{1 - e^{-2\lambda_2 T}}}. \tag{2.2.8}$$

Before introducing our method, we present a thorough analysis of the exercise boundary of the spread option. The exercise boundary is defined to be the minimal standardized log price of asset one for the option to be in the money as a function of the standardized log price of asset two. A detailed study on the exercise boundary is important because as

we will see later, the existence of a closed-form formula for exchange options but not for general spread options results exactly from the linearity of the exercise boundary when the spread is zero.

At time T, the options are in-the-money if $S_1(T) - S_2(T) - K \geq 0$. Let $K \geq 0$. By the definitions of X and Y in equation (2.2.3), this condition is the same as

$$X \geq \frac{\log(e^{\nu_2 Y + \mu_2} + K) - \mu_1}{\nu_1}. \tag{2.2.9}$$

Thus, conditioning on $Y = y$, the option is in-the-money if $X \geq \underline{x}(y)$, where the (conditional) exercise boundary $\underline{x}(y)$ is given by

$$\underline{x}(y) \equiv \frac{\log(e^{\nu_2 y + \mu_2} + K) - \mu_1}{\nu_1}. \tag{2.2.10}$$

When $K < 0$, the condition in equation (2.2.9) is not always well-defined because it is possible that $e^{\nu_2 Y + \mu_2} + K < 0$. However, by making use of the identities

$$1_{S_1(T) \geq S_2(T) + K} = 1 - 1_{S_2(T) \geq S_1(T) - K}, \tag{2.2.11}$$

$$[S_1(T) - S_2(T) - K]^+ = S_1(T) - S_2(T) - K + (S_2(T) - S_1(T) + K)^+, \tag{2.2.12}$$

we can transform the problems of computing Π^{D} and Π in the $K < 0$ case to the $K > 0$ case. For example, by equation (2.2.11), to compute the price of a digital spread option with final payoff $1_{S_1(T) \geq S_2(T) + K}$ where $K < 0$, we can switch the roles of S_1 and S_2 and compute the price of the digital spread option with final payoff $1_{S_2(T) \geq S_1(T) + |K|}$. Similarly, equation (2.2.12) allows us to only consider spread options with $K \geq 0$. Consequently, throughout this chapter we assume that $K \geq 0$, so that equation (2.2.9) is always well-defined.

The risk-neutral valuation in equation (2.2.1) gives Π^{D} and Π in terms of two-dimensional integrations. However, in the following proposition, we utilize a method introduced in Pearson (1995) which reduces the two-dimensional integrations to one-dimensional integrations. Reducing the two-dimensional integration problem in equation (2.2.1) to a one-dimensional integration is useful not only for our approximation later, but also for numerical methods. For example, if one uses numerical integration, then by Proposition 2.2.1 below, we only need to evaluate one-dimensional integrals, which is considerably faster than

evaluating two-dimensional integrals. Also, Proposition 2.2.1 is useful for Monte Carlo simulation. Carrying out Monte Carlo directly using equation (2.2.1) is not very efficient because many realizations of $(S_1(T) - S_2(T) - K)^+$ will be zero, especially for out-of-the-money spread options. Also, we need to simulate a bivariate distribution. With Proposition 2.2.1, we can simulate a single random variable y using a standard normal density and then compute the $\mathbf{I}_i$'s by taking the sample averages of the three cumulative normal distribution functions. In this way, information in each realization of y is utilized and thus Proposition 2.2.1 plays a similar role as importance sampling in variance reduction.

Proposition 2.2.1. *Under the jointly-normal returns setup, the prices of the spread option and the digital spread option are given by*

$$\Pi = e^{\nu_1^2/2+\mu_1-rT}\,\mathbf{I}_1 - e^{\nu_2^2/2+\mu_2-rT}\,\mathbf{I}_2 - Ke^{-rT}\,\mathbf{I}_3, \quad \textit{and} \quad \Pi^{\mathrm{D}} = e^{-rT}\mathbf{I}_3, \tag{2.2.13}$$

where the integrals $\mathbf{I}_i$*'s are given by*

$$\mathbf{I}_1 = \int_{-\infty}^{\infty} N\Big(A(y+\rho\nu_1) + \sqrt{1-\rho^2}\nu_1\Big)\, n(y)\,\mathrm{d}y, \tag{2.2.14}$$

$$\mathbf{I}_2 = \int_{-\infty}^{\infty} N(A(y+\nu_2))\, n(y)\,\mathrm{d}y, \tag{2.2.15}$$

$$\mathbf{I}_3 = \int_{-\infty}^{\infty} N(A(y))\, n(y)\,\mathrm{d}y, \tag{2.2.16}$$

where $n(\cdot)$ *and* $N(\cdot)$ *are the standard normal density function and the cumulative normal distribution function, respectively, and the function* $A(\cdot)$ *is given by*

$$A(y) = \frac{\rho y - \underline{x}(y)}{\sqrt{1-\rho^2}}, \tag{2.2.17}$$

with the exercise boundary $\underline{x}(y)$ *given in equation* (2.2.10)*.*

Equation (2.2.13) in Proposition 2.2.1 gives a formula for the spread option price very similar to the Black-Scholes formula (Black and Scholes 1973). In particular, the price of the spread option Π consists of three terms. The first term is the present value of the risk-neutral expected future benefit of receiving asset one. The second term is the present value

of expected future cost of giving up asset two if the option expires in the money. The last term is the present value of the expected cost of giving up an additional monetary amount K.

The quantities $A(y)$ and $\mathbf{I}_i$'s have intuitive meanings. We will call $A(y)$ the **conditional moneyness** of the spread option because $A(y)$ plays a similar role as d_2 in the Black-Scholes formula. This can be seen from the proof of Proposition 2.2.1 that the quantity $N(A(y))$ is the risk-neutral probability that the spread option expires in the money conditioning on that the standardized log price of asset two is y. Written out explicitly, we have

$$N(A(y)) = \text{Prob}^{\mathbb{Q}}\left[S_1(T) \geq S_2(T) + K \;\middle|\; Y \equiv \frac{\log S_2(T) - \mu_2}{\nu_2} = y\right]. \tag{2.2.18}$$

In the Black-Scholes formula, y is a constant, while in the case of spread options, y is distributed as a standard normal random variable. Integrating over y in equation (2.2.16) then gives the unconditional exercise probability $\mathbf{I}_3$. That is, $\mathbf{I}_3$ is the probability that the spread option will expire in the money under the risk-neutral distribution. The proof of Proposition 2.2.1 shows that $\mathbf{I}_1$ and $\mathbf{I}_2$ have similar meanings as $\mathbf{I}_3$. They are the probabilities that the spread option will expire in the money under the two measures in which asset one and asset two are taken to be the numeraire asset, respectively. This is similar to the case of the Black-Scholes formula, where the term $N(d_1)$ is the probability that the option will expire in the money under the probability measure in which the underlying stock is taken as the numeraire asset. For general change of numeraire technique, see Geman et al. (1995). The quantities $\mathbf{I}_i$'s are also related to the Greeks. As we will see later, in the GBMs case, $\mathbf{I}_1$ and $-\mathbf{I}_2$ are also the deltas of the spread option price with respect to the initial prices of asset one and asset two, respectively, while $\mathbf{I}_3$ is related to the price sensitivity of the spread option with respect to the spread K.

In Proposition 2.2.1, we have given the spread option price in terms of three one-dimensional integrals $\mathbf{I}_1$, $\mathbf{I}_2$ and $\mathbf{I}_3$. In the rest of the chapter, we will develop closed-form approximations based on Proposition 2.2.1. We carry this out in a few steps. First, in Proposition 2.2.2 below, we will show that these integrals can be computed in closed-form

to yield the Margrabe formula if the exercise boundary $\underline{x}(y)$ (and hence the conditional moneyness function $A(y)$) is linear, which happens exactly when the spread K is zero. Second, we study the monotonicity and convexity properties of the exercise boundary and the conditional moneyness function in detail in Proposition 2.2.3. Finally, in later sections, we approximate the exercise boundary by making use of these properties. These approximations in turn allow us to derive price bounds for digital options in Proposition 2.3.1 and Proposition 2.3.2, as well as approximate spread option prices in Proposition 2.4.1.

We first take a look at the special case when $K = 0$. Proposition 2.2.2 derives the Margrabe formula (Margrabe 1978) for this special case using a new mathematical identity (equation 2.2.19), which will also be very useful for our approximation later on. This lemma is a result by Li (2008). If we interpret $n(y; \mu, \sigma^2)$ in the proposition as the density of the log price of asset two and $a + by$ as the conditional moneyness $A(y)$, then this identity says that the unconditional moneyness can be computed in closed-form when the conditional moneyness $A(y)$ is a linear function of y. For spread options, from the expression for the exercise boundary $\underline{x}(y)$ in equation (2.2.10), we see that $\underline{x}(y)$ is linear in y precisely when $K = 0$. Notice also that $A(y)$ is linear in y if and only if $\underline{x}(y)$ is linear in y. Thus, Proposition 2.2.2 offers a direct proof of the Margrabe formula which differs from the original partial differential equation approach in Margrabe (1978). Also, the Margrabe formula we give is more general than the original form as it applies to all models in which the returns are jointly normally distributed, and just the GBMs case. The proof of Proposition 2.2.2 is given in the Appendix.

Proposition 2.2.2. *Let a and b be real numbers. Then we have*

$$\int_{-\infty}^{\infty} N(a + by) n(y; \mu, \sigma^2) \mathrm{d}y = N\left(\frac{a + b\mu}{\sqrt{1 + b^2\sigma^2}} \right). \tag{2.2.19}$$

For exchange options (spread options with $K = 0$), the conditional moneyness function $A(y)$ is linear in y. Thus, from equation (2.2.19)*, the price of an exchange option under the*

jointly-normal returns setup is given by the following Margrabe formula

$$\Pi = e^{\nu_1^2/2+\mu_1-rT} N\left(\frac{\mu_1-\mu_2+(\nu_1^2-\rho\nu_1\nu_2)}{\sqrt{\nu_1^2+\nu_2^2-2\rho\nu_1\nu_2}}\right) - e^{\nu_2^2/2+\mu_2-rT} N\left(\frac{\mu_1-\mu_2-(\nu_2^2-\rho\nu_1\nu_2)}{\sqrt{\nu_1^2+\nu_2^2-2\rho\nu_1\nu_2}}\right). \quad (2.2.20)$$

For general spread options, $K \neq 0$. An immediate difficulty to apply Proposition 2.2.2 in this case is that the arguments for the cumulative normal distributions in the integrals $\mathbf{I}_1$, $\mathbf{I}_2$ and $\mathbf{I}_3$, namely, $A(y+\rho\nu_1)+\sqrt{1-\rho^2}\nu_1$, $A(y+\nu_2)$ and $A(y)$, are not linear functions of y. From the expression for $A(y)$, we see that this is precisely because the exercise boundary $\underline{x}(y)$ is not linear in y. However, a closer examination reveals that $\underline{x}(y)$ is quite close to linear locally. When y is very negative, $\underline{x}(y)$ behaves like a constant function. When y is very positive, $\underline{x}(y)$ behaves like a linear function. Figure 2.2.1 plots the function $\underline{x}(y)$ for different values of K. The parameters used are for the GBMs case with $S_1 = 90$, $S_2 = 100$, $r = 5\%$, $q_1 = q_2 = 0$, $\sigma_1 = 0.4$, $\sigma_2 = 0.5$ and $T = 0.25$. The idea of our approximation is to approximate the exercise boundary $\underline{x}(y)$ using a lower-order Taylor expansion, for example, a linear or quadratic function. This has the advantage that we approximate the $\mathbf{I}_i$'s separately. Notice that $\underline{x}(y)$ is exactly linear when either $\sigma_2 = 0$ or $K = 0$. Thus, as we shall see, our approximation is exact when $\sigma_2 = 0$ or $K = 0$. This is appealing because when $\sigma_2 = 0$, our formula collapses to the Black-Scholes formula for an ordinary European call option, and when $K = 0$, our formula collapses to the Margrabe formula for an exchange option.

Because our approximation tries to catch the deviation of the exercise boundary from linearity, a closer look at the regions of monotonicity and convexity of the exercise boundary $\underline{x}(y)$, the risk-neutral conditional moneyness $A(y)$, and the conditional exercise probability $N(A(y))$ is crucial. In addition, by making use of the monotonicity and convexity properties, we are able to look at price bounds for digital spread options as we will do in the next section. The results of this monotonicity and convexity analysis are given in the following proposition. For readers who are less interested in the mathematical details, it suffices to understand the following three points from Proposition 2.2.3. First, the exercise

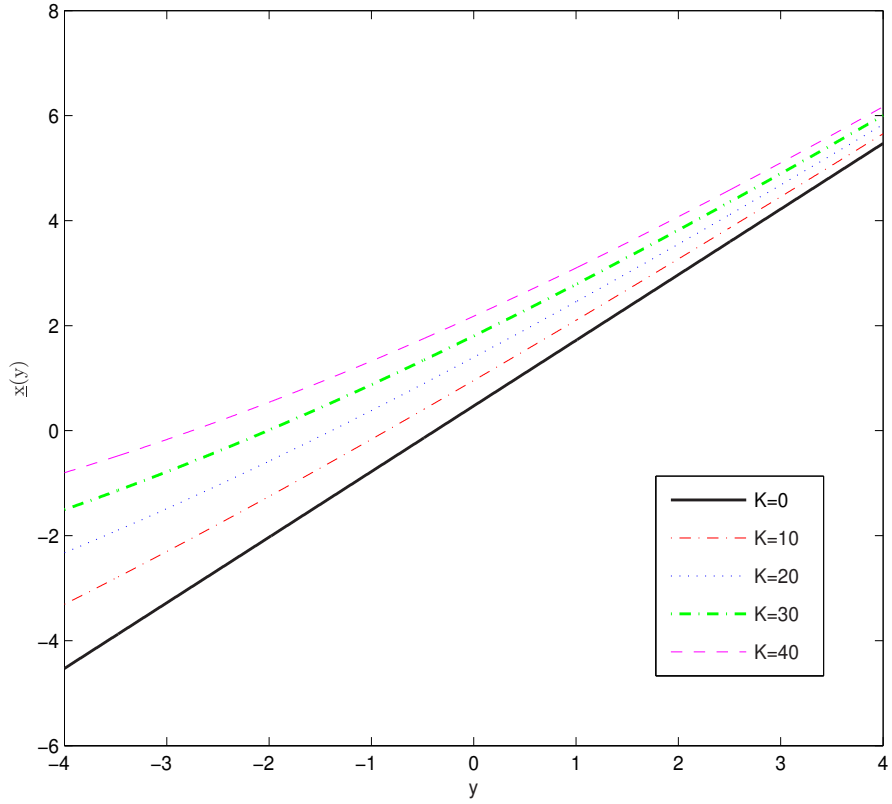

Figure 2.2.1: The Exercise Boundary

boundary $\underline{x}(y)$ is convex in y while the conditional moneyness function $A(y)$ is concave in y. Second, the behavior of $A(y)$ and $N(A(y))$ is influenced by the sign and size of the correlation coefficient ρ. Third, the behavior of $A(y)$ and $N(A(y))$ could be different for different regions of y. These properties will be used later on. For example, as we will see later, the sign and size of ρ has influence on the signs of spread option vegas. The proof of Proposition 2.2.3 is given in the Appendix.

Proposition 2.2.3. *Let $K \geq 0$ and $|\rho| < 1$.*

1. *The exercise boundary $\underline{x}(y)$ is an increasing and convex function of y.*

2. *If $\rho \geq \nu_2/\nu_1$, the conditional moneyness $A(y)$ and risk-neutral conditional exercise probability $N(A(y))$ are both monotonically increasing in y. If $\rho \leq 0$, $A(y)$ and*

$N(A(y))$ are both monotonically decreasing in y. If $0 < \rho < \nu_2/\nu_1$, both $A(y)$ and $N(A(y))$ have exactly one maximum at

$$\widehat{y} = \frac{1}{\nu_2} \log\left(\frac{e^{-\mu_2} K\rho\nu_1}{\nu_2 - \rho\nu_1}\right). \tag{2.2.21}$$

3. *The conditional moneyness $A(y)$ is a concave function of y.*

4. *If $e^{\mu_1+\rho\nu_1 y} > e^{\mu_2+\nu_2 y} + K$, then the conditional exercise probability $N(A(y))$ is locally concave at y. Furthermore, suppose the solution of $e^{\mu_1+\rho\nu_1 y} = e^{\mu_2+\nu_2 y} + K$ exists and denote it by $\widetilde{y}$. Then $N(A(y))$ is concave in the region $(\widetilde{y}, +\infty)$ if $\nu_2 < \rho\nu_1$, and concave in the region $(-\infty, \widetilde{y})$ if $\rho < 0$.*

Now that we have studied the monotonicity and convexity properties of the conditional moneyness $A(y)$ in Proposition 2.2.3, we are ready to develop our approximations. In the next section, we establish lower and upper bounds on the digital spread option with the help of Proposition 2.2.2 and 2.2.3. Readers who are interested in spread option prices can go directly to Section 2.4 where we develop closed-form approximations for spread option prices.

2.3 Bounds for digital spread option prices

2.3.1 The upper bound — tangent line approximation

In this section, we derive upper and lower bounds for digital spread options by approximating the exercise boundary. Pricing bounds for spread options can be obtained similarly. Pricing bounds are useful when no closed-form formula exists. Early studies in this area include Perrakis and Ryan (1984) and Lo (1987). More recently, Nielsen and Sandmann (2003), and Henderson, et al. (2007) derive pricing bounds for Asian options. Pricing bounds for American options are studied in Broadie and Detemple (1996), Chen and Yeh (2002), Chung and Chang (2007), among others. Carmona and Durrleman (2006) study pricing bounds for spread options.

By approximating the exercise boundary $\underline{x}(y)$ more or less favorably, we can establish price bounds for digital spread options. We look at the upper bound first. By Proposition 2.2.3, the conditional moneyness $A(y)$ is concave in y. Thus, if we draw any tangent line of $A(y)$, it will lie completely above the graph of $A(y)$. Pick an arbitrary point y_0. By the expression of $A(y)$ in equation (2.2.17), the tangent line of $A(y)$ at y_0 is given by $G(y_0) + H(y_0)y$, where

$$G(y_0) = \frac{1}{\nu_1\sqrt{1-\rho^2}}\left(\mu_1 - \log(R+K) + \frac{R}{R+K}\nu_2 y_0\right), \tag{2.3.1}$$

$$H(y_0) = \frac{1}{\sqrt{1-\rho^2}}\left(\rho - \frac{R\nu_2}{(R+K)\nu_1}\right), \tag{2.3.2}$$

with

$$R = e^{\nu_2 y_0 + \mu_2}. \tag{2.3.3}$$

For any tangent position y_0, the conditional moneyness approximation $G(y_0) + H(y_0)y$ is more favorable than the actual conditional moneyness $A(y)$. Proposition 2.2.1 and 2.2.2 now give us the following inequality:

$$\mathbf{I_3} = \int_{-\infty}^{\infty} N(A(y))n(y)\mathrm{d}y \le \int_{-\infty}^{\infty} N(G(y_0) + H(y_0)y)n(y)\mathrm{d}y = N\left(\frac{G(y_0)}{\sqrt{1+H^2(y_0)}}\right). \tag{2.3.4}$$

Since the above derivation is valid for any y_0, we can establish an upper bound for the price of a digital spread option:

Proposition 2.3.1. *Let $K \ge 0$ and $|\rho| < 1$. Then*

$$\Pi^{\mathrm{D}} \le \inf_{y_0 \in \mathbb{R}} e^{-rT} N\left(\frac{G(y_0)}{\sqrt{1+H^2(y_0)}}\right). \tag{2.3.5}$$

In the above proposition, each candidate in the infimum is the price of a digital option whose exercise boundary is more favorable than the one in our digital spread option. Different values of y_0 match the slopes of the actual and approximating exercise boundaries at different future log prices of asset two. For example, setting $y_0 = 0$ amounts to matching the slope of the exercise boundary exactly when the log price of asset two equals its mean.

The two limiting cases $y_0 \to \pm\infty$ correspond to the prices of an ordinary digital option and a digital exchange option, respectively. For example, when $y_0 \to -\infty$, from the expressions for $G(y_0)$ and $H(y_0)$, the conditional moneyness approximation $G(y_0) + H(y_0)y$ for $A(y)$ becomes

$$A(y) \approx G(-\infty) + H(-\infty)y = \frac{1}{\nu_1\sqrt{1-\rho^2}}(\mu_1 - \log K) + \frac{\rho}{\sqrt{1-\rho^2}}y. \tag{2.3.6}$$

Thus,

$$e^{-rT}N\left(\frac{G(-\infty)}{\sqrt{1+H^2(-\infty)}}\right) = e^{-rT}N\left(\frac{\mu_1 - \log K}{\nu_1}\right), \tag{2.3.7}$$

which is exactly the price of a plain-vanilla digital option with final payoff $1_{S_1(T)\geq K}$. Similarly, one can show that the upper bound in equation (2.3.5) when $y_0 \to +\infty$ is the price of the digital exchange option with final payoff $1_{S_1(T)\geq S_2(T)}$. Thus the infimum in Proposition 2.3.1 automatically incorporates the following inequalities

$$1_{S_1(T)\geq S_2(T)+K} \leq 1_{S_1(T)\geq K}, \quad \text{and} \quad 1_{S_1(T)\geq S_2(T)+K} \leq 1_{S_1(T)\geq S_2(T)}. \tag{2.3.8}$$

This upper bound in Proposition 2.3.1 is very tight and can be used as an approximation for the digital spread option price. Numerical analysis shows that the relative pricing errors, defined as the pricing errors divided by the actual prices, are typically of order 10^{-3}.

In order to make Proposition 2.3.1 more useful in practice, we need to have a quick estimate of the optimal value for y_0 that achieves the infimum in equation (2.3.5). The optimal value for y_0 is given by the solution of the following equation

$$\frac{\mathrm{d}}{\mathrm{d}y_0}N\left(\frac{G(y_0)}{\sqrt{1+H^2(y_0)}}\right) = 0. \tag{2.3.9}$$

An analytical solution to the best y_0 from the above nonlinear equation turns out to be not possible. However, we can linearize equation (2.3.9) around $y_0 = 0$ and then solve for the best y_0 approximately. This should be a very accurate approximation because the best expansion point for y_0 ought to be very close to 0 since $n(y)$ peaks at 0. The result is the

following choice of y_0:

$$\widehat{y_0} = \frac{\xi(\lambda\xi + K\nu_2)\log(e^{\mu_1}/\xi)}{\xi^2(\nu_2^2 + 2\lambda\nu_2 - \nu_1^2) - K^2\nu_2^2 - 2K\xi\lambda\nu_2 + e^{\mu_2}\xi\lambda\nu_2\log(e^{\mu_1}/\xi)}, \tag{2.3.10}$$

where

$$\lambda = \rho\nu_1 - \nu_2, \quad \xi = e^{\mu_2} + K. \tag{2.3.11}$$

Although the expression of $\widehat{y_0}$ is complicated, it is a simple function of the input parameters and can be computed very quickly. Numerical analysis shows that for all reasonable parameter values, we have

$$0 \le N\left(\frac{G(\widehat{y_0})}{\sqrt{1+H^2(\widehat{y_0})}}\right) - \inf_{y_0\in\mathbb{R}} N\left(\frac{G(y_0)}{\sqrt{1+H^2(y_0)}}\right) \sim 10^{-4}\cdot \inf_{y_0\in\mathbb{R}} N\left(\frac{G(y_0)}{\sqrt{1+H^2(y_0)}}\right). \tag{2.3.12}$$

Thus, in practice, we can replace the infimum in Proposition 2.3.1 by this particular choice of $\widehat{y_0}$ without losing much accuracy.

2.3.2 The lower bound — chord approximation

A lower bound can also be established for the digital spread option by using the chords of the exercise boundary $\underline{x}(y)$. Pick two points y_l and y_r on the real line with $y_r > y_l$. The line passing through points $(y_l, A(y_l))$ and $(y_r, A(y_r))$ is given by $B(y) = P(y_l, y_r) + Q(y_l, y_r)y$, where

$$P(y_l, y_r) = \frac{y_r A(y_l) - y_l A(y_r)}{y_r - y_l}, \quad Q(y_l, y_r) = \frac{A(y_r) - A(y_l)}{y_r - y_l}. \tag{2.3.13}$$

The segment of $B(y)$ between points $(y_l, A(y_l))$ and $(y_r, A(y_r))$ is a chord of the conditional moneyness function $A(y)$. By Proposition 2.2.3, the line $B(y)$ lies below the exercise boundary $\underline{x}(y)$ in the region (y_l, y_r) and above the exercise boundary $\underline{x}(y)$ outside this region. Because of this, if we directly use $B(y)$ to approximate the conditional moneyness $A(y)$, the resulting price could be either an upper bound or a lower bound. However, notice that we always have

$$N(A(y)) \ge N(B(y)) - [N(A(y)) - N(B(y))]^+. \tag{2.3.14}$$

This fact can be used to derive a lower bound for the digital spread option given in the following proposition. In the second line of equation (2.3.15), we add back two terms by looking at the behavior of the conditional moneyness $A(y)$ in more detail with the help of Proposition 2.2.3. The proof of Proposition 2.3.2 is in the Appendix.

Proposition 2.3.2. *Let $K \geq 0$ and $|\rho| < 1$. Then*

$$\Pi^{\mathrm{D}} \geq \sup_{\substack{y_l, y_r \in \mathbb{R} \\ y_r > y_l}} e^{-rT} \left(N\left(\frac{P(y_l, y_r)}{\sqrt{1 + Q^2(y_l, y_r)}} \right) - N(y_l) - N(-y_r) \right.$$
$$\left. + N(-y_r) N(A(y_r)) 1_{\rho \geq \nu_2/\nu_1} + N(y_l) N(A(y_l)) 1_{\rho \leq 0} \right). \tag{2.3.15}$$

In the above proposition, each candidate in the supremum is the price of a digital option whose exercise boundary is less favorable than the one in our digital spread option. Since the digital spread option price is greater than each of the candidate, it is greater than the supremum of them too. For given values of y_l and y_r, the lower bound can be computed quickly to give an approximation for Π^D.

This lower bound is not as accurate as the upper bound, yielding relative pricing errors of about 2% in many cases in our numerical analysis. We can also approximate the optimal y_l and y_r as we have done for the upper bound. We choose not to do it and instead introduce a new approximation which is extremely accurate with relative pricing errors being less than 10^{-4} most of the time.

The upper and lower bounds for digital spread options are useful because the delta's and kappa (defined as the option price sensitivity with respect to the spread K) of a spread option can themselves be considered digital spread option prices, as we will see in Proposition 2.4.3 later. Thus our bounds for digital spread options give us bounds on the Greeks of spread options.

2.4 Closed-form approximations for spread option prices and Greeks

2.4.1 Approximation for spread option prices

We are now ready to obtain the main result of this chapter, that is, a fast and accurate approximation for spread options prices. Our improved approximation is based on a quadratic approximation of the exercise boundary and hence a quadratic approximation of the conditional moneyness function $A(y)$. Suppose we approximate $A(y)$ using a parabola by $C^3(y_0) + D^3(y_0)y + \epsilon(y_0)y^2$ around $y = y_0$, then

$$\mathbf{I}_3 = \int_{-\infty}^{\infty} N(A(y))n(y)\mathrm{d}y \approx \int_{-\infty}^{\infty} N(C^3 + D^3 y + \epsilon y^2)n(y)\mathrm{d}y. \tag{2.4.1}$$

The expressions for C^3, D^3 and ϵ will be given in Proposition 2.4.1. The superscripts 3 in C^3 and D^3 indicate that these quantities are for the third term $\mathbf{I}_3$. They should not be misinterpreted as powers. We use superscripts instead of subscripts because later we will use subscripts for partial derivatives. The quantities C^3, D^3 and ϵ are the intercept, slope, and curvature at $y = 0$, respectively, of the quadratic approximating boundary $C^3(y_0) + D^3(y_0)y + \epsilon(y_0)y^2$.

By Proposition 2.2.2, the last integral in the above equation cannot be evaluated in closed-form unless we let $\epsilon = 0$. However, if the curvature ϵ is small around the expansion point y_0, then we can expand the above integral around $\epsilon = 0$. Numerical analysis shows this is indeed the case. Similar observations are made to the integrals $\mathbf{I}_1$ and $\mathbf{I}_2$. The resulting approximation is given in the following proposition. Proposition 2.4.1 approximates $\mathbf{I}_1$, $\mathbf{I}_2$ and $\mathbf{I}_3$ with a second-order Taylor expansion in terms of the curvature ϵ of the conditional moneyness function $A(y)$. The proof of Proposition 2.4.1 is given in the Appendix.

Proposition 2.4.1. *Let $K \geq 0$ and $|\rho| < 1$. Let y_0 be any real number close to 0. The spread option price Π under the general jointly-normal returns setup is given by*

$$\Pi = e^{\nu_1^2/2+\mu_1-rT}\,\mathbf{I}_1 - e^{\nu_2^2/2+\mu_2-rT}\,\mathbf{I}_2 - Ke^{-rT}\,\mathbf{I}_3. \tag{2.4.2}$$

The integrals $\mathbf{I}_i$'s are approximated to second order in ϵ as

$$\mathbf{I}_i \approx \mathbf{J}_0(C^i, D^i) + \mathbf{J}_1(C^i, D^i)\epsilon + \frac{1}{2}\mathbf{J}_2(C^i, D^i)\epsilon^2, \tag{2.4.3}$$

where the function $\mathbf{J}_i$'s are defined as

$$\mathbf{J}_0(u, v) = N\left(\frac{u}{\sqrt{1+v^2}}\right), \tag{2.4.4}$$

$$\mathbf{J}_1(u, v) = \frac{1 + (1+u^2)v^2}{(1+v^2)^{5/2}} \cdot n\left(\frac{u}{\sqrt{1+v^2}}\right), \tag{2.4.5}$$

$$\mathbf{J}_2(u, v) = \frac{(6-6u^2)v^2 + (21-2u^2-u^4)v^4 + 4(3+u^2)v^6 - 3}{(1+v^2)^{11/2}} u \cdot n\left(\frac{u}{\sqrt{1+v^2}}\right), \tag{2.4.6}$$

and the arguments C^i, D^i,and ϵ are given by

$$C^1 = C^3 + D^3\rho\nu_1 + \epsilon\rho^2\nu_1^2 + \sqrt{1-\rho^2}\nu_1, \tag{2.4.7}$$

$$D^1 = D^3 + 2\rho\nu_1\epsilon, \tag{2.4.8}$$

$$C^2 = C^3 + D^3\nu_2 + \epsilon\nu_2^2, \tag{2.4.9}$$

$$D^2 = D^3 + 2\nu_2\epsilon, \tag{2.4.10}$$

$$C^3 = \frac{1}{\nu_1\sqrt{1-\rho^2}}\left(\mu_1 - \log(R+K) + \frac{\nu_2 R}{R+K}y_0 - \frac{1}{2}\frac{\nu_2^2 RK}{(R+K)^2}y_0^2\right), \tag{2.4.11}$$

$$D^3 = \frac{1}{\nu_1\sqrt{1-\rho^2}}\left(\rho\nu_1 - \frac{\nu_2 R}{R+K} + \frac{\nu_2^2 RK}{(R+K)^2}y_0\right), \tag{2.4.12}$$

$$\epsilon = -\frac{1}{2\nu_1\sqrt{1-\rho^2}}\frac{\nu_2^2 RK}{(R+K)^2}, \tag{2.4.13}$$

with $R = e^{\nu_2 y_0 + \mu_2}$.

Note that Proposition 2.4.1 also allows us to approximate the digital spread option price Π^D. Systematic numerical analysis demonstrates that a first order approximation in ϵ by setting $\mathbf{J}_2 = 0$ already yields very accurate spread option prices, although its accuracy seems to be consistently dominated by a second order approximation in ϵ. Moreover, the choice of $y_0 = 0$ works very well and generally produces relative price errors smaller than 10^{-4}. A zero y_0 also results in simpler expressions for C^i's and D^i's and makes our approximation faster. Thus, we shall fix $y_0 = 0$ throughout this chapter. Setting $y_0 = 0$

amounts to matching the slope and curvature of the exercise boundary exactly when the log price of asset two equals its mean.

Our approximation in Proposition 2.4.1 has some nice properties. First, it satisfies many boundary conditions. For example, it collapses to the Black-Scholes formula when either μ_1 or μ_2 approaches $-\infty$. Also, as μ_1 goes to infinity, we have $\lim_{\mu_1\to\infty} \Pi/e^{\nu_1^2/2+\mu_1-rT} = 1$, and as $\mu_2 \to \infty$, we have $\lim_{\mu_2\to\infty} \Pi = 0$. The approximation also satisfies the terminal boundary condition when $T \to 0$. Second, our approximation collapses exactly to the Margrabe formula when $K = 0$ and converges to 0 when $K \to \infty$. Third, our approximation collapses exactly to the Black-Scholes formula when $\nu_2 \to 0$. These nice properties add to the attractiveness of our approximation.

In Section 2.5, we will perform a thorough comparison of our method with other methods in terms of computational speed and accuracy. We shall see that our method is extremely fast and accurate. Before we do that, we study the price sensitivity of spread options. We first perform an analysis for the general jointly-normal return setup in Proposition 2.4.2. We then study the special geometric Brownian motions case and the results are given in Proposition 2.4.3 and 2.4.4. Readers who are less interested to see the analysis on price sensitivity and Greeks can proceed directly to Section 2.5.

2.4.2 Price sensitivity analysis of spread options

The price Π of the spread option is a function of $\nu_1, \nu_2, \rho, r, T, \mu_1, \mu_2$ and $\log K$. Sometimes we view Π as a function of e^{μ_1}, e^{μ_2} or K instead of μ_1, μ_2, and K. For example, in the geometric Brownian motions case, it is usually more natural to look at price sensitivity with respect to S_i's instead of $\log S_i$'s. It should be clear from the context which point of view we use. The sensitivities of spread option prices with respect to these parameters are not well understood under the jointly-normal returns setup, mainly because of the lack of a closed-form formula. We fill this gap with the following two propositions. Proofs are provided in the Appendix.

Proposition 2.4.2. *Let $K \geq 0$. Under the jointly-normal returns setup, we have:*

1. *Holding all other variables constant,* Π *is increasing and convex in* e^{μ_1}.
2. *Holding all other variables constant,* Π *is decreasing and convex in* e^{μ_2}.
3. *Holding all other variables constant,* Π *is decreasing and convex in* K.
4. *Holding all other variables constant,* Π *is convex in* μ_1.
5. *Holding all other variables constant,* Π *is decreasing in* ρ.
6. *Holding all other variables constant,* $\partial^2\Pi/\partial\mu_1\partial\mu_2 < 0$.

This proposition generalizes the known price sensitivities of the Black-Scholes formula and the Margrabe formula to the case of spread options. It is easy to understand that Π is increasing in μ_1, and decreasing in μ_2 and K. For exchange options, from the Margrabe formula, it is well-known that the option price is convex in S_1 and S_2. Proposition 2.4.2 generalizes this result to spread options by pointing out that Π is convex in e^{μ_1}, e^{μ_2} and K. Statement 4 is a new and interesting result. The fact that Π decreases with ρ agrees with intuition and generalizes the result for exchange options. Intuitively, for larger values of ρ, when the value of asset one increases, the value of asset two tends to increase more, resulting in a smaller value for the spread option.

Notice that under the general jointly-normal returns setup, we cannot say too much on the Greeks because we have not specified the functional forms for μ_i's and ν_i's. For example, μ_i's could be complicated functions of the volatilities, time to maturity, etc. Thus, we do not examine the sensitivities of Π with respect to ν_i's in Proposition 2.4.2. However, if we assume geometric Brownian motions for the $S_i(t)$'s, the functional forms of μ_i's and ν_i's are determined and we can obtain more results. For simplicity, we assume that $q_1 = q_2 = 0$ throughout this chapter. This does not incur any loss of generality since nonzero q_1 and q_2 can be absorbed into a redefinition of S_1 and S_2. Notice first that in this special

case, equation (2.2.5) holds and we have

$$\Pi = S_1\mathbf{I}_1 - S_2\,\mathbf{I}_2 - Ke^{-rT}\,\mathbf{I}_3. \tag{2.4.14}$$

The following proposition expresses the Greeks in terms of one-dimensional integrations and points out the signs of the Greeks. These one-dimensional integrals are potentially very useful if one computes the Greeks using Monte Carlo simulation. Proposition 2.4.3 also characterizes the signs of various Greeks for the spread option under the geometric Brownian motions assumption.

Proposition 2.4.3. *Let $K \geq 0$ and assume that $S_i(t)$'s follow geometric Brownian motions with correlation ρ.*

1. *The sensitivities of the spread option price to initial stock prices S_i and spread K are given by*

$$\Delta_1 \equiv \frac{\partial \Pi}{\partial S_1} = \mathbf{I}_1 = \int_{-\infty}^{\infty} N\left(A(y+\rho\nu_1) + \sqrt{1-\rho^2}\nu_1\right) n(y)\mathrm{d}y, \tag{2.4.15}$$

$$\Delta_2 \equiv \frac{\partial \Pi}{\partial S_2} = -\mathbf{I}_2 = -\int_{-\infty}^{\infty} N(A(y+\nu_2))\, n(y)\mathrm{d}y, \tag{2.4.16}$$

$$\kappa \equiv \frac{\partial \Pi}{\partial K} = -e^{-rT}\mathbf{I}_3 = -e^{-rT}\int_{-\infty}^{\infty} N(A(y))\, n(y)\mathrm{d}y. \tag{2.4.17}$$

   Furthermore, we have

$$0 < \Delta_1 < 1, \quad -1 < \Delta_2 < 0, \quad \textit{and} \quad -e^{-rT} < \kappa < 0. \tag{2.4.18}$$

2. *The signs of the gamma's are given by*

$$\Gamma_{11} \equiv \frac{\partial^2 \Pi}{\partial S_1^2} > 0, \quad \Gamma_{12} \equiv \frac{\partial^2 \Pi}{\partial S_1 \partial S_2} < 0, \quad \Gamma_{22} \equiv \frac{\partial^2 \Pi}{\partial S_2^2} > 0. \tag{2.4.19}$$

3. *The spread option price is a decreasing function of ρ and we have*

$$\frac{\partial \Pi}{\partial \rho} = S_1 S_2 \sigma_1 \sigma_2 T\, \Gamma_{12} < 0. \tag{2.4.20}$$

4. The vega's of the spread option price are given by

$$\mathcal{V}_1 \equiv \frac{\partial \Pi}{\partial \sigma_1} = e^{-rT}\sqrt{1-\rho^2}\sqrt{T}\int_{-\infty}^{\infty} n(A(y))(K + e^{\mu_2+\nu_2 y})\, n(y)\mathrm{d}y$$
$$+ \rho S_1 \sqrt{T}\int_{-\infty}^{\infty} yN(A(y+\rho\nu_1) + \sqrt{1-\rho^2}\nu_1)\, n(y)\mathrm{d}y, \tag{2.4.21}$$

$$\mathcal{V}_2 \equiv \frac{\partial \Pi}{\partial \sigma_2} = -S_2\sqrt{T}\int_{-\infty}^{\infty} yN(A(y+\nu_2))\, n(y)\mathrm{d}y. \tag{2.4.22}$$

Furthermore, if $\rho \leq 0$, we have $\mathcal{V}_1 \geq 0$ and $\mathcal{V}_2 \geq 0$. If $\sigma_2/\sigma_1 \leq \rho \leq 1$, we have $\mathcal{V}_1 \geq 0$ and $\mathcal{V}_2 \leq 0$.

While the signs of the Greeks in the first three statements are well-known, statement 4 gives us some insights on the vegas. It is interesting to note that unlike the Black-Scholes formula, in which both call and put option prices are increasing functions of the volatility, the spread option price can be either increasing or decreasing in the two volatilities. For exchange options, from the Margrabe formula, it can be easily shown the sign of $\mathcal{V}_1$ is the same as that of $\nu_1 - \nu_2\rho$, and the sign of $\mathcal{V}_2$ is the same as that of $\nu_2 - \nu_1\rho$. Proposition 2.4.3 is consistent with these results and partially generalizes them to spread options. It is only a partial generalization because the signs of the vegas are still not known when $0 \leq \rho \leq \sigma_2/\sigma_1$. The difficulty lies in Proposition 2.2.3, which points out that for values of ρ in this range, the conditional moneyness $A(y)$ is no longer monotone in y. Besides expressing the Greeks in simple one-dimensional integrals, Proposition 2.4.3 is useful for other purposes. In particular, bounds on the vega's can be established with the help of Proposition 2.4.3. For example, by equation (2.4.22), it is easy to show that when $K \geq 0$, we have $|\mathcal{V}_2| \leq S_2\sqrt{T}/\sqrt{2\pi}$.

Finally, in Propositions 2.4.2 and 2.4.3, we have assumed that $K \geq 0$. For the case $K \leq 0$, we need to use equation (2.2.12) to reduce to the $K \geq 0$ case. The modifications are as follows. For Proposition 2.4.2, all statements are still true when $K \leq 0$ except statement 4. Most expressions in Proposition 2.4.3 can no longer be directly used when $K \leq 0$. The correct expressions in this case can be worked out easily with the help of equation (2.2.12). Because this process is not completely trivial, we use κ as an illustration. Writing

$\Pi = \Pi(S_1, S_2, \sigma_1, \sigma_2, \rho, K)$, we have by equation (2.2.12) that

$$\Pi(S_1, S_2, \sigma_1, \sigma_2, \rho, K) = S_1 - S_2 - Ke^{-rT} + \Pi(S_2, S_1, \sigma_2, \sigma_1, \rho, -K). \tag{2.4.23}$$

We will call the above equation the generalized put-call parity for spread options. Indeed, if $S_2 = 0$ and $\sigma_2 = 0$, then the above relation reduces to the put-call parity for plain-vanilla European options in the Black-Scholes formula. If $K = 0$, then the above equation reduces to the put-call parity for exchange options in the Margrabe formula. Now let $K \leq 0$ in equation (2.4.23). To compute κ, we have by the generalized put-call parity and Proposition 2.4.3 that

$$\begin{aligned}\kappa &= \frac{\partial}{\partial K}\Pi(S_1, S_2, \sigma_1, \sigma_2, \rho, K) = -e^{-rT} + \frac{\partial}{\partial K}\Pi(S_2, S_1, \sigma_2, \sigma_1, \rho, -K) \\ &= -e^{-rT} + e^{-rT}\int_{-\infty}^{\infty} N(A^{\dagger}(x))\, n(x)\mathrm{d}x = -e^{-rT}\int_{-\infty}^{\infty} N(-A^{\dagger}(x))\, n(x)\mathrm{d}x,\end{aligned} \tag{2.4.24}$$

where $A^{\dagger}(x)$ is the mirror image of $A(y)$ given as

$$A^{\dagger}(x) = \frac{\rho x - \underline{y}(x)}{\sqrt{1-\rho^2}} \tag{2.4.25}$$

with

$$\underline{y}(x) = \frac{\log(e^{\nu_1 x + \mu_1} + |K|) - \mu_2}{\nu_2}. \tag{2.4.26}$$

Equations (2.4.17) and (2.4.24) seem to give two different expressions for κ when $K = 0$. They actually lead to exactly the same result if we evaluate them using Proposition 2.2.2. The reason that the function $A^{\dagger}(x)$ now gets involved is that by using the put-call parity, the roles of asset one and asset two get switched. Other Greeks can be modified similarly when $K \leq 0$ and are omitted here. It is worthwhile pointing out that when $K \leq 0$, the expression for $\mathcal{V}_1$ now involves only one integral while the expression for $\mathcal{V}_2$ now involves two integrals. Also, equations (2.4.18), (2.4.19) and (2.4.20) in Proposition 2.4.3 are still correct. The last sentence in statement 4 when $K \leq 0$ should be changed to: If $\sigma_1/\sigma_2 \leq \rho \leq 1$, we have $\mathcal{V}_1 \leq 0$ and $\mathcal{V}_2 \geq 0$. Again, it is easy to check that this new statement is consistent with the known behavior of $\mathcal{V}_1$ and $\mathcal{V}_2$ for the exchange option case.

2.4.3 Approximations for the Greeks in the GBMs case

Proposition 2.4.1 gives the approximate price for the spread option in closed form. However, in practice one often needs to compute the Greeks efficiently. This can be done by differentiating the approximate price Π in Proposition 2.4.1. However, the algebra is quite complicated. Instead, we design separate approximations for the Greeks in the special geometric Brownian motions case in Proposition 2.4.4 below. This proposition allows for fast and accurate computation of the Greeks for the spread option in this important special case. The proof relies on Proposition 2.4.3 and is again based heavily on the boundary approximation. It is given in the Appendix.

Proposition 2.4.4. *Let $K \geq 0$ and assume that $S_i(t)$'s follow geometric Brownian motions with correlation ρ.*

1. *The delta's and kappa can be approximated as*

$$\Delta_1 \approx \mathbf{J}_0(C^1, D^1) + \mathbf{J}_1(C^1, D^1)\epsilon + \frac{1}{2}\mathbf{J}_2(C^1, D^1)\epsilon^2, \tag{2.4.27}$$

$$\Delta_2 \approx -\mathbf{J}_0(C^2, D^2) - \mathbf{J}_1(C^2, D^2)\epsilon - \frac{1}{2}\mathbf{J}_2(C^2, D^2)\epsilon^2, \tag{2.4.28}$$

$$\kappa \approx -\mathbf{J}_0(C^3, D^3) - \mathbf{J}_1(C^3, D^3)\epsilon - \frac{1}{2}\mathbf{J}_2(C^3, D^3)\epsilon^2. \tag{2.4.29}$$

2. *The gamma's can be approximated as*

$$\Gamma_{11} \approx \Phi(C^1, D^1, C^1_{S_1}, D^1_{S_1}, \epsilon_{S_1}), \tag{2.4.30}$$

$$\Gamma_{12} \approx \Phi(C^1, D^1, C^1_{S_2}, D^1_{S_2}, \epsilon_{S_2}), \tag{2.4.31}$$

$$\Gamma_{22} \approx -\Phi(C^2, D^2, C^2_{S_2}, D^2_{S_2}, \epsilon_{S_2}), \tag{2.4.32}$$

where the function Φ is defined by

$$\Phi(x, y, u, v, w) = n\Big(\frac{x}{\sqrt{1+y^2}}\Big)\frac{(1+y^2)^2 u - x(y+y^3)v + (1+(1+x^2)y^2)w}{(1+y^2)^{5/2}}, \tag{2.4.33}$$

and the partial derivatives are given by

$$C^1_{S_1} = \frac{1}{\nu_1 S_1\sqrt{1-\rho^2}}, \quad D^1_{S_1} = 0, \quad \epsilon_{S_1} = 0, \tag{2.4.34}$$

and

$$C^1_{S_2} = \frac{\epsilon}{S_2}\Big(\frac{2(R+K)}{\nu_2^2 K} + \frac{2\rho\nu_1}{\nu_2} + \Big(1 - \frac{2R}{R+K}\Big)\rho^2\nu_1^2\Big), \tag{2.4.35}$$

$$D^1_{S_2} = \frac{\epsilon}{S_2}\Big(\frac{2}{\nu_2} + 2\rho\nu_1\Big(1 - \frac{2R}{R+K}\Big)\Big), \tag{2.4.36}$$

$$C^2_{S_2} = \frac{\epsilon}{S_2}\Big(\frac{2(R+K)}{\nu_2^2 K} + 2 + \Big(1 - \frac{2R}{R+K}\Big)\nu_2^2\Big), \tag{2.4.37}$$

$$D^2_{S_2} = \frac{\epsilon}{S_2}\Big(\frac{2}{\nu_2} + 2\nu_2\Big(1 - \frac{2R}{R+K}\Big)\Big), \tag{2.4.38}$$

$$\epsilon_{S_2} = \frac{\epsilon}{S_2}\Big(1 - \frac{2R}{R+K}\Big). \tag{2.4.39}$$

3. *The approximation for vega with respect to σ_1 is given by*

$$\begin{aligned}\mathcal{V}_1 \approx\ & S_1\Phi(C^1, D^1, C^1_{\sigma_1}, D^1_{\sigma_1}, \epsilon_{\sigma_1}) \\ & - S_2\Phi(C^2, D^2, C^2_{\sigma_1}, D^2_{\sigma_1}, \epsilon_{\sigma_1}) - Ke^{-rT}\Phi(C^3, D^3, C^3_{\sigma_1}, D^3_{\sigma_1}, \epsilon_{\sigma_1}),\end{aligned} \tag{2.4.40}$$

where

$$C^1_{\sigma_1} = -\frac{C^3}{\sigma_1} + \epsilon\rho^2\sigma_1 T, \qquad D^1_{\sigma_1} = D^3_{\sigma_1}, \tag{2.4.41}$$

$$C^2_{\sigma_1} = C^3_{\sigma_1} + D^3_{\sigma_1}\nu_2 + \epsilon_{\sigma_1}\nu_2^2, \qquad D^2_{\sigma_1} = D^3_{\sigma_1} + 2\nu_2\epsilon_{\sigma_1}, \tag{2.4.42}$$

$$C^3_{\sigma_1} = -\frac{\sqrt{T}}{\sqrt{1-\rho^2}} - \frac{C^3}{\sigma_1}, \qquad D^3_{\sigma_1} = \frac{\sigma_2}{\sigma_1^2\sqrt{1-\rho^2}}\frac{R}{R+K}, \tag{2.4.43}$$

$$\epsilon_{\sigma_1} = -\frac{\epsilon}{\sigma_1}. \tag{2.4.44}$$

The approximation for vega with respect to σ_2 is given by

$$\begin{aligned}\mathcal{V}_2 \approx\ & S_1\Phi(C^1, D^1, C^1_{\sigma_2}, D^1_{\sigma_2}, \epsilon_{\sigma_2}) \\ & - S_2\Phi(C^2, D^2, C^2_{\sigma_2}, D^2_{\sigma_2}, \epsilon_{\sigma_2}) - Ke^{-rT}\Phi(C^3, D^3, C^3_{\sigma_2}, D^3_{\sigma_2}, \epsilon_{\sigma_2}),\end{aligned} \tag{2.4.45}$$

where

$$C^1_{\sigma_2} = C^3_{\sigma_2} + \rho\sigma_1\sqrt{T}D^3_{\sigma_2} + \rho^2\sigma_1^2 T\epsilon_{\sigma_2}, \qquad D^1_{\sigma_2} = D^3_{\sigma_2} + 2\rho\sigma_1\sqrt{T}\epsilon_{\sigma_2}, \tag{2.4.46}$$

$$C^2_{\sigma_2} = \frac{\rho\sqrt{T}}{\sqrt{1-\rho^2}} - C^3_{\sigma_2} + \sigma_2^2 T\epsilon_{\sigma_2}, \qquad D^2_{\sigma_2} = -\frac{1}{\sigma_2\sqrt{T}}C^3_{\sigma_2} + 2\sigma_2\sqrt{T}\epsilon_{\sigma_2}, \tag{2.4.47}$$

$$C^3_{\sigma_2} = \frac{R\sigma_2\sqrt{T}}{(R+K)\sigma_1\sqrt{1-\rho^2}}, \qquad D^3_{\sigma_2} = -\frac{R(R+K-K\sigma_2^2 T)}{(R+K)^2\sigma_1\sqrt{1-\rho^2}}, \tag{2.4.48}$$

$$\epsilon_{\sigma_2} = -\frac{1}{2}C^3_{\sigma_2} + \frac{(K-R)\sigma_2\sqrt{T}}{2(R+K)}D^3_{\sigma_2}. \tag{2.4.49}$$

or

$$\mathcal{V}_2 \approx S_2\sqrt{T}\,\Upsilon(C^2, D^2, \epsilon), \tag{2.4.50}$$

where the function Υ *is given by*

$$\Upsilon(u,v,w) = n\Big(\frac{u}{\sqrt{1+v^2}}\Big)v\frac{(1+v^2)^3 - uw(3+(3+u^2)v^2)}{(1+v^2)^{7/2}}. \tag{2.4.51}$$

Although we do not discuss them here, higher-order Greeks such as the vomma's and vanna's (defined as the sensitivities of option vegas with respect to volatilities and spot prices, respectively) can be easily approximated as well using our method. Our approximations for the Greeks involve only simple arithmetic and are very fast to compute. Also, they are derived using the same idea as for the price approximation and are thus extremely accurate, often giving relative errors well within 0.1%.

2.5 Comparison of accuracy and speed with existing methods

2.5.1 Existing approximation methods

Various methods have been proposed for pricing spread options, which can be broadly divided into two groups. The first group follows the numerical approach and includes Pearson (1995)'s one-dimensional numerical integration method, fast Fourier transform methods as in Dempster and Hong (2000), numerical solutions to partial differential equations, and Monte Carlo methods. The second group tries to approximate the spread option price

and Greeks analytically, and includes Bachelier approximation, Bachelier approximation with Gram-Charlier adjustment, Kirk's approximation, Carmona-Durrleman approximation, and others. Eydeland and Wolyniec (2003) also contain a closed-form approximation for spread options, which is not very accurate. In this section, we will compare the speed and accuracy of our method with alternative methods. We first discuss some of the alternative methods, namely, the Bachelier approximation, Bachelier approximation with Gram-Charlier adjustment, Kirk's approximation and the Carmona-Durrleman approximation. In the next subsection, we then perform a comparison of speed and accuracy of existing methods with our approximation.

In the Bachelier approximation, the quantity $B \equiv e^{-rT}(S_1(T) - S_2(T))$ is approximated as a normal random variable, with mean μ_B and standard deviation σ_B given by

$$\mu_B = S_1 - S_2, \quad \sigma_B = \sqrt{S_1^2(\theta_1 - 1) - 2S_1S_2(\theta_2 - 1) + S_2^2(\theta_3 - 1)}, \tag{2.5.1}$$

where

$$\theta_1 = e^{\sigma_1^2 T}, \quad \theta_2 = e^{\sigma_2^2 T}, \quad \theta_3 = e^{\rho\sigma_1\sigma_2 T}. \tag{2.5.2}$$

The spread option price is then approximated using the Bachelier formula for a plain-vanilla European call option (Bachelier 1900) as

$$\Pi_{\mathrm{B}} = (\mu_B - Ke^{-rT})N(d_B) + \sigma_B\, n(d_B), \tag{2.5.3}$$

where

$$d_B = \frac{\mu_B - Ke^{-rT}}{\sigma_B}. \tag{2.5.4}$$

The assumption that B is normal is very crude. Mbafeno (1997) proposes a skewness and kurtosis adjustment based on the Gram-Charlier approximation in Jarrow and Rudd (1982). However, the formula in Mbafeno (1997) contains a typo. Also, he does not give explicit expressions for the skewness and kurtosis under the GBMs setup. Thus, we present the result for the Gram-Charlier approximation in the following proposition, which takes

into account the nonzero skewness γ_B and excess kurtosis κ_B explicitly. The proof is given in the Appendix.

Proposition 2.5.1. *Suppose that the asset prices $S_1(t)$ and $S_2(t)$ follow geometric Brownian motions with initial prices S_1 and S_2. Assume that $B \equiv e^{-rT}(S_1(T) - S_2(T))$ follows a Gram-Charlier approximation which includes skewness and kurtosis adjustments. Then the approximate spread option prices is*

$$\Pi_{\text{GC}} = (\mu_B - Ke^{-rT})N(d_B) + \sigma_B\, n(d_B)\left(1 - \frac{d_B}{6}\gamma_B + \frac{d_B^2 - 1}{24}\kappa_B\right), \tag{2.5.5}$$

with skewness γ_B and excess kurtosis κ_B given by

$$\gamma_B = \frac{\mathbb{E}^{\mathbb{Q}}(B - \mu_B)^3}{\sigma_B^3}, \quad \kappa_B = \frac{\mathbb{E}^{\mathbb{Q}}(B - \mu_B)^4}{\sigma_B^4} - 3, \tag{2.5.6}$$

where

$$\begin{aligned}\mathbb{E}^{\mathbb{Q}}(B - \mu_B)^3 =& (\theta_1 - 1)^2(\theta_1 + 2)S_1^3 - (\theta_2 - 1)^2(\theta_2 + 2)S_2^3 \\ &- 3(\theta_3 - 1)(\theta_1 + \theta_1\theta_3 - 2)S_1^2S_2 + 3(\theta_3 - 1)(\theta_2 + \theta_2\theta_3 - 2)S_1S_2^2,\end{aligned} \tag{2.5.7}$$

and

$$\begin{aligned}\mathbb{E}^{\mathbb{Q}}(B - \mu_B)^4 =& (6\theta_1 - 4\theta_1^3 + \theta_1^6 - 3)S_1^4 + (6\theta_2 - 4\theta_2^3 + \theta_2^6 - 3)S_2^4 \\ &+ 4(3 - 3\theta_1 + \theta_1^3 - 3\theta_3 - \theta_1^3\theta_3^3 + 3\theta_1\theta_3^2)S_1^3S_2 + 4(3 - 3\theta_2 + \theta_2^3 - 3\theta_3 - \theta_2^3\theta_3^3 + 3\theta_2\theta_3^2)S_1S_2^3 \\ &+ 6(\theta_1 + \theta_2 + 3\theta_3 - 2\theta_2\theta_3^2 - 2\theta_1\theta_3^2 + \theta_1\theta_2\theta_3^4 - 3)S_1^2S_2^2.\end{aligned} \tag{2.5.8}$$

Except for the fact that the expressions for the skewness γ_B and excess kurtosis κ_B are complicated, equation (2.5.5) in Proposition 2.5.1 is a standard result. For example, it is well-known that the skewness adjustment is proportional to the moneyness d_B while the excess kurtosis adjustment is quadratic in d_B. Unlike the Bachelier approximation, in the Gram-Charlier approximation the spread option price can become negative, especially when the skewness and excess kurtosis are large. Whenever this happens, we will assume the approximated spread option price is 0. Also, as many researchers have noticed, it is

possible for the Gram-Charlier approximation to perform worse than the Bachelier approximation if the deviation of B from normality is significant. We found that this is indeed the case.

In Kirk's approximation, $Z(T) = S_2(T) + K$ is considered as a lognormal random variable. The initial value of Z is given by $z = S_2 + Ke^{-rT}$. The volatility for $Z(T)$ is value weighted using the relative proportions of the stock and bond positions and is given by

$$\sigma_Z = \frac{S_2}{S_2 + Ke^{-rT}}\sigma_2. \tag{2.5.9}$$

The correlation of $S_1(T)$ and $Z(T)$ are still ρ. Kirk then uses the Margrabe formula to price the spread option (now viewed as a simple exchange option):

$$\Pi_K = e^{-rT}\mathbb{E}^{\mathbb{Q}}[S_1(T) - S_2(T) - K]^+ \approx e^{-rT}\mathbb{E}^{\mathbb{Q}}[S_1(T) - Z(T)]^+ \tag{2.5.10}$$

$$= S_1 N\Big(d_K + \sigma_K\sqrt{T}/2\Big) - (S_2 + Ke^{-rT})N\Big(d_K - \sigma_K\sqrt{T}/2\Big), \tag{2.5.11}$$

where

$$d_K = \frac{\log(S_1/(S_2 + Ke^{-rT})}{\sigma_K\sqrt{T}}, \quad \sigma_K = \sqrt{\sigma_1^2 - 2\rho\sigma_1\sigma_2\frac{S_2}{S_2 + Ke^{-rT}} + \sigma_2^2\Big(\frac{S_2}{S_2 + Ke^{-rT}}\Big)^2}. \tag{2.5.12}$$

Although not obvious, Kirk's approximation can be thought of as a rough version of our approximation, in which the exercise boundary is approximated using three straight lines very close to it. Details are available upon request from the authors. Kirk's approximation is relatively accurate given its simple form, with relative price errors usually within a few percentages.

More recently, a new approximation formula is proposed in Carmona and Durrleman (2003a, 2003b). In this method, one first solves the following equation to get an optimal θ^*:

$$\frac{1}{\sigma_2\sqrt{T}\cos\theta}\log\left(-\frac{\sigma_1 Ke^{-rT}\sin(\theta+\phi)}{S_2(\sigma_1\sin(\theta+\phi) - \sigma_2\sin\theta)}\right) + \frac{\sigma_2\sqrt{T}\cos\theta}{2} \tag{2.5.13}$$

$$= \frac{1}{\sigma_1\sqrt{T}\cos(\theta+\phi)}\log\left(-\frac{\sigma_2 Ke^{-rT}\sin\theta}{S_1(\sigma_1\sin(\theta+\phi) - \sigma_2\sin\theta)}\right) + \frac{\sigma_1\sqrt{T}\cos(\theta+\phi)}{2},$$

where $\phi = \arccos(\rho)$. Now let

$$d^* = \frac{1}{\sigma\sqrt{T}\cos(\theta^* - \psi)} \log\left(\frac{S_1\sigma_1 \sin(\theta^* + \phi)}{S_2\sigma_2 \sin\theta^*}\right) + \frac{1}{2}\left(\sigma_1 \cos(\theta^* + \phi) + \sigma_2 \cos\theta^*\right)\sqrt{T}, \tag{2.5.14}$$

where

$$\sigma = \sqrt{\sigma_1^2 - 2\rho\sigma_1\sigma_2 + \sigma_2^2}, \quad \psi = \arccos\left(\frac{\sigma_2 - \rho\sigma_1}{\sigma}\right). \tag{2.5.15}$$

In the above equations, we have corrected a few typos in Carmona and Durrleman (2003a, 2003b), ranging from missing minus signs and switching of cos and sin functions. Carmona and Durrleman (2003a, 2003b) show that the spread option price is always larger than the following lower bound

$$\Pi_{\text{CD}} = S_1 N\left(d^* + \sigma_1\sqrt{T}\cos(\theta^* + \phi)\right) - S_2 N\left(d^* + \sigma_2\sqrt{T}\cos\theta^*\right) - Ke^{-rT}N(d^*). \tag{2.5.16}$$

In addition, they show that the lower bound is very tight and can be used as a good approximation for the actual price. Our numerical analysis confirms their claim. It is also noteworthy to point out that recently Carmona and Durrleman (2006) have extended their results to multiple assets cases.

Our method improves upon existing approximations in many aspects. First, previous approximations have focused on the spread option as a single identity and developed formulas for the whole spread option, while in our method, we approximate the three individual terms separately. Each individual term in our method is approximated extremely accurately. This contrasts many previous methods. For example, the accuracy of Kirk's method relies on a delicate cancellation of errors between the three terms in equation (2.5.11). The individual terms in Kirk's approximation are very inaccurate, often having relative pricing errors reaching 200%. Approximating individual terms also allows us to compute digital-type spread options, such as asset-or-nothing and cash-or-nothing spread options. Although we do not develop formulas in this chapter, our boundary approximation method also allows us to compute more exotic spread options, for example, options with quadratic payoff $S_1(T)^2 1_{S_1(T)\geq S_2(T)+K}$.

Second, and perhaps the most significant advantage of our method, is that we provide extremely accurate and fast approximations for the Greeks. For example, delta's in our method often have relative errors in the order of 0.1%.

Third, our method achieves a good balance between speed and accuracy. It is more accurate than the Bachelier approximation and Kirk's method. While the Carmona-Durrleman approximation is more accurate than Kirk's approximation, it is still about one or two orders' of magnitude less accurate than our method. Furthermore, like most analytical methods, our method is very fast. The computing times of Bachelier approximation, Kirk's approximation and ours are roughly of the same order of magnitude. However, the Carmona-Durrleman approximation is slower than most analytical approximations since one needs to solve a complicated trigonometrical equation to get the optimal θ^*. This is time-consuming even if one utilizes fast algorithms such as the Newton-Raphson method.

Finally, our approximation is very straightforward to implement and is very robust. We find that it is not trivial to find θ^* for equation (2.5.13) in the Carmona-Durrleman approximation because sometimes the objective function is not smooth in θ^* and there is little guidance on the initial value for θ. Thus, it is hard to use the Newton-Raphson method. The lack of guidance on the initial value for θ also prevents us from comparing systematically the performance of Carmona-Durrleman approximation with ours. The important case $K = 0$ also poses some problems in Carmona-Durrleman because equation (2.5.13) breaks down. Another issue is that whenever θ^* is the solution to equation (2.5.13), so is $\theta^* + \pi$. Only one of the two solutions will correspond to the lower bound. Lacking any guidance on how to select θ^* and $\theta^* + \pi$, one would have to compute option prices for both solutions and then compare. Thus, the Carmona-Durrleman approximation is not as straightforward as our method.

2.5.2 Comparison of accuracy and speed with existing methods

For definiteness, we shall assume the special GBMs case and compare our method with Bachelier approximation, Bachelier approximation with Gram-Charlier adjustment, Kirk's approximation and one-dimensional numerical integration method. The one-dimensional numerical integration is based on Proposition 2.2.1.

Notice that the spread option price is a function of many variables, namely, S_1, S_2, T, r, q_1, q_2, σ_1, σ_2, K, and ρ. We will set $q_1 = q_2 = 0$ as nonzero q_i's can be absorbed into S_1 and S_2. Also, since σ_i's and $\sqrt{T}$ always go together, we set $T = 1$. Because the spread option price is homogeneous of degree 1 in S_1, S_2 and K, we fix $S_1 = 100$. The interest rate r usually does not play a major role so we fix it at 5%. In order to perform a systematic accuracy comparison, we vary S_2/S_1, K/S_1, σ_1, σ_2 and ρ. We set the range of S_2/S_1 to be $[0.7, 1.2]$, the range of K/S_1 to be $[0, 0.4]$, the range of σ_1 and σ_2 to be both $[0.1, 0.8]$, and the range of ρ to be $[-0.75, 0.75]$. In addition, we impose the restriction $S_1 - S_2 - Ke^{-rT} \geq -30$ so that we exclude deeply out-of-the-money options. Parameters are *uniformly* generated from these ranges. All together, we generate 123,783 individual options. Generating options uniformly will tend to weigh extreme scenarios more heavily and thus tend to exaggerate an approximation method's pricing errors.

We then compute the spread option prices for those 123,783 options using Bachelier approximation, Bachelier approximation with Gram-Charlier adjustment, Kirk's approximation and the approximation in this chapter. We also compute the prices using one-dimensional numerical integration with recursive adaptive Simpson quadrature method. Two error tolerance levels are used: 10^{-6} and 10^{-8}. The prices computed from the latter tolerance level are then used as the actual option prices. All methods are implemented in MATLAB 7.0 on an IBM computer with 1.60 GHz Intel Pentium CPU and 768M memory and some other computers. The computing times of different methods do not seem to vary with the specification of the computer on which they are run. For each option and for each approximation method, we first compute the pricing error $\Delta\Pi = \Pi_{\text{Approximation}} - \Pi_{\text{Actual}}$ and

then compute the relative pricing error $\Delta\Pi/\Pi_{\text{Actual}}$. Because the actual prices vary greatly from 0 to around 65, we focus on the relative pricing errors.

The results are reported in Table 2.5.2. For the numerical methods, we do not list their accuracy since it has been specified. Looking at $\Delta\Pi/\Pi_{\text{Actual}}$, Bachelier approximation gives quite inaccurate spread option prices. Also, Bachelier approximation with Gram-Charlier adjustment seems to perform worse than no adjustment. Detailed analysis shows that the deviations of B from normality are often quite significant, with mean excess kurtosis for those 123,783 options being around 10. In addition, Bachelier approximation and Kirk's approximation seem to be biased upward. Most of the time, they give a price larger than the actual price. The bias in our method seems to be extremely small. Also, we see that our method is extremely accurate, with a median $|\Delta\Pi/\Pi_{\text{Actual}}|$ of 3.8×10^{-6}. In terms of speed, Bachelier approximation and Kirk's approximation are the fastest while our method is not too far behind. In particular, we see that our method is capable of computing one million spread option prices within 10 seconds. The numerical integration methods are much slower, with computing times roughly two orders of magnitude larger than those of the analytical methods.

Figure 2.5.1 compares the accuracy of three important Greeks for both Kirk's approximation and ours, namely, the two deltas and the kappa. The Greeks for Kirk's approximation are obtained by differentiating Kirk's formula. The Greeks for our approximation are those in Proposition 2.4.4. The actual values for the Greeks are computed using numerical integration and Proposition 2.4.3. The parameter are chosen to be: $S_1 = 100$, $S_2 = 90$, $K = 25$, $r = 0.05$, and $T = 1$. The relative errors of the Greeks are plotted against σ_1 and σ_2, which are allowed to vary in the range $[0.1, 0.5]$. As we see, the Greeks computed from our method are much more accurate than those from Kirk's approximation. Other parameter combinations give qualitatively the same pictures.

Table 2.5.1: Performance Comparison of Various Methods in Computing Spread Option Prices

This exhibit reports the speed and accuracy of Bachelier approximation, Bachelier approximation with Gram-Charlier adjustment, Kirk's approximation, the approximation in this chapter and one-dimensional numerical integration. Total number of options is 123,783. NI stands for numerical integration.

	Methods					
	Ours	Bachelier	Gram-Charlier	Kirk	NI–10^{-6}	NI–10^{-8}
$\Delta\Pi/\Pi_{\text{Actual}}$						
max	0.027	2.558	0.411	0.460		
min	−0.030	−0.621	−1.000	−0.018		
mean	-5.1×10^{-5}	0.139	−0.337	0.007		
median	-1.3×10^{-7}	0.117	−0.209	9.1×10^{-4}		
std. deviation	7.6×10^{-4}	0.142	0.338	0.017		
$\lvert\Delta\Pi/\Pi_{\text{Actual}}\rvert$						
max	0.030	2.558	1.000	0.460		
min	$\sim 10^{-15}$	2.5×10^{-6}	1.0×10^{-7}	$\sim 10^{-15}$		
mean	1.7×10^{-4}	0.147	0.338	0.008		
median	3.8×10^{-6}	0.119	0.209	0.0015		
std. deviation	7.4×10^{-4}	0.133	0.337	0.016		
time (seconds)	1.02	0.22	1.12	0.25	363.57	891.60

2.6 Conclusion

In this chapter, we first obtain lower and upper bounds for digital spread options by analyzing the exercise boundary. We then develop a new closed-form approximation for pricing spread options. Numerical analysis demonstrates that our method is more accurate than existing analytical approximations. It is also extremely fast, capable of computing one million spread options within 10 seconds. Thus, our method enables the accurate pricing of a bulk volume of spread options with different specifications in real time which offers traders a potential edge in financial markets. The availability of a closed-form formula for

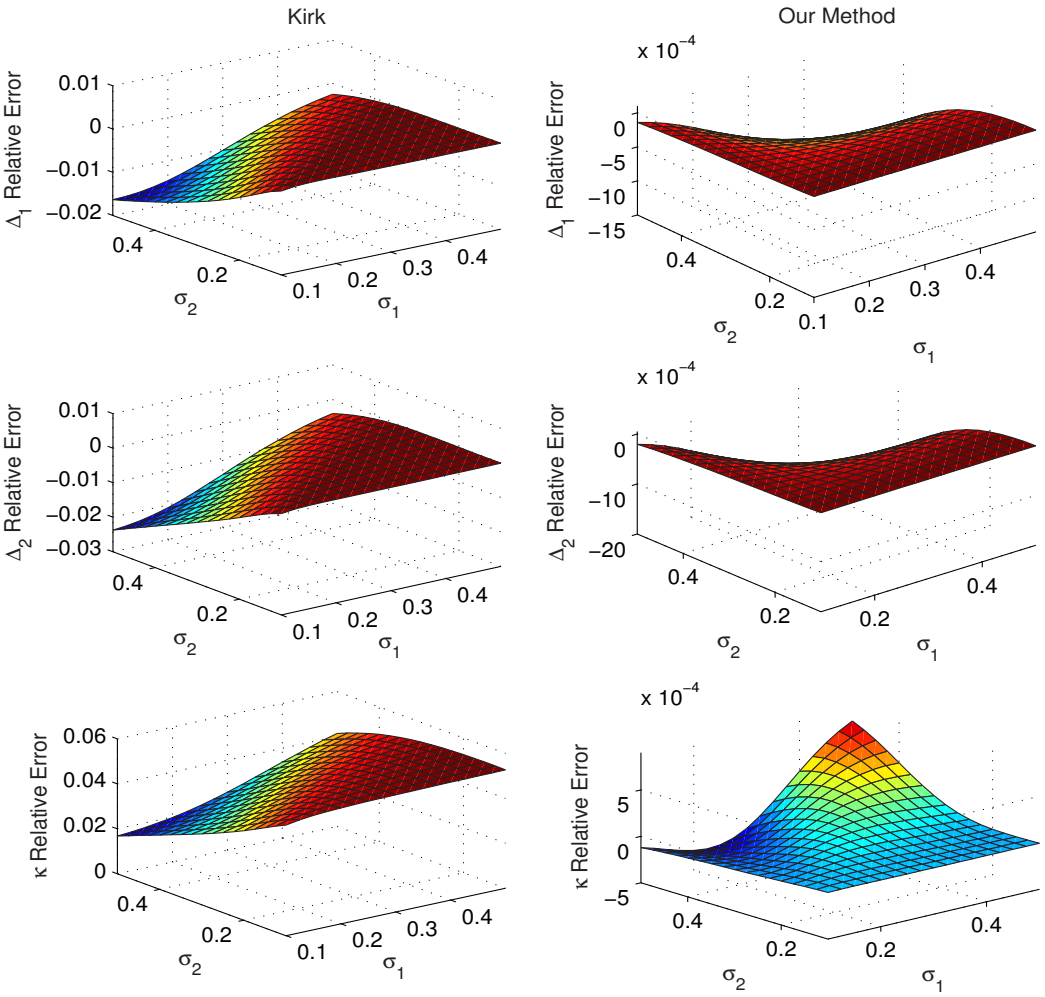

Figure 2.5.1: Accuracy comparison of Greeks in Kirk's approximation and ours.

spread options also helps us design and analyze real and financial contracts with embedded spread-option-like features.

We also derive closed-form approximations for the greeks of spread options. The closed-form approximations of greeks serve as valuable tools in financial applications. For instance, they can be used for calculating Value-at-Risk for a portfolio containing spread options. As byproducts, we analyze the price sensitivities of spread options. In particular, we point out the signs of vegas when the correlation is negative and when the correlation is positive and large. The analysis of the price sensitivities leads to improved understanding of

the price behavior of spread options and is useful in formulating effective dynamic-hedging strategies.

CHAPTER III

MULTI-ASSET SPREAD OPTIONS PRICING AND HEDGING

Results in Chapter 2 can be extended to spread options on a basket of risky assets. Spread options play an increasingly important role in hedging correlation risks among a set of assets of concern. In terms of the contract structure, the level of complexity rises constantly and the scope covers more and more asset classes. For instance, in the fixed income markets, instruments are traded on exchanging securities with different maturities (such as Treasury notes and bonds), with different quality levels (such as the Treasury bills and Eurodollars), and with different issuers (such as French and German bonds, or Municipal bonds and Treasury bonds). In the agricultural markets, the crush spread options traded on the Chicago Board of Trade (CBOT) exchanges raw soybeans with a combination of soybean oil and soybean meal (Johnson et al 1991). Asset pricing and risk management in energy markets embody a large variety of spread options. In the crude oil markets, crack spread options, which either exchange crude oil and unleaded gasoline or exchange crude oil and heating oil, are traded on the New York Mercantile Exchange (NYMEX). In the electricity markets, spark spread option and its variants designed for exchanging one or several types of fuel for electricity are commonly utilized in hedging both short-term and long-term cross-commodity risks. Moreover, there is a growing demand for pricing spread options involving 3, 4 and even more commodities in bulk quantity with contract parameters spanning a large range. Such scenarios arise from the application of valuing physical assets such as fossil fuel electric power plants, transmission assets (see Deng et al. 2001 and Routledge et al. 2001) and natural gas storage facilities. In valuing a fossil-fuel power plant, one could approximate the plant value by a portfolio of spread options with maturity spanning 15 to 20 years. At each time instant over the life span of the plant, owner of the

plant receives a payoff resembling that of a spread option paying off the positive part of electricity price less fuel price, emission permit prices, operating and maintenance costs. If considering the granularity in maturity to be as fine as one day, then the total number of spread option prices that need to be computed is between 5000 and 7500. Similarly, in valuing a natural gas storage facility, a portfolio consisting of hundreds to thousands of daily spread options on forward contracts of different terms with maturities spanning from one year to ten years, are commonly used for approximating the facility value. In these kinds of applications, numerical algorithms that are capable of pricing a large quantities of spread options on multiple assets with varying parameters fast and accurately, are in great demand. As for applications of spread options on multi-assets in the corporate finance arena, there have been proposals on using the spread between own firm's stock performance and an index level reflecting the average performance of a basket of peer firms as compensation for executives working in the own firm (see Johnson and Tian 2000).

While the spread options written on more than two underlyings are becoming more and more popular, it is very challenging to price such spread options efficiently and accurately since closed-form expressions are not available. A number of research works have studied the pricing of two-asset spread options, such as Jarrow and Rudd (1982), Wilcox (1990), Shimko (1994), Pearson (1995), Mbanefo (1997), Zhang (1997), and Carmona and Durrleman (2003). More recently, Deng, Li and Zhou (2006) provide a very accurate closed-form approximation formula for the efficient pricing of two-asset spread options. However, when the number of asset involved in the spread option is larger than two, not many approaches are available for computing the spread option price efficiently and accurately, even under the classical Black-Scholes framework. This is because when the dimension (the number of assets) is high, numerical approaches, such as numerical integration method, numerical solutions to partial differential equations and Monte Carlo simulation, become extremely slow and often inapplicable. A noticeable work that approximates the multi-asset spread option price is Carmona and Durrleman (2005). While Carmona and Durrleman's method

is quite accurate, it suffers from a somewhat major shortcoming. Carmona and Durrleman's method does not give the option price in closed form. To compute each option price, one would have to solve a high-dimensional system of nonlinear equations numerically, usually by using the Newton-Raphson's algorithm. However, our extensive experiments with these equations indicate that it takes considerable effort to solve them because the convergence of numerical algorithms depends very sensitively on the initial values, and a good understanding of how to choose the initial values is still lacking.

In this chapter, we directly approximate multi-asset spread option prices under the jointly normal return framework based on the approximation of the exercise boundary. There are several main contributions of this chapter. The most important contribution of this chapter is that we give two closed-form approximation methods. The first method is an extension of Kirk's approximation (1995) for two-asset spread options to the multi-asset case. As pointed out in Deng, Li and Zhou (2006), Kirk's method can be thought of as a linear approximation of the exercise boundary. Our numerical experiment shows that in most cases, the extended Kirk approximation is quite accurate. The main advantage of the extended Kirk approximation is that it is extremely fast and robust. The second method is an extension of Deng, Li and Zhou (2006)'s method of approximating the exercise boundary using a quadratic function. Using matrix algebra, we show that the computational cost of the second-order boundary approximation is very low. Compared with the method in Carmona and Durrleman (2005), both our methods are in closed-form and only involve arithmetic calculations, thus they are quite straightforward to implement. We also extend both our methods to price hybrid spread-basket options through a technique commonly used in valuing Asian options.

Second, we consider the Greeks of the multi-asset spread option. In practical applications such as dynamic hedging and Value-at-Risk calculations, the calculation of Greeks is very important. Because the second-order boundary approximation is more accurate than the extended Kirk approximation, we use the former to compute the Greeks. We give

closed-form approximations for the deltas and kappa of the multi-asset spread option in two important cases of our general framework, namely, the geometric Brownian motions case and the log-Ornstein-Uhlenbeck process case. Because the second-order boundary approximation is extremely fast and accurate, Greeks other than the deltas and kappa can be very efficiently computed using finite difference approximation.

Finally, we perform extensive numerical experiments to study the performance of our methods and other existing methods, including Monte Carlo simulation, Carmona and Durrleman's method and numerical integration. We first perform the comparisons with different number of assets in the spread option, namely, 3, 20, 50 and 150 assets. Numerical integration is only performed for the three-asset case because it quickly gets inapplicable when the dimension gets higher. All results indicate that our methods are extremely fast and accurate. Between our methods, the second-order boundary approximation is a little bit slower than the extended Kirk approximation but more accurate. In particular, for the second-order boundary approximation, it takes about 3×10^{-3} second to compute the price of a spread option written on 50 underlying assets. The relative pricing error of the second-order boundary approximation is usually in the order of 10^{-4}. For the three-asset case, because computation of the Greeks using numerical integration is still feasible, we also perform a comparison of the deltas and kappa between the extended Kirk approximation and the second-order boundary approximation. We find that for the purpose of calculating Greeks, it is preferable to use the latter method. Our last comparison uses two hypothetical spread options. The first one is between the S&P 500 index and the 30 component stocks of the Dow Jones Industrial Average (DJIA) index, while the second one is between the S&P SmallCap 600 index and the DJIA components. The purpose of this experiment is to examine the performance of our methods with more realistic parameters. Also, in practice, the spreads between large company stocks and the whole market and between large and small company stocks are closely watched by industry practitioners. The results again show that our methods are fast and most accurate.

The chapter is organized as follows. Section 3.1 discusses the general framework under which our spread option pricing results are derived, and then gives the spread option price in integration form. Section 3.2 develops two closed-form approximations for multi-asset spread option prices, namely, the extended Kirk approximation and the second-order boundary approximation. The implementation of the latter method is discussed in detail. We also study the Greeks of multi-asset spread options and extend both our methods to hybrid spread-basket options. Section 3.3 compares our methods with alternative numerical approaches and other approximations in terms of both speed and accuracy. Section 3.4 concludes. Proofs are given in the Appendix.

3.1 The model setup

Consider $N+1$ assets whose prices at time t are denoted by $S_0(t)$, $S_1(t), \cdots$, and $S_N(t)$. We are interested in spread options with time-T payoff $[S_0(T) - \sum_{k=1}^{N} S_k(T) - K]^+$, where the strike K is a pre-specified constant. We will first assume that $K \geq 0$. Negative K cases are treated later when we discuss hybrid basket-spread options. Assuming that the interest rate r is a constant, by the martingale pricing approach, the price of a spread option Π is given by

$$\Pi = e^{-rT}\mathbb{E}^{\mathbb{Q}}[S_0(T) - \sum_{k=1}^{N} S_k(T) - K]^+ \tag{3.1.1}$$

where $\mathbb{Q}$ is the risk-neutral measure under which discounted security prices are martingales. To compute these option prices, we assume that $\log S_0(T)$, $\log S_1(T)$, $\cdots$, and $\log S_N(T)$ are jointly normally distributed conditioning on the initial asset prices. Specifically, conditioning on $S_0(0) = s_0$, $S_1(0) = s_1, \cdots$, and $S_N(0) = s_N$, we assume

$$\mathbb{E}^{\mathbb{Q}}[\log S_k(T)] = \mu_k, \quad \text{Var}^{\mathbb{Q}}[\log S_k(T)] = \nu_k^2, \quad k = 0, 1, \cdots, N$$

where $\boldsymbol{\mu} \equiv \{\mu_k\}$ and $\boldsymbol{\nu} \equiv \{\nu_k\}$ are two deterministic vectors. Recasting in more familiar terms of asset returns $R_{k,T} \equiv \log(S_k(T)/s_k)$, we have

$$\mu_k = \log s_k + \mathbb{E}^{\mathbb{Q}}[R_{k,T}], \quad \text{and} \quad \nu_k^2 = \text{Var}^{\mathbb{Q}}[R_{k,T}], \quad k = 0, 1, \cdots, N. \tag{3.1.2}$$

Next, we define

$$X = \frac{\log S_0(T) - \mu_0}{\nu_0}, \quad Y_k = \frac{\log S_k(T) - \mu_k}{\nu_k}, \quad k = 1, 2, \cdots, N. \tag{3.1.3}$$

In our setup, we will assume that X and $Y_k's$ are jointly normally distributed with mean vector $\mathbf{0}$, variance vector $\mathbf{1}$, and the following $(N+1)\times(N+1)$ correlation matrix

$$\mathbf{\Sigma} = (\rho_{i,j}) = \begin{pmatrix} 1 & \mathbf{\Sigma_{10}}' \\ \mathbf{\Sigma_{10}} & \mathbf{\Sigma_{11}} \end{pmatrix},$$

where $\mathbf{\Sigma_{10}}$ is a $N\times 1$ column vector and $\mathbf{\Sigma_{11}}$ is the $N\times N$ correlation matrix of the Y_k's. We assume that the determinant of $\mathbf{\Sigma}$ is not zero. That is, the returns of the $N+1$ assets are not perfectly correlated.

This general setup incorporates two important cases, namely, the geometric Brownian motions (GBMs) case and the mean-reverting log-Ornstein-Uhlenbeck (log-OU) case. Geometric Brownian motions are frequently used to model stock prices while the log-OU processes are frequently used to model commodity prices. Specifically, let $W_k(t)$, $k = 0, 1, \cdots, N$, be Brownian motions with correlation matrix $\boldsymbol{\varrho} = (\varrho_{i,j})$. In the GBMs case, we have

$$\mathrm{d}S_k = (r - q_k)S_k\mathrm{d}t + \sigma_k S_k \mathrm{d}W_k, \tag{3.1.4}$$

where r is the risk-free interest rate, σ_k's are the volatilities, and q_k's are the dividend rates. A simple application of Ito's lemma yields

$$\mu_k = \log s_k + (r - q_k - \sigma_k^2/2)T, \quad \nu_k = \sigma_k\sqrt{T}, \quad \rho_{i,j} = \varrho_{i,j}, \tag{3.1.5}$$

The GBMs case can be easily generalized to incorporate seasonality in parameters by allowing σ_k's, q_k's and $\mathbf{\Sigma}$ to be deterministic functions of the calendar time t. This is useful since for some spread options, their underlying assets exhibit strong seasonality in price volatilities and in their return correlations. Our general framework incorporates this generalized GBMs case.

In the log-OU case, we have

$$\mathrm{d}S_k = -\lambda_k(\log S_k - \eta_k)S_k\mathrm{d}t + \sigma_k S_k \mathrm{d}W_k, \tag{3.1.6}$$

where λ_k's are the mean-reverting strength parameters and η_k's are parameters controlling the long-run means. The application of Ito's lemma now gives

$$\mu_k = \eta_k - \frac{\sigma_k^2}{2\lambda_k} + e^{-\lambda_k T}\Big(\log s_k - \eta_k + \frac{\sigma_k^2}{2\lambda_k}\Big), \quad \nu_k = \sigma_k\sqrt{\frac{1-e^{-2\lambda_k T}}{2\lambda_k}}, \tag{3.1.7}$$

$$\rho_{i,j} = 2\varrho_{i,j}\frac{\sqrt{\lambda_i\lambda_j}}{\lambda_i+\lambda_j}\frac{1-e^{-(\lambda_i+\lambda_j)T}}{\sqrt{1-e^{-2\lambda_i T}}\sqrt{1-e^{-2\lambda_j T}}}. \tag{3.1.8}$$

Again, with some modifications on the μ_k's, ν_k's and $\mathbf{\Sigma}$, our general framework can incorporate the log-OU case with time-varying parameters.

Before introducing our methods for computing the spread option price, we present an analysis of the exercise boundary. At time T, the spread option is in-the-money if $S_0(T) - \sum_{k=1}^N S_k(T) - K \geq 0$. If $K \geq 0$, this condition is the same as

$$X \geq \frac{\log(\sum_{k=1}^N e^{\nu_k Y_k + \mu_k} + K) - \mu_0}{\nu_0}.$$

Thus, conditioning on $Y_k = y_k$, the option is in-the-money if $X \geq \underline{x}(\mathbf{y})$, where

$$\underline{x}(\mathbf{y}) \equiv \frac{\log(\sum_{k=1}^N e^{\nu_k y_k + \mu_k} + K) - \mu_0}{\nu_0}. \tag{3.1.9}$$

Notice that since $K \geq 0$, equation (3.1.9) is always binding since the right hand side is a finite real number. Also notice that $\underline{x}(\mathbf{y})$ is a nonlinear function in the components of $\mathbf{y}$.

Throughout the chapter, we use $\phi(\mathbf{z}; \mathbf{m}, \mathbf{\Sigma})$ to stand for the multivariate normal density function with mean vector $\mathbf{m}$ and covariance matrix $\mathbf{\Sigma}$, and $\Phi(z)$ for the one-dimensional cumulative normal distribution function. If $\mathbf{m}$ and $\mathbf{\Sigma}$ are scalers with $\mathbf{m} = 0$, and $\mathbf{\Sigma} = 1$, we will simply write $\phi(z)$ for $\phi(z; 0, 1)$. Notice that the random variables X and Y in equation (3.1.3) are jointly normally distributed with density $\phi(\{x, \mathbf{y}\}; \mathbf{0}, \mathbf{\Sigma})$. By risk-neutral valuation, the computation of spread option price Π involves an $(N+1)-$dimensional integration as follows:

$$\Pi = \Pi(\boldsymbol{\mu}, \boldsymbol{\nu}, \mathbf{\Sigma}) = e^{-rT}\int_{\mathbb{R}^N}\int_{\mathbb{R}}\Big(e^{\nu_0 x + \mu_0} - \sum_{k=1}^N e^{\nu_k y_k + \mu_k} - K\Big)^+ \phi(\{x, \mathbf{y}\}; \mathbf{0}, \mathbf{\Sigma})\,\mathrm{d}x\mathrm{d}\mathbf{y}. \tag{3.1.10}$$

However, in the following proposition, we reduce the above integral to $N+2$ N-dimensional integrations based on a technique in Pearson (1995).

Proposition 3.1.1. *Under the jointly-normal returns setup with* $K \geq 0$ *and* $\det \mathbf{\Sigma} \neq 0$*, the price of the spread option can be written as*

$$\Pi = e^{-rT+\mu_0+\frac{1}{2}\nu_0^2}\, \mathbf{I}_0 - \sum_{k=1}^{N} e^{-rT+\mu_k+\frac{1}{2}\nu_k^2}\, \mathbf{I}_k - Ke^{-rT}\, \mathbf{I}_{N+1}. \tag{3.1.11}$$

The integrals $\mathbf{I}_i$*'s are given by*

$$\mathbf{I}_0 = \int_{\mathbb{R}^N} \phi(\mathbf{y}; \mathbf{0}, \mathbf{\Sigma_{11}})\, \Phi\Big(A(\mathbf{y} + \nu_0 \mathbf{\Sigma_{10}}) + \nu_0 \sqrt{\Sigma_{x|\mathbf{y}}}\Big)\, \mathrm{d}\mathbf{y}, \tag{3.1.12}$$

$$\mathbf{I}_k = \int_{\mathbb{R}^N} \phi(\mathbf{y}; \mathbf{0}, \mathbf{\Sigma_{11}})\, \Phi\Big(A(\mathbf{y} + \nu_k \mathbf{\Sigma_{11}} \mathbf{e_k})\Big)\, \mathrm{d}\mathbf{y}, \quad k = 1, 2, \cdots, N \tag{3.1.13}$$

$$\mathbf{I}_{N+1} = \int_{\mathbb{R}^N} \phi(\mathbf{y}; \mathbf{0}, \mathbf{\Sigma_{11}})\, \Phi(A(\mathbf{y}))\, \mathrm{d}\mathbf{y}, \tag{3.1.14}$$

where $\mathbf{e_k}$ *is the unit column vector* $(0, \cdots, 0, 1, 0, \cdots, 0)'$ *with* 1 *at the k-th position, and*

$$A(\mathbf{y}) = \frac{\mu_{x|\mathbf{y}} - \underline{x}(\mathbf{y})}{\sqrt{\Sigma_{x|\mathbf{y}}}}, \tag{3.1.15}$$

with

$$\mu_{x|\mathbf{y}} = \mathbf{\Sigma_{10}}' \mathbf{\Sigma_{11}^{-1}} \mathbf{y}, \quad \Sigma_{x|\mathbf{y}} = 1 - \mathbf{\Sigma_{10}}' \mathbf{\Sigma_{11}^{-1}} \mathbf{\Sigma_{10}}. \tag{3.1.16}$$

Notice that when $\det \mathbf{\Sigma} \neq 0$, we have $\Sigma_{x|\mathbf{y}} \neq 0$ and $\det \mathbf{\Sigma}_{11} \neq 0$, so $A(\mathbf{y})$ is always well-defined. Also, notice that in the geometric Brownian motions case, the price Π reduces to the more familiar form

$$\Pi = s_0 e^{-q_0 T}\, \mathbf{I}_0 - \sum_{k=1}^{N} s_k e^{-q_k T}\, \mathbf{I}_k - Ke^{-rT}\, \mathbf{I}_{N+1}.$$

Proposition 3.1.1 gives a formula for the spread option price which resembles the Black-Scholes formula (Black and Scholes 1973). In particular, the price of the spread option Π in equation (3.1.11) consists of three terms. The first term is the present value of the risk-neutral expected future benefit of receiving asset S_0. The second term is the present value of expected future cost of giving up assets S_k, where $k = 1, \cdots, N$. The last term is the

present value of the expected cost of giving up an additional monetary amount K. The quantities $A(\mathbf{y})$ and $\mathbf{I}_i$'s also have intuitive meanings. The quantity $A(\mathbf{y})$ is the **conditional moneyness** of the spread option because $A(\mathbf{y})$ plays a similar role as d_2 in the Black-Scholes formula. This can be seen from the proof of Proposition 3.1.1 that the quantity $\Phi(A(\mathbf{y}))$ is the risk-neutral probability that the spread option expires in the money conditioning on that the vector of standardized log prices of assets $\{S_k\}$ is $\mathbf{y}$. Written out explicitly, we have

$$\Phi(A(\mathbf{y})) = \text{Prob}^{\mathbb{Q}}\left[S_0(T) \geq \sum_{k=1}^{N} S_k(T) + K \;\middle|\; Y_k \equiv \frac{\log S_k(T) - \mu_k}{\nu_k} = y_k,\ k = 1, \cdots, N\right]. \tag{3.1.17}$$

Similar to the Black-Scholes formula, the quantity $\mathbf{I}_{N+1}$ is the unconditional probability that the spread option will expire in the money under the risk-neutral distribution. The proof of Proposition 3.1.1 shows that $\mathbf{I}_0$ and $\mathbf{I}_k$ have similar meanings as $\mathbf{I}_{N+1}$. They are the probabilities that the spread option will expire in the money under the measures in which asset S_0 and S_k are taken to be the numeraire asset, respectively. This is similar to the case of the Black-Scholes formula, where the term $\Phi(d_1)$ is the probability that the option will expire in the money under the probability measure in which the underlying stock is taken as the numeraire asset.

Proposition 3.1.1 highlights the importance of the exercise boundary and is the starting point of our approximation. Our goal now is to approximate $A(\mathbf{y})$ so that the $\mathbf{I}_k$'s can be performed in closed form. In the next section, we give two closed-form approximations for computing the spread option price Π.

3.2 Closed-form approximations

3.2.1 Extended Kirk approximation

Kirk (1995) gives a fairly accurate closed-form approximation for two-asset spread option prices. Li, Deng, and Zhou (2008) compare its performance with other methods and point out that Kirk's formula can be obtained by a linear approximation of the exercise boundary. In this subsection, we extend Kirk's approximation to a multi-asset setting. Our idea is to

first approximate $\sum_{k=1}^{N} S_k(T)$ as a lognormal random variable and then apply Kirk's approximation for two-asset spread options. This can be achieved by approximating $\sum_{k=1}^{N} S_k(T)/N$ by the corresponding geometric average $\big(\prod_{k=1}^{N} S_k(T)\big)^{1/N}$, a technique commonly used in pricing Asian options. The result is the following

Proposition 3.2.1. *Under the general jointly-normal returns setup, the multi-asset spread option price can be approximated as*

$$\Pi \approx e^{-rT+\mu_0+\frac{1}{2}\nu_0^2}\Phi\Big(d_K+\frac{\nu_K}{2}\Big)-\Big(\sum_{k=1}^{N} e^{-rT+\mu_k+\frac{1}{2}\nu_k^2}+Ke^{-rT}\Big)\Phi\Big(d_K-\frac{\nu_K}{2}\Big), \tag{3.2.1}$$

where

$$\nu_K=\sqrt{\nu_0^2-2\rho_a\nu_0\nu_a m+\nu_a^2 m^2}, \quad d_K=\frac{\log m_0}{\nu_K},$$

with

$$m_0=\frac{e^{\mu_0+\frac{1}{2}\nu_0^2}}{\sum_{k=1}^{N} e^{\mu_k+\frac{1}{2}\nu_k^2}+K}, \quad m=\frac{\sum_{k=1}^{N} e^{\mu_k+\frac{1}{2}\nu_k^2}}{\sum_{k=1}^{N} e^{\mu_k+\frac{1}{2}\nu_k^2}+K},$$
$$\nu_a=\frac{1}{N}\sqrt{\sum_{i=1}^{N}\sum_{j=1}^{N}\rho_{i,j}\nu_i\nu_j}, \quad \rho_a=\frac{1}{N\nu_a}\Big(\sum_{k=1}^{N}\rho_{0,k}\nu_k\Big).$$

Notice that the above proposition works for all models in our general jointly normal returns setup, in particular, for the GBMs and the log-OU case. In the GBMs case, equation (3.2.1) becomes

$$\Pi \approx s_0 e^{-q_0 T}\Phi\Big(d_K+\frac{\nu_K}{2}\Big)-\Big(\sum_{k=1}^{N} s_k e^{-q_k T}+Ke^{-rT}\Big)\Phi\Big(d_K-\frac{\nu_K}{2}\Big), \tag{3.2.2}$$

and resembles the Black-Scholes formula or more closely, the Margrabe formula (Margrabe 1978). The extended Kirk approximation is extremely easy to implement and extremely fast. Another advantage of the above approximation is that it also works when $\det \mathbf{\Sigma}$ is very close to 0.

Numerical experiments show that the extended Kirk approximation is most accurate when the $S_k(T)$'s $(k=1,\cdots,N)$ are more symmetric. That is, the $\rho_{i,j}$'s are about the same,

initial asset prices s_i's are about the same, and μ_i's and ν_i's are about the same. The reason is that in this case, the geometric average of the $S_k(T)$ is closer to the arithmetic average. We also conduct an experiment where the $S_k(T)$'s $(k = 1, \cdots, N)$ are not very symmetric using a hypothetical spread option between the S&P 500 Index and the 30 component stocks of the Dow Jones Industrial Average Index. We see that when the assets are not very symmetric, the extended Kirk approximation is not as accurate as the second-order boundary approximation which we are introducing below. Also, by the nature of its design, the extended Kirk approximation does not give as accurate Greeks as the second-order boundary approximation does.

3.2.2 Second-order boundary approximation

As Li, Deng, and Zhou (2008) point out, one will obtain Kirk's approximation if one uses linear approximations to approximate the conditional moneyness function $A(\mathbf{y})$. Li, Deng, and Zhou (2008) derive an approximation for two-asset spread options based on a second-order approximation of the exercise boundary. They also show that when the curvature of the exercise boundary is not large, the second-order boundary approximation is extremely efficient and more accurate than existing methods such as Kirk's approximation. It turns out that their method could be generalized to arbitrary number of assets. Below we give the generalized results for multi-asset spread options.

Two observations of Proposition 3.1.1 are very useful. First, the integrals $\mathbf{I}_i$'s all involve $\phi(\mathbf{y}; \mathbf{0}, \mathbf{\Sigma_{11}})$ which is quite peaked around $\mathbf{y} = 0$. Second, around $\mathbf{y} = 0$, the exercise boundary $\underline{x}(\mathbf{y})$ is quite close to being linear in $\mathbf{y}$. Hence the same is true for the function $A(\mathbf{y})$. Figure 3.2.1 confirms this by giving a sample plot of $A(\mathbf{y})$ when $N = 2$. The parameters used are the same ones we use later for numerical comparisons in the three-asset case, and we fix $K = 30$ with $\sigma_i = 0.3$ for all three assets.

We now derive the approximations for the exercise boundary $\underline{x}(\mathbf{y})$ of the spread option and the function $A(\mathbf{y})$ to second order in $\mathbf{y}$ around $\mathbf{y} = \mathbf{0}$ as follows:

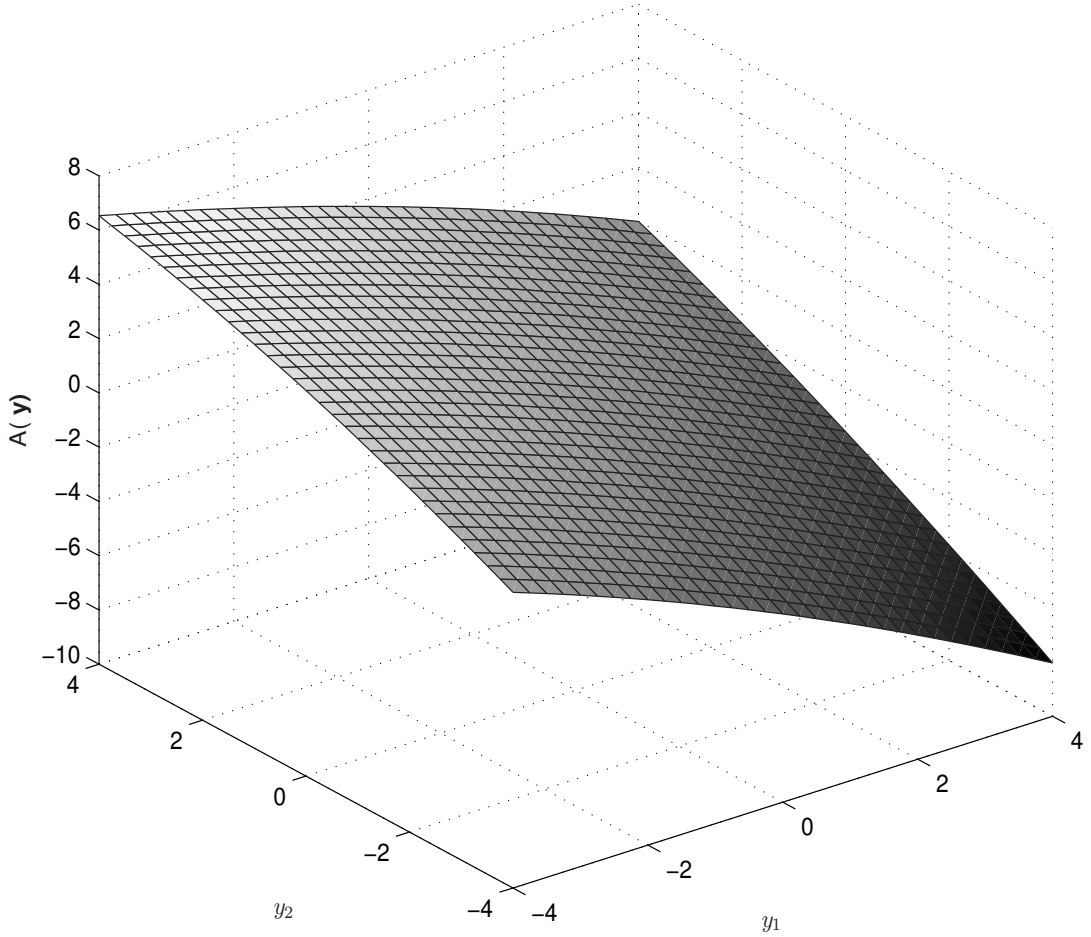

Figure 3.2.1: The function $A(\mathbf{y})$ near $\mathbf{y} = \mathbf{0}$. Notice that $A(\mathbf{y})$ is approximately linear in $\mathbf{y}$ around $\mathbf{y} = \mathbf{0}$, with some modest curvature.

Proposition 3.2.2. *The exercise boundary* $\underline{x}(\mathbf{y})$ *can be approximated to second order in* $\mathbf{y}$ *as*

$$\underline{x}(\mathbf{y}) \approx \underline{x}(\mathbf{0}) + \nabla \underline{x}|_{\mathbf{0}}' \, \mathbf{y} + \frac{1}{2} \mathbf{y}' \nabla^2 \underline{x}|_{\mathbf{0}} \, \mathbf{y},$$

where

$$\underline{x}(\mathbf{0}) = \frac{\log(R+K)-\mu_0}{\nu_0},$$
$$(\nabla \underline{x}|_{\mathbf{0}})_k = \frac{e^{\mu_k}\nu_k}{\nu_0(R+K)}, \quad k = 1, 2, \cdots, N,$$
$$(\nabla^2 \underline{x}|_{\mathbf{0}})_{i,j} = -\frac{\nu_i \nu_j e^{\mu_i+\mu_j}}{\nu_0(R+K)^2} + \delta_{i,j}\frac{\nu_j^2 e^{\mu_j}}{\nu_0(R+K)}, \quad i, j = 1, 2, \cdots$$

with $\delta_{i,j}$ *being the Kronecker delta function, and*

$$R = \sum_{k=1}^{N} e^{\mu_k}.$$

Accordingly, the function $A(\mathbf{y})$ *can be approximated as*

$$A(\mathbf{y}) = \frac{\mu_{x|\mathbf{y}} - \underline{x}(\mathbf{y})}{\sqrt{\Sigma_{x|\mathbf{y}}}} \approx c + \mathbf{d}'\mathbf{y} + \mathbf{y}'\mathbf{E}\mathbf{y},$$

where

$$c = -\frac{\log(R+K)-\mu_0}{\nu_0\sqrt{\Sigma_{x|\mathbf{y}}}}, \tag{3.2.3}$$
$$\mathbf{d} = \frac{1}{\sqrt{\Sigma_{x|\mathbf{y}}}}(\mathbf{\Sigma}_{11}^{-1}\mathbf{\Sigma}_{\mathbf{10}} - \nabla \underline{x}|_{\mathbf{0}}), \tag{3.2.4}$$
$$\mathbf{E} = -\frac{1}{2\sqrt{\Sigma_{x|\mathbf{y}}}}(\nabla^2 \underline{x}|_{\mathbf{0}}). \tag{3.2.5}$$

Our goal is to use an approximation of $A(\mathbf{y})$ in Proposition 3.1.1 so that we can perform the integrals $\mathbf{I}_k$'s. For this purpose, we further expand $\Phi(c + \mathbf{d}'\mathbf{y} + \mathbf{y}'\mathbf{E}\mathbf{y})$ into three terms to second order in $\mathbf{y}'\mathbf{E}\mathbf{y}$ around $\mathbf{y}'\mathbf{E}\mathbf{y} = \epsilon$, for some suitably chosen ϵ. Intuitively, we should choose ϵ to be the unconditional mean of $Y'\mathbf{E}Y$, which is given by the trace of the matrix $\mathbf{F}$ below. With the help of an identity in Li (2008), we are now able to perform the integration and obtain a closed-form approximation for the spread option price as presented in Proposition 3.2.3. Proposition 3.2.3 is one of the most important results of this chapter.

Proposition 3.2.3. *Let* $K \geq 0$ *and* $\det \mathbf{\Sigma} \neq 0$. *The spread option price* Π *under the general jointly-normal returns setup is given by*

$$\Pi = e^{-rT+\mu_0+\frac{1}{2}\nu_0^2}\,\mathbf{I}_0 - \sum_{k=1}^{N} e^{-rT+\mu_k+\frac{1}{2}\nu_k^2}\,\mathbf{I}_k - Ke^{-rT}\,\mathbf{I}_{N+1}. \tag{3.2.6}$$

The integrals $\mathbf{I}_i$*'s are approximated as*

$$\mathbf{I}_i \approx \mathbf{J}^0(c_i, \mathbf{d_i}) + \mathbf{J}^1(c_i, \mathbf{d_i}) - \frac{1}{2}\mathbf{J}^2(c_i, \mathbf{d_i}), \quad i = 0, 1, \cdots, N+1 \tag{3.2.7}$$

where the scaler function $\mathbf{J}^i$*'s are defined as*

$$\mathbf{J}^0(u, \mathbf{v}) = \Phi\left(\frac{u}{\sqrt{1+\mathbf{v}'\mathbf{v}}}\right), \tag{3.2.8}$$

$$\mathbf{J}^1(u, \mathbf{v}) = \frac{\lambda}{\sqrt{1+\mathbf{v}'\mathbf{v}}} \cdot \phi\left(\frac{u}{\sqrt{1+\mathbf{v}'\mathbf{v}}}\right), \tag{3.2.9}$$

$$\mathbf{J}^2(u, \mathbf{v}) = \frac{u}{(1+\mathbf{v}'\mathbf{v})^{3/2}} \cdot \phi\left(\frac{u}{\sqrt{1+\mathbf{v}'\mathbf{v}}}\right) \tag{3.2.10}$$

$$\left\{\lambda^2 + 2tr[(\mathbf{PFP})^2] - 4\lambda(1+\mathbf{v}'\mathbf{v})(\mathbf{v}'\mathbf{P}^2\mathbf{F}\mathbf{P}^2\mathbf{v}) + (4u^2 - 8 - 8\mathbf{v}'\mathbf{v})\|\mathbf{PFP}^2\mathbf{v}\|^2\right\},$$

with

$$\mathbf{P} = \mathbf{P}(\mathbf{v}) \equiv (\mathbf{I} + \mathbf{v}\mathbf{v}')^{-1/2}, \tag{3.2.11}$$

$$\lambda = \lambda(u, \mathbf{v}) \equiv u^2\mathbf{v}'\mathbf{P}^2\mathbf{F}\mathbf{P}^2\mathbf{v} + tr(\mathbf{PFP}) - tr(\mathbf{F}), \tag{3.2.12}$$

where tr stands for the trace operator of a matrix. The scalers c_i*, vectors* $\mathbf{d_i}$*,and matrix* $\mathbf{F}$ *are given by*

$$c_0 = c + tr(\mathbf{F}) + \nu_0\sqrt{\Sigma_{x|\mathbf{y}}} + \nu_0\boldsymbol{\Sigma_{10}}'\mathbf{d} + \nu_0^2\boldsymbol{\Sigma_{10}}'\mathbf{E}\boldsymbol{\Sigma_{10}}, \tag{3.2.13}$$

$$\mathbf{d_0} = \boldsymbol{\Sigma}_{\mathbf{11}}^{\frac{1}{2}}(\mathbf{d} + 2\nu_0\mathbf{E}\boldsymbol{\Sigma_{10}}), \tag{3.2.14}$$

$$c_k = c + tr(\mathbf{F}) + \nu_k\mathbf{e_k}'\boldsymbol{\Sigma_{11}}\mathbf{d} + \nu_k^2\mathbf{e_k}'\boldsymbol{\Sigma_{11}}\mathbf{E}\boldsymbol{\Sigma_{11}}\mathbf{e_k}, \quad k = 1, 2, \cdots, N \tag{3.2.15}$$

$$\mathbf{d_k} = \boldsymbol{\Sigma}_{\mathbf{11}}^{\frac{1}{2}}(\mathbf{d} + 2\nu_k\mathbf{E}\boldsymbol{\Sigma_{11}}\mathbf{e_k}), \quad k = 1, 2, \cdots, N \tag{3.2.16}$$

$$c_{N+1} = c + tr(\mathbf{F}), \tag{3.2.17}$$

$$\mathbf{d_{N+1}} = \boldsymbol{\Sigma}_{\mathbf{11}}^{\frac{1}{2}}\mathbf{d}, \tag{3.2.18}$$

$$\mathbf{F} = \boldsymbol{\Sigma}_{\mathbf{11}}^{\frac{1}{2}}\mathbf{E}\boldsymbol{\Sigma}_{\mathbf{11}}^{\frac{1}{2}}, \tag{3.2.19}$$

with $\Sigma_{x|\mathbf{y}}$ *given in Proposition 3.1.1 and* $c, \mathbf{d}, \mathbf{E}$ *given in Proposition 3.2.2.*

Notice that we have used boldface subscript $\boldsymbol{i}$ in $\mathbf{d_i}$ to denote the i-th vector in order to avoid confusion with the i-th component $\mathbf{d}_i$ of the vector $\mathbf{d}$. That is, each $\mathbf{d_i}$ is a vector, and

we have $N+2$ of them, for $i = 0, 1, \cdots, N+1$. As we see, the calculation of the spread option price is quite straightforward in the second-order boundary approximation. If one is not too concerned with accuracy, he could omit the $\mathbf{J}^2$'s in the approximation, which we call the first-order boundary approximation.

A naive look at Proposition 3.2.3 might imply that we need to perform a lot of costly matrix multiplications. However, Proposition 3.2.4 below shows that we only need to perform a very limited number of matrix multiplications. The critical observation in obtaining Proposition 3.2.4 is that $\mathbf{v}$ is an eigenvector of $\mathbf{P}(\mathbf{v})$ defined in equation (3.2.11).

Proposition 3.2.4. *With* $\mathbf{P} = \mathbf{P}(\mathbf{v})$ *as defined in equation* (3.2.11)*, we have*

$$\mathbf{P} = \mathbf{I} - \theta\mathbf{v}\mathbf{v}', \quad \mathbf{P}^2 = \mathbf{I} - \psi\mathbf{v}\mathbf{v}',$$

where the scalars θ *and* ψ *are given by*

$$\theta = \theta(\mathbf{v}) = \frac{\sqrt{1+\mathbf{v}'\mathbf{v}}-1}{\mathbf{v}'\mathbf{v}\sqrt{1+\mathbf{v}'\mathbf{v}}}, \quad \psi = \psi(\mathbf{v}) = \frac{1}{1+\mathbf{v}'\mathbf{v}}. \tag{3.2.20}$$

Furthermore, we have

$$tr[(\mathbf{PFP})^2] = tr(\mathbf{F}^2) - \psi(1+\psi)\mathbf{v}'\mathbf{F}^2\mathbf{v}, \tag{3.2.21}$$

$$\mathbf{v}'\mathbf{P}^2\mathbf{F}\mathbf{P}^2\mathbf{v} = \psi^2\mathbf{v}'\mathbf{F}\mathbf{v}, \tag{3.2.22}$$

$$\|\mathbf{PFP}^2\mathbf{v}\|^2 = \psi^2[\mathbf{v}'\mathbf{F}^2\mathbf{v} - \psi(\mathbf{v}'\mathbf{F}\mathbf{v})^2], \tag{3.2.23}$$

$$tr(\mathbf{PFP}) = tr(\mathbf{F}) - \psi\mathbf{v}'\mathbf{F}\mathbf{v}. \tag{3.2.24}$$

Thus the scaler function $\mathbf{J}^i$*'s given in (3.2.8) can be simplified as*

$$\mathbf{J}^0(u,\mathbf{v}) = \Phi\left(u\sqrt{\psi}\right), \tag{3.2.25}$$

$$\mathbf{J}^1(u,\mathbf{v}) = \psi^{\frac{3}{2}}(\psi u^2 - 1)\mathbf{v}'\mathbf{F}\mathbf{v}\cdot\phi\left(u\sqrt{\psi}\right), \tag{3.2.26}$$

$$\begin{aligned}\mathbf{J}^2(u,\mathbf{v}) = u\psi^{\frac{3}{2}}\cdot\phi\left(u\sqrt{\psi}\right)\Big\{&2tr(\mathbf{F}^2) - 4(1-tr(\mathbf{F}))(\psi-\psi^2)\mathbf{v}'\mathbf{F}\mathbf{v} \\ &+ \psi^2(9+(2-3u^2)\psi - u^2(4-u^2)\psi^2)(\mathbf{v}'\mathbf{F}\mathbf{v})^2 - 2\psi(5+(1-2u^2)\psi)\mathbf{v}'\mathbf{F}^2\mathbf{v}\Big\}.\end{aligned} \tag{3.2.27}$$

Proposition 3.2.4 is very useful in the actual implementation of the second-order boundary approximation because it reduces the calculation of the four computationally costly terms in Proposition 3.2.3, $tr[(\mathbf{PFP})^2]$, $\mathbf{v}'\mathbf{P}^2\mathbf{F}\mathbf{P}^2\mathbf{v}$, $||\mathbf{PFP}^2\mathbf{v}||^2$ and $tr(\mathbf{PFP})$, to four much simpler expressions, namely, $tr(\mathbf{F})$, $tr(\mathbf{F}^2)$, $\mathbf{v}'\mathbf{F}\mathbf{v}$, and $\mathbf{v}'\mathbf{F}^2\mathbf{v}$. Our numerical analysis shows that Proposition 3.2.4 reduces the computational time of the second-order boundary approximation as presented in Proposition 3.2.3 by about several hundred times for relatively large N. The larger the N, the more important it is to use Proposition 3.2.4. When $N = 1$ so that we are dealing with two-asset spread options, $\mathbf{v}$'s are all scalers and so are $\mathbf{P}$ and $\mathbf{F}$. In this case, we could use either Proposition 3.2.3 or Proposition 3.2.4.

It is worthwhile emphasizing that in addition to being applicable to spread options with arbitrary number of assets, the second-order boundary approximation above in this chapter is also more accurate than the one in Li, Deng, and Zhou (2008) when specialized to the case of two-asset spread options. The mathematical reason is that in developing Proposition 3.2.3, we have changed the expansion point for the second-order boundary approximation. For two-asset spread options, $\mathbf{E}$ (denoted as ϵ in Li, Deng, and Zhou 2008) and y are both scalars. In Li, Deng, and Zhou (2008), the expansion point is chosen to be $\epsilon y^2 = 0$, while in this chapter we have chosen the expansion point to be $\epsilon y^2 = \epsilon$. Intuitively, the new expansion point works much better because the mean of y^2 is 1, so we are expanding around the mean. Later we will compare the performance of the second-order boundary approximation with other existing methods.

Proposition 3.2.3 gives an approximation for the multi-asset spread option price but does not provide an error estimate. There are a few approaches to deal with the error estimate. First, Li, Deng, and Zhou (2008) provide lower and upper bounds for the digital spread options in the two-asset spread option case. Although the algebra would be much more complicated, it is possible to generalize these bounds to the multi-asset spread option case. Second, as long as the nonlinearity in $A(\mathbf{y})$ is relatively mild, the approximation method in this chapter is convergent in that if we keep more and more higher-order terms,

then the approximating option prices will approach the true price (see the remarks in the proof of Proposition 3.2.3). In this chapter, we have only kept the lowest two orders. It is possible to get an estimate (or lower and upper bounds) for the third-order term, which takes into account the higher-order nonlinearity in the conditional moneyness $A(\mathbf{y})$. Third, as we will see in our numerical analysis, the second-order approximation is extremely accurate when compared to Monte Carlo estimates of the true prices. The absolute difference between the Monte Carlo price and the second-order boundary approximation when added to the standard error of the Monte Carlo approximation could be used as an estimate for the approximation error of the second-order boundary approximation. Finally, as an operationally extremely simple but relatively conservative method, we could simply use the difference between the first-order and second-order boundary approximations as the error bound for the second-order boundary approximation.

In the next subsection, we consider the Greeks of the spread options.

3.2.3 Spread option Greeks and their approximation

Proposition 3.2.1 and Proposition 3.2.3 give approximations for multi-asset spread options prices. Below we derive approximations for the important Greeks in our setup. Fast and accurate calculation of these Greeks is very important because the Greeks are very useful in hedging, portfolio rebalancing, risk assessment such as VaR calculations, among other things. There are many approaches to calculating the Greeks, including finite difference method using Monte Carlo, numerical integration, and more recently, Malliavin calculus. For multi-asset spread options, especially when the number of assets is large, numerical methods often prove to be extremely slow to be applicable in practice. Thus a closed-form approximation is extremely useful. We use the second-order boundary approximation in the computation of the Greeks because although the extended Kirk approximation is fairly accurate for the prices, it does not give as accurate Greeks as the second-order boundary approximation does.

We will focus on the most important Greeks, the deltas and kappa. Because the second-order boundary approximation is extremely fast and accurate, Greeks other than the deltas and kappa can be very efficiently computed using finite difference method.

To compute the deltas and kappa, we need to know the dependence of μ_k's and ν_k's on the initial asset prices s_k's and the strike price K. We will assume that for each k, μ_k is a function of s_k while ν_k is independent of s_k. This is not very restrictive because both the two important special cases of our general setup, namely, the GBMs case and the log-OU case, satisfy this requirement.

Now let us define the price vector

$$\mathbf{S} = (e^{-rT+\mu_0+\frac{1}{2}\nu_0^2}, -e^{-rT+\mu_1+\frac{1}{2}\nu_1^2}, \cdots, -e^{-rT+\mu_N+\frac{1}{2}\nu_N^2}, -Ke^{-rT})'.$$

Be careful with the minus signs in the above definition. This definition allows us to write the spread option price formally as $\Pi = \mathbf{S}'\mathbf{I}$. Notice that in the GBMs case, equation (3.1.5) holds so

$$\mathbf{S} = (s_0 e^{-q_0 T}, -s_1 e^{-q_1 T}, \cdots, -s_N e^{-q_N T}, -Ke^{-rT}). \tag{3.2.28}$$

In the log-OU case, equation (3.1.7) gives us that for $k = 0, 1, \cdots, N$,

$$\mathbf{S}_k = (1_{k=0} - 1_{k>0}) \exp\Big(- rT + \eta_k(1 - e^{-\lambda_k T}) + e^{-\lambda_k T} \log s_k - \frac{\sigma_k^2}{4\lambda_k}(1 - e^{-\lambda_k T})^2\Big). \tag{3.2.29}$$

From Proposition 3.1.1 and 3.2.3 , we have the following result for the deltas and kappa.

Proposition 3.2.5. *Let $K \geq 0$. Suppose that in the general jointly normal returns setup, μ_k is only a function of s_k while ν_k is independent of s_k for each $k = 1, \cdots, N$. Then*

$$\Delta_0 \equiv \frac{\partial \Pi}{\partial s_0} = \frac{\partial \mu_0}{\partial s_0}\mathbf{S}_0\mathbf{I}_0, \tag{3.2.30}$$

$$\Delta_k \equiv \frac{\partial \Pi}{\partial s_k} = -\frac{\partial \mu_k}{\partial s_k}|\mathbf{S}_k|\mathbf{I}_k, \quad k = 1, 2, \cdots, N \tag{3.2.31}$$

$$\kappa \equiv \frac{\partial \Pi}{\partial K} = -e^{-rT}\mathbf{I}_{N+1}. \tag{3.2.32}$$

In particular, in the geometric Brownian motions case, we have

$$\Delta_0 = e^{-q_0 T}\mathbf{I}_0, \quad \Delta_k = -e^{-q_k T}\mathbf{I}_k, \quad k = 1, 2, \cdots, N.$$

In the log-Ornstein-Uhlenbeck case, with $\mathbf{S}_k$*'s given in equation* (3.2.29)*, we have*

$$\Delta_0 = \frac{e^{-\lambda_0 T}}{s_0}\mathbf{S}_0\mathbf{I}_0, \quad \Delta_k = -\frac{e^{-\lambda_k T}}{s_k}|\mathbf{S}_k|\mathbf{I}_k, \quad k = 1, 2, \cdots, N.$$

The vector $\mathbf{I} = \{\mathbf{I}_k\}$ *can then be approximated by Proposition 3.2.3.*

Proposition 3.2.5 shows that Proposition 3.2.3 is not only useful for computing spread option prices, but also useful for computing the deltas and kappa of the spread option. In particular, if Proposition 3.2.3 is implemented with the vectorization technique, then the computation of the vector $\mathbf{I}$ simultaneously gives us all the deltas and kappa. This is not the case if one uses Monte Carlo simulation to compute the prices and then uses finite difference to approximate the Greeks.

3.2.4 Extension to hybrid spread-basket option prices

We now extend both the extended Kirk approximation and the second-order boundary approximation to a generic hybrid spread-basket option with time-T payoff

$$\Big[\sum_{i=1}^{M} w_i S_i(T) - \sum_{j=M+1}^{M+N} w_j S_j(T) - K\Big]^+,$$

where K, w_i's are positive constants. Again, we assume that conditioning on the initial asset prices, $\log S_i(T)$ are jointly normally distributed with mean μ_i, variance ν_i^2, and correlation matrix $(\rho_{i,j})$ for $i, j = 1, 2, \cdots, M+N$. Without loss of generality, we will assume that all w_i equal 1 as the weights w_i can be easily absorbed by defining $\widetilde{S}_i = w_i S_i$ and noticing that $\widetilde{\mu}_i = \log w_i + \mu_i$, $\widetilde{\nu}_i = \nu_i$ and $\widetilde{\rho}_{i,j} = \rho_{i,j}$. In addition, we allow one of S_i ($i = 1, \cdots, M$) to be a constant, thus effectively allowing K to be negative. Except for the possibility of a constant S_i for some i, we assume the correlation matrix of $\log S_i$'s is positive definite.

To compute the price of this hybrid spread-basket option, we again utilize the well-known technique in pricing Asian options. Specifically, let

$$H_0(t) \equiv \sum_{i=1}^{M} S_i(t), \quad \text{and} \quad H_k(t) \equiv S_{k+M}(t) \quad k = 1, 2, \cdots, N.$$

Notice that the final payoff of the hybrid option now formally reduces to that of a standard spread option

$$\Big[H_0(T) - \sum_{k=1}^{N} H_k(T) - K\Big]^+.$$

However, the H_i's are no longer jointly normally distributed, nor is $H_0(T)$ normally distributed. The idea is to approximate the distribution of $H_0(T)$ by the corresponding geometric average of the S_i's. In addition, in order to apply Proposition 3.2.3, we need the correlation matrix of the H_i's. The detailed procedure is as follows.

Define random variables X and Y_k's by

$$X = \frac{\log H_0(T) - \mu_0^H}{\nu_0^H}, \quad Y_k = \frac{\log H_k(T) - \mu_k^H}{\nu_k^H}, \quad k = 1, 2, \cdots, N$$

with $\mu_k^H = \mu_{k+M}$ and $\nu_k^H = \nu_{k+M}$ for $k = 1, \cdots, N$, and

$$\mu_0^H = \log\Big(\sum_{i=1}^{M} e^{\mu_i + \frac{1}{2}\nu_i^2}\Big) - \frac{1}{2}(\nu_0^H)^2, \quad \nu_0^H = \frac{1}{M}\sqrt{\sum_{i=1}^{M}\sum_{j=1}^{M}\rho_{i,j}\nu_i\nu_j}\,.$$

Then X and the Y_i's can be approximated as jointly normally distributed with mean vector $\mathbf{0}$, variance vector $\mathbf{1}$, and correlation matrix $\mathbf{\Sigma} = (\varrho_{i,j})$, $i, j = 0, 1, \cdots, N$, where

$$\begin{aligned}
&\varrho_{0,0} = 1,\\
&\varrho_{0,k} = \varrho_{k,0} = \frac{1}{M\nu_0^H}\Big(\sum_{i=1}^{M}\rho_{i,k}\nu_i\Big), \quad k = 1, 2, \cdots, N\\
&\varrho_{i,j} = \rho_{M+i,M+j}, \quad i, j = 1, 2, \cdots, N.
\end{aligned}$$

The above equations can be proven in a very similar way to Proposition 3.2.1. Notice that under the GBMs case, the quantity μ_0^H are usually further approximated as

$$\mu_0^H = \log H_0(0) + \Big(rT - \frac{1}{M}\sum_{i=1}^{M} q_i T - \frac{1}{2M}\sum_{i=1}^{M}\nu_i^2\Big).$$

Once we have approximated the H_i's using the jointly normal setup, we can use either the extended Kirk approximation in Proposition 3.2.1 or the second-order boundary approximation in Proposition 3.2.3 to compute the price of the hybrid spread-basket option. This extension to hybrid spread-basket options greatly enhances the applicability of our approximation methods.

3.3 Comparison of accuracy and speed with existing methods

3.3.1 Existing pricing methods

When the number of assets is small, numerical integration method can be used to calculate spread option prices by using Proposition 3.1.1. Although very accurate, it is not quite applicable for multi-asset spread options when the number of assets is large because of the huge computation cost. The same is true for partial differential equation technique. Another widely used numerical method is Monte Carlo simulation. The advantage of Monte Carlo simulation is that it is very flexible and is able to value spread options under many different distributional assumptions. The shortcomings are that the results are not always accurate enough, even after variance reduction techniques such as antithetic method, control variate and importance sampling are applied. Also, the Greeks need to be calculated with extra effort, usually by approximating them using finite difference. The biggest shortcoming is that Monte Carlo simulation is generally very time-consuming, especially when the dimension is high and the number of option prices need to be computed is large.

Given the high computational cost of numerical methods for multi-asset spread option, it is extremely useful to design approximation techniques. However, until very recently, not much work has been done on this subject. Carmona and Durrleman (2005) propose approximate formulas for the lower and upper bounds of multi-asset spread options by solving a nonlinear optimization problem. They only consider the geometric Brownian motions case. The lower bound is quite accurate while the upper bound is less accurate. Therefore we just compare our method with their lower bound. We give a brief description

of the Carmona and Durrleman method below. Interpreting $\sigma_{N+1} = 0$ and letting $\mathbf{C} = \mathbf{\Sigma} \oplus 1$, the lower bound of the spread option price is given as follows.

$$\Pi = \sum_{i=0}^{N+1} \mathbf{S}_i \Phi\Big(d^* + (\mathbf{C}^{\frac{1}{2}}\mathbf{z}^*)_i \, \sigma_i \sqrt{T}\Big),$$

where the scaler d^* and unit length vector $\mathbf{z}^*$ satisfy the following system of nonlinear equations

$$\sum_{i=0}^{N+1} \mathbf{S}_i \sigma_i \sqrt{T} (\mathbf{C}^{\frac{1}{2}})_{ij} \, \phi\Big(d^* + (\mathbf{C}^{\frac{1}{2}}\mathbf{z}^*)_i \sigma_i \sqrt{T}\Big) - \mu \mathbf{z}_j^* = 0, \quad \text{for } \; j = 0, \cdots, N+1 \tag{3.3.1}$$

$$\sum_{i=0}^{N+1} \mathbf{S}_i \, \phi\Big(d^* + (\mathbf{C}^{\frac{1}{2}}\mathbf{z}^*)_i \sigma_i \sqrt{T}\Big) = 0, \tag{3.3.2}$$

and μ is the Lagrangian multiplier. Notice that Carmona and Durrleman's method is not in closed-form because it requires the numerical solution of a system of nonlinear equations. In addition, like our second-order boundary approximation, Carmona and Durrleman's method also requires the somewhat expensive calculation of the square root of $\mathbf{\Sigma}$. Interpreting $s_{N+1} \equiv K$, the deltas and kappa are given by

$$\frac{\partial \Pi}{\partial s_i} = \frac{\mathbf{S}_i}{s_i} \cdot \Phi\Big(d^* + (\mathbf{C}^{\frac{1}{2}}\mathbf{z}^*)_i \sigma_i \sqrt{T}\Big), \quad i = 0, 1, \cdots, N+1. \tag{3.3.3}$$

One very nice feature about this method is that it always gives a lower bound for the actual price. The main difficulty of applying Carmona and Durrleman's method is in solving the system of nonlinear equations, because there is not much guidance on the choice of initial values for d^*, $\mathbf{z}^*$ and μ.

3.3.2 Numerical performance

We now compare our methods, namely, the extended Kirk approximation and the second-order boundary approximation, with Monte Carlo simulation, numerical integration method based on Proposition 3.1.1, and Carmona and Durrleman's method. We perform the comparisons for four different dimensions $N + 1$, namely, $3, 20, 50$, and 150 using an artificial correlation matrix similar to the one used in Carmona and Durrleman (2005). In addition,

in order to test various methods using a more plausible correlation matrix, we also apply the methods to two hypothetical spread options. One is between the S&P 500 index and the 30 component stocks of the Dow Jones Industrial Average (DJIA) index and the other is between the S&P SmallCap 600 index and the DJIA components. All methods are implemented in MATLAB 7.0 on a Dell Optiplex GX620 with 3.80 GHz Intel Pentium(R) 4 CPU and 3G RAM. For the purpose of definiteness and the fact that Carmona and Durrleman (2005) only consider the geometric Brownian motions case, we will only compare models in this special case.

For the Monte Carlo simulation, we generate 10,000,000 replicates. We use Proposition 3.1.1 rather than equation (3.1.10) because if one uses equation (3.1.10), then the information on the random variables x and $\mathbf{y}$ is completely lost if the option happens to be out of money. The use of Proposition 3.1.1 amounts to an importance sampling technique. In the actual implementation we find that it gives very large variance reduction in Π. The numerical integration method is only used for the 3-dimension case because the computational cost is exceedingly high when the dimension is high. The numerical integration results computed with error tolerance level 10^{-8} are used as actual option prices to calculate the relative pricing errors $(\Pi_{\text{Approximation}} - \Pi_{\text{Actual}})/\Pi_{\text{Actual}}$. For Carmona and Durrleman's method, we use the globally convergent Newton-Raphson method as described in Press et al. (1992). We find that the globally convergent Newton-Raphson method is slightly more stable than the Newton-Raphson method and slightly faster to converge to the optimal solution. However, the optimization is still extremely sensitive to the choice of initial values and very often fails. The region of initial values that will lead to solutions is an unknown function of the parameters of the spread option, namely, μ_i, ν_i and $\mathbf{\Sigma}$, and Carmona and Durrleman (2005) does not give much guidance on how to choose the initial values. Because of this, extensive numerical experiments are often needed to find out the appropriate initial values for different options, which can take from one minute to as long as half an hour. We thus conclude that some guidance on how to choose the initial values

in Carmona and Durrleman's method is crucial for the method to be useful in large scale real-life computations.

Spread options on 3 assets.

As a first example, we consider spread options on 3 assets. We set $T = 0.25$, $r = 5\%$, and the dividend rate zero. The initial asset prices are $s_0 = 150, s_1 = 60$, and $s_2 = 50$. The volatilities of all three assets are given by the same σ and we vary σ to be 0.3 and 0.5. We vary K to be from 30 to 50 with increment 5. The correlation matrix for the asset returns is given by

$$\mathbf{\Sigma} = \begin{pmatrix} 1 & 0.2 & 0.8 \\ 0.2 & 1 & 0.4 \\ 0.8 & 0.4 & 1 \end{pmatrix}.$$

Table 3.3.1 reports the prices for each of the five methods we compare together with the average computing times. The numerical integration results are used as the actual prices. Looking at the relative errors, both our methods are quite accurate with the second-order boundary approximation being more accurate than the extended Kirk approximation. In particular, the relative pricing error of the extended Kirk approximation is in the order of 10^{-2}, while that of the second-order boundary approximation is in the order of 10^{-5}. Monte Carlo simulation with 10,000,000 replications and the use of Proposition 3.1.1 gives quite accurate results, but usually still not as accurate as the second-order boundary approximation. Carmona and Durrleman's method is also quite accurate but not as good as our second-order boundary approximation. Furthermore, in the actual implementation we need to spend about 20 minutes to find good starting values for the nonlinear equations that one has to solve in their method. Even if good starting values are found, their method is still slower than both our methods. The average computing times for both our methods are in the order of 10^{-3} second, while both the numerical integration and Monte Carlo simulation methods take considerably more time.

Table 3.3.2 lists the results for four important Greeks for all the methods, namely, the

Table 3.3.1: Prices of spread options on 3 assets

This table reports the three-asset spread option prices of different methods. Numbers in parenthesis are the relative errors. NI represents two-dimensional numerical integration. EK represents the extended Kirk approximation. SB represents the second-order boundary approximation. CD represents Carmona an Durrleman's method, using globally convergent Newton-Raphson algorithm to solve the set of nonlinear equations. MC represents Monte Carlo simulation with 10,000,000 replications, whose standard error is in the order of 10^{-3} or 10^{-4}. The time listed is the average computing time of one option price. The asterisk on Carmona and Durrleman's method indicates that the searching time for initial values is not included.

	σ = **30**%					σ = **60**%				
K	**NI**	**EK**	**SB**	**CD**	**MC**	**NI**	**EK**	**SB**	**CD**	**MC**
30	13.5762	13.3426	13.5761	13.5751	13.5767	20.2066	19.6953	20.2063	20.1952	20.2043
		(-2×10^{-2})	(-7×10^{-6})	(-8×10^{-5})	(4×10^{-5})		(-3×10^{-2})	(-1×10^{-5})	(-6×10^{-4})	(-1×10^{-4})
35	10.3573	10.1171	10.3572	10.3560	10.3584	17.4770	16.9978	17.4769	17.4641	17.4759
		(-2×10^{-2})	(-1×10^{-5})	(-1×10^{-4})	(1×10^{-4})		(-3×10^{-2})	(-8×10^{-6})	(-7×10^{-4})	(-6×10^{-5})
40	7.6610	7.4337	7.6610	7.6594	7.6597	15.0280	14.5889	15.0281	15.0135	15.0293
		(-3×10^{-2})	(-1×10^{-6})	(-2×10^{-4})	(-2×10^{-4})		(-3×10^{-2})	(2×10^{-6})	(-1×10^{-3})	(9×10^{-5})
45	5.4914	5.2921	5.4914	5.4897	5.4901	12.8516	12.4580	12.8518	12.8361	12.8514
		(-4×10^{-2})	(-2×10^{-6})	(-3×10^{-4})	(-2×10^{-4})		(-3×10^{-2})	(2×10^{-5})	(-1×10^{-3})	(-2×10^{-5})
50	3.8150	3.6523	3.8150	3.8132	3.8142	10.9347	10.5891	10.9351	10.9186	10.9332
		(-4×10^{-2})	(3×10^{-6})	(-4×10^{-4})	(5×10^{-5})		(-3×10^{-2})	(4×10^{-5})	(-2×10^{-3})	(-1×10^{-4})
Time(s)	21.87	0.00017	0.00034	0.016*	8.06					

three deltas and the kappa. Here we fix $K = 30$. Again, the qualitative conclusions are the same for the prices. Both our methods are extremely fast, with the second-order boundary approximation gives the most accurate results.

Figure 3.3.1 further compares the accuracy of the four important Greeks between the extended Kirk approximation and the second-order boundary approximation. Parameters are still the same, but now with K varies in the range $[30, 50]$ and σ varies in the range $[0.1, 0.9]$. The actual values for the Greeks are computed using numerical integration. The Greeks for the extended Kirk approximation are obtained by differentiating equation (3.2.1) in Proposition 3.2.1. The Greeks for the second-order boundary approximation are given in Proposition 3.2.5. The Greeks for Carmona and Durrleman's method is given in equation (3.3.3). Figure 3.3.1 indicates that for the purpose of calculating the Greeks, the second-order boundary approximation should be preferred to the extended Kirk approximation.

Spread options on 20, 50 and 150 assets.

Next, we consider spread options on multiple assets with numbers of assets $N + 1$ equal 20, 50 and 150, respectively. We will consider symmetric target assets with initial prices $s_0 = 10(N + 1)$ and $s_1 = \cdots = s_N = 10$. We set $T = 0.25$, $r = 5\%$, and dividend rate zero. The correlation matrix is set to be

$$\mathbf{\Sigma} = \begin{pmatrix} 1 & \rho & \cdots & \rho \\ \rho & 1 & \ddots & \vdots \\ \vdots & \vdots & \ddots & \rho \\ \rho & \cdots & \rho & 1 \end{pmatrix} \tag{3.3.4}$$

with $\rho = 0.4$. All assets returns have the same volatility σ and we vary σ to be either 0.3 or 0.6. We vary K from 0 to 20 with increment 5.

Table 3.3.3 reports the prices of spread options with different number of assets, different volatilities σ and strikes K for each of the four methods we consider, together with the average computing time of each method. The results for different dimension $N + 1$ are reported in three different panels. Since N is large, numerical integration is no longer

Table 3.3.2: Greeks of spread options on 3 assets

This table reports the three-asset spread option Greeks of different methods. Numbers in parenthesis are the relative errors. NI represents two-dimensional numerical integration. EK represents the extended Kirk approximation. SB represents the second-order boundary approximation. CD represents Carmona and Durrleman's method, using globally convergent Newton-Raphson method to solve the set of nonlinear equations. MC represents Monte Carlo simulation with 10,000,000 replications, whose standard error is in the order of 10^{-3} or 10^{-4}. The time listed is the average computing time of one Greek. The asterisk on Carmona and Durrleman's method indicates that the searching time for initial values is not included.

	σ = **30**%					σ = **60**%				
Greeks	**NI**	**EK**	**SB**	**CD**	**MC**	**NI**	**EK**	**SB**	**CD**	**MC**
Δ_1	0.7405	0.7436	0.7404	0.7413	0.7405	0.6674	0.6619	0.6672	0.6675	0.6675
		(4×10^{-3})	(-7×10^{-5})	(1×10^{-3})	(4×10^{-5})		(-8×10^{-3})	(-3×10^{-4})	(2×10^{-4})	(2×10^{-4})
Δ_2	-0.6786	-0.7025	-0.6785	-0.6776	-0.6784	-0.5283	-0.5684	-0.5280	-0.5283	-0.5284
		(4×10^{-2})	(-9×10^{-5})	(-1×10^{-3})	(-2×10^{-4})		(8×10^{-2})	(-5×10^{-4})	(-8×10^{-5})	(2×10^{-4})
Δ_3	-0.7194	-0.7025	-0.7193	-0.7185	-0.7192	-0.6195	-0.5684	-0.6193	-0.6198	-0.6195
		(-2×10^{-2})	(-7×10^{-5})	(-1×10^{-3})	(-2×10^{-4})		(-8×10^{-2})	(-4×10^{-4})	(4×10^{-4})	(5×10^{-5})
κ	-0.6938	-0.7058	-0.6937	-0.6929	-0.6938	-0.5741	-0.5759	-0.5741	-0.5745	-0.5745
		(2×10^{-2})	(-6×10^{-5})	(-1×10^{-3})	(2×10^{-5})		(3×10^{-3})	(-9×10^{-5})	(5×10^{-4})	(7×10^{-4})
Time(s)	7.62	0.00011	0.00013	0.029*	12.60					

feasible so we do not know the exact actual option prices and as a result, we do not know the exact relative pricing errors. However, the results from Monte Carlo simulation can serve as a rough comparison benchmark. The results indicate that when the target assets are more symmetric, the extended Kirk approximation is more accurate. Again, both our methods are among the fastest and the second-order boundary approximation is much more accurate than the extended Kirk approximation and Carmona and Durrleman's method.

Figure 3.3.2 gives the computing time as a function of dimensions $N+1$. The horizontal axis is dimension $N+1$, which we vary from 3 to 200. The vertical axis is time in log scale. We do not plot the computing times for Carmona and Durrleman's method because it often takes more than 20 minutes to search for good initial starting values for their algorithm. If we do not include the search time, which is significant, the curve for Carmona and Durrleman's method would lie somewhere between the second-order boundary approximation and Monte Carlo simulation. As we see, up to dimension 25, both our methods take less than 10^{-3} second to compute the price of one spread option. The extended Kirk approximation remains within 10^{-3} second for all dimensions, while the second order boundary approximation remains within 10^{-1} second. Monte Carlo simulation takes considerable more time, ranging from 8 seconds in dimension 3 to over 500 seconds in dimension 200. For all dimensions, the computing times in the extended Kirk approximation are about 0.001% or 0.0001% of those in Monte Carlo simulation while the computing times in the second-order boundary approximation are about 0.01% of those in Monte Carlo simulation.

Spread options on two S&P indices and DJIA components.

Our final numerical example considers two hypothetical spread options. The first one is written on the S&P 500 index and the 30 component stocks of the Dow Jones Industrial Average (DJIA) index. The second one is written on the S&P SmallCap 600 index and DJIA components. Both options are very interesting in practice because industrial practitioners pay very close and constant attention to the different performance among large

Table 3.3.3: Prices of spread options on 20, 50 and 150 assets

This table reports the spread option prices of different methods when the numbers of assets are 20, 50 and 150. EK represents the extended Kirk approximation. SB represents the second-order boundary approximation. CD represents Carmona and Durrleman's method, using globally convergent Newton-Raphson method to solve the set of nonlinear equations. MC represents Monte Carlo simulation with 10,000,000 replications, whose standard error is in the order of 10^{-3} or 10^{-4}. The time listed is the average computing time of one option price. The asterisk on Carmona and Durrleman's method indicates that the searching time for initial values is not included.

Panel A: 20 assets

	σ = **30**%				σ = **60**%			
K	**EK**	**SB**	**CD**	**MC**	**EK**	**SB**	**CD**	**MC**
0	15.1119	15.1132	15.1122	15.1133	23.9279	23.9394	23.9283	23.9395
5	12.1229	12.1243	12.1233	12.1243	21.3570	21.3684	21.3577	21.3685
10	9.5495	9.5509	9.5498	9.5509	19.0032	19.0144	19.0038	19.0146
15	7.3867	7.3881	7.3870	7.3880	16.8596	16.8706	16.8603	16.8708
20	5.6119	5.6132	5.6122	5.6131	14.9173	14.9280	14.9180	14.9282
Time(s)	0.00018	0.00069	0.57*	51.81				

Panel B: 50 assets

	σ = **30**%				σ = **60**%			
K	**EK**	**SB**	**CD**	**MC**	**EK**	**SB**	**CD**	**MC**
0	28.5062	28.5078	28.5070	28.5078	51.4195	51.4316	51.4211	51.4318
5	25.8944	25.8959	25.8952	25.8959	49.0466	49.0586	49.0482	49.0588
10	23.4514	23.4529	23.4522	23.4528	46.7603	46.7722	46.7620	46.7715
15	21.1754	21.1769	21.1761	21.1769	44.5593	44.5712	44.5611	44.5714
20	19.0633	19.0647	19.0641	19.0648	42.4423	42.4541	42.4442	42.4543
Time(s)	0.00021	0.0032	7.39*	136.24				

Panel C: 150 assets

	σ = **30**%				σ = **60**%			
K	**EK**	**SB**	**CD**	**MC**	**EK**	**SB**	**CD**	**MC**
0	74.6046	74.6062	74.6066	74.6044	143.8020	143.8143	143.8070	143.8268
5	72.1642	72.1657	72.1666	72.1640	141.5173	141.5296	141.5239	141.5421
10	69.7800	69.7815	69.7818	69.7818	139.2615	139.2737	139.2653	139.2741
15	67.4519	67.4534	67.4544	67.4537	137.0342	137.0464	137.0404	137.0589
20	65.1795	65.1810	65.1820	65.1811	134.8354	134.8477	134.8396	134.8601
Time(s)	0.00038	0.035	292.91*	452.10				

company stocks, small company stocks and the whole market. For our numerical experiments, these options are very interesting because now the target assets are not completely symmetric.

For the first spread options, the final payoff is given by $[S_0(T) - \sum_{k=1}^{30} S_k(T) - K]^+$, where S_0 is chosen to be the S&P 500 index multiplied by 1.15, and $S_1, \cdots, S_{30}$ the prices of the DJIA component stocks. The weight 1.15 is chosen such that the spread option is near the money. Because of occasional additions and deletions of the DJIA components, the DJIA component stocks are fixed as those on August 29th, 2007. For the second spread option, S_0 is chosen to be the S&P SmallCap 600 index multiplied by 4.

We consider two different maturities, $T = 1/6$ and $T = 1/3$. For each maturity T, to obtain μ_k and ν_k, we use equation (3.1.2) and compute the mean and variance of the historical T-period returns $R_{k,T}$. For the first option, we use historical daily price data from the CRSP (Center for Research in Security Prices) data base from July 9th, 1986 to August 29th, 2007 because the stock prices for several companies are only available after July 9th, 1986. The returns are calculated using daily close prices after adjusting for stock splits. The prices on August 29th, 2007 are used to determine the initial asset prices s_k's. Alternatively, we could have used equations (3.1.5) to compute μ_k's and ν_k's by estimating the dividend rates. The correlation matrix $\mathbf{\Sigma}$ is estimated from the historical correlation matrix of the $R_{k,T}$'s. For the second option, we use historical daily price data from August 16th, 1995 to August 29th, 2007 because the S&P SmallCap 600 index is only available after August 16th, 1995. To include both in-the-money and out-of-the-money options, we vary K from 0 to 75 with increment 15 for the first option, and vary K from 0 to 120 with increment 30 for the second one.

Table 3.3.4 and Table 3.3.5 report the prices of the two spread option with different maturities T and strikes K, together with the average computing time of each method. Because actual prices are not available, we use the results from the Monte Carlo simulation as a rough benchmark. As we see, the extended Kirk approximation in this nonsymmetric

Table 3.3.4: Prices of spread options on S&P 500 and DJIA components
This table reports the spread option prices of different methods, where the options are written between the S&P 500 index and the Dow Jones Industrial Average (DJIA) component stocks. EK represents the extended Kirk approximation. SB represents the second-order boundary approximation. CD represents Carmona and Durrleman's method, using globally convergent Newton-Raphson method to solve the set of nonlinear equations. MC represents Monte Carlo simulation with 10,000,000 replications. Numbers in parenthesis are the standard errors. The time listed is the average computing time of one option price. The asterisk on Carmona and Durrleman's method indicates that the searching time for initial values is not included.

	T = 1/6				**T = 1/3**			
K	**EK**	**SB**	**CD**	**MC**	**EK**	**SB**	**CD**	**MC**
0	49.7453	50.1471	50.1336	50.1464 (6×10^{-3})	53.5266	53.5267	53.4684	53.5260 (8×10^{-3})
15	36.5853	37.2481	37.2276	37.2481 (5×10^{-3})	40.7162	41.9215	41.8499	41.9211 (7×10^{-3})
30	24.9909	25.9129	24.8859	25.9125 (5×10^{-3})	30.2193	31.6552	31.5736	31.6558 (6×10^{-3})
45	15.5874	16.6634	16.6329	16.6635 (4×10^{-3})	21.3773	22.9449	22.8581	22.9449 (5×10^{-3})
60	8.7325	9.7825	9.7531	9.7820 (3×10^{-3})	14.3348	15.9007	15.8156	15.9045 (4×10^{-3})
75	4.3312	5.1864	5.1628	5.1866 (2×10^{-3})	9.0686	10.4988	10.4218	10.5013 (3×10^{-3})
90	1.8802	2.4619	2.4457	2.4622 (1×10^{-3})	5.3921	6.5866	6.5227	6.5874 (2×10^{-3})
Time(s)	0.00019	0.0013	1.71*	82.83				

case becomes less accurate, with relative pricing error sometimes quite significant. Our second-order boundary approximation give more accurate approximation for the option prices than Carmona and Durrleman's method.

3.4 Conclusion

In this chapter, we study spread options written on multiple assets. We develop two closed-form approximations for pricing them, namely, the extended Kirk approximation and the second-order boundary approximation. Numerical analysis demonstrates that both

Table 3.3.5: Prices of spread options on S&P SmallCap 600 and DIJA components
This table reports the spread option prices of different methods, where the options are written between the S&P SmallCap 600 index and the Dow Jones Industrial Average (DJIA) component stocks. EK represents the extended Kirk approximation. SB represents the second-order boundary approximation. CD represents Carmona and Durrleman's method, using globally convergent Newton-Raphson method to solve the set of nonlinear equations. MC represents Monte Carlo simulation with 10,000,000 replications. Numbers in parenthesis are the standard errors. The time listed is the average computing time of one option price. The asterisk on Carmona and Durrleman's method indicates that the searching time for initial values is not included.

	T = 1/6				**T = 1/3**			
K	**EK**	**SB**	**CD**	**MC**	**EK**	**SB**	**CD**	**MC**
0	46.7497	47.0864	47.0697	47.0878 (8×10^{-3})	61.0999	61.6068	61.5581	61.6163 (1×10^{-2})
30	31.1304	31.4923	31.4754	31.4994 (7×10^{-3})	45.8508	46.3877	46.3389	46.3960 (9×10^{-3})
60	19.4500	19.7945	19.7799	19.7963 (5×10^{-3})	33.3758	33.9092	33.8627	33.9161 (8×10^{-3})
90	11.3518	11.6436	11.6315	11.6475 (3×10^{-3})	23.5374	24.0361	23.9946	24.0426 (6×10^{-3})
120	6.1692	6.3901	6.3811	6.3914 (6×10^{-3})	16.0680	16.5082	16.4726	16.5094 (4×10^{-3})
150	3.1157	3.2657	3.2599	3.2668 (1×10^{-3})	10.6130	10.9806	10.9517	10.9851 (3×10^{-3})
180	1.4610	1.5529	1.5494	1.5535 (7×10^{-4})	6.7817	7.0730	7.0511	7.0735 (2×10^{-3})
Time(s)	0.00019	0.0013	1.71*	82.83				

our methods are very robust, fast and accurate, with the second-order approximation being more accurate than the extended Kirk approximation and Carmona and Durrleman's method. For spread options written on 3 assets, the relative pricing error of the second-order approximation is in the order of 10^{-4} with an average computing time for each option of 2×10^{-4}. For dimensions up to about 100, the second-order boundary approximation takes less than 10^{-2} second. Thus, our method enables the accurate pricing of a bulk volume of spread options on multiple assets with different contract specifications in real time, which offer traders a potential edge in financial markets. We also extend our results to hybrid spread-basket options.

In addition, our approximations, especially the second-order boundary approximation, can be used to approximate the Greeks of spread options, which serve as valuable tools in financial applications such as calculating the delta-hedging position of a portfolio containing spread options.

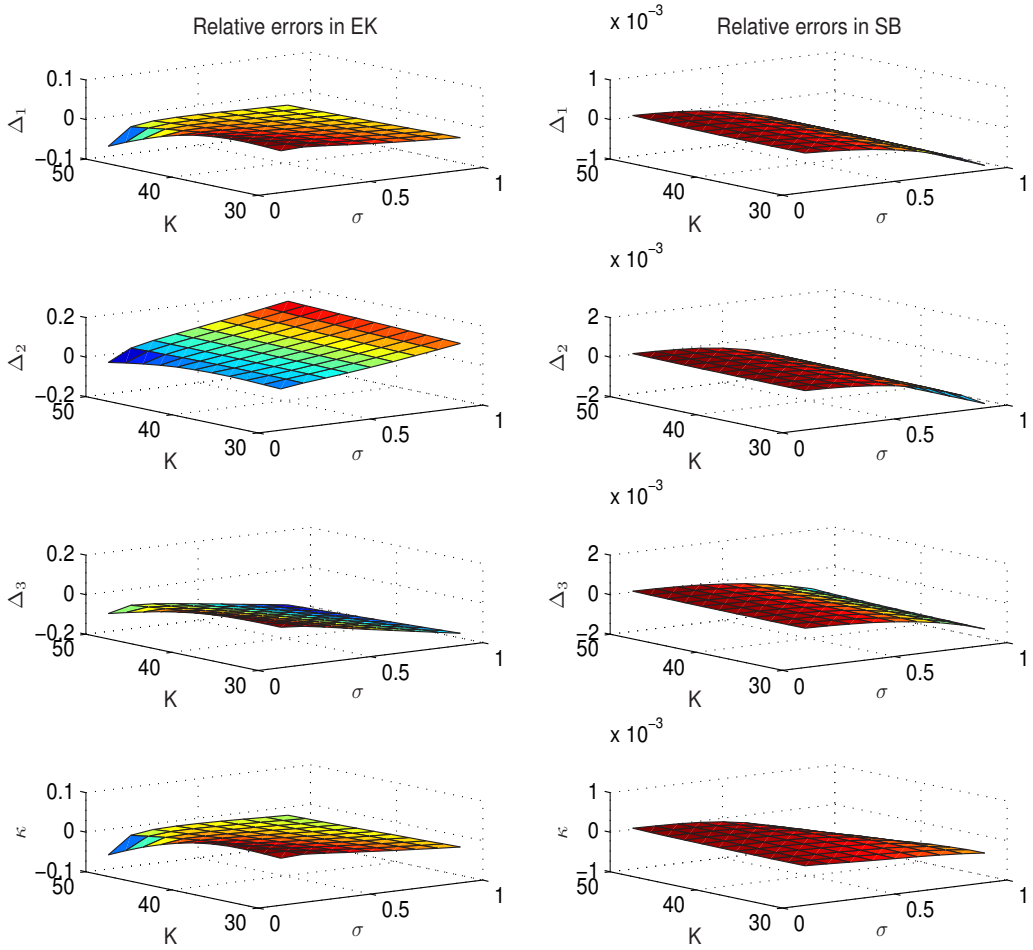

Figure 3.3.1: Accuracy comparison of deltas and kappa between the extended Kirk (EK) approximation and the second-order boundary (SB) approximation. The actual values for the Greeks are computed using numerical integration.

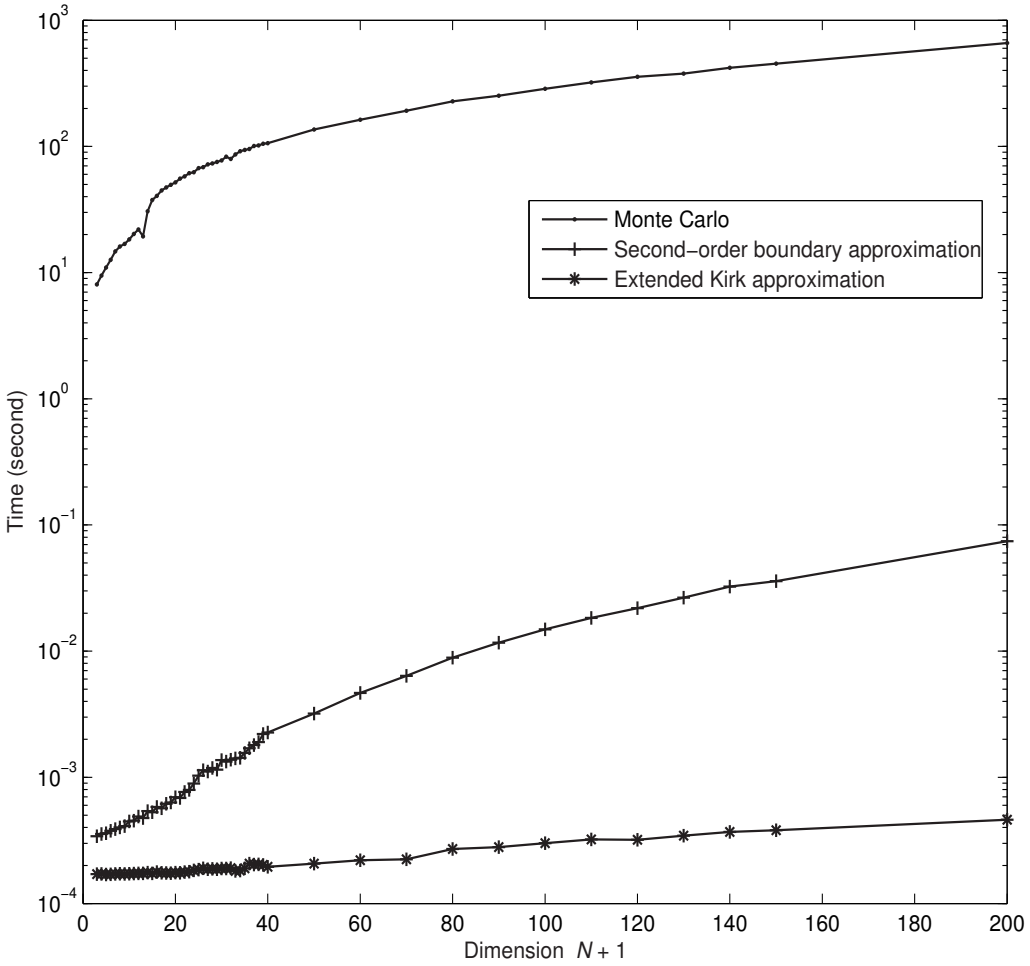

Figure 3.3.2: Average computing time as a function of dimension $N + 1$ for one spread option in Monte Carlo simulation, the extended Kirk approximation and the second-order boundary approximation.

CHAPTER IV

GENERALIZED GAUSSIAN QUADRATURE METHOD FOR NATURAL GAS STORAGE VALUATION

4.1 Introduction

With deregulation of the U.S. natural gas market, natural gas storage becomes increasingly important. According to Energy Information Administration, in 2009 there was about 3,889 billion cubic feet (Bcf) aggregate peak capacity for U.S. underground natural gas storage, and interest in developing more storage facilities has been growing. Besides the traditional function of serving a balance purpose, many storage capacities can now be leased by the owner to third parties through storage contracts. In the current competitive market, it is crucial to make the most of the operational flexibilities of the storage facility to capture any possible revenues.

The valuation of these storage contracts is a challenging problem because both the physical and the financial aspects of storage need to be considered. Storage facility operations are subject to various physical constraints. The three major types of underground storage facilities are depleted fields, aquifers, and salt caverns. Each storage type has different physical characteristics, among which the maximum capacity and deliverability rates are the most important. Eydeland and Wolyniec (2003) compare different types of storage facilities. Financial consideration is important because natural gas can be traded both in active spot markets and in forward or futures markets. Depending on the trading strategy adapted, different valuation methods have been developed.

Under spot-trading strategy, storage valuation is usually modeled as a stochastic dynamic programming problem. Ahn et al. (2002),Weston (2002), Chen and Forsyth (2007),

and Thompson et al. (2009) translate the Bellman equations into quasi-variational partial differential equations, which are solved using finite difference methods. Ghiuvea et al. (2003), Manoliu (2004), Parsons (2005), and Barrera-Esteve et al. (2006) apply tree-building techniques for swing-option pricing developed by Jaillet et al. (2004) for storage valuation. The most commonly used approaches are simulation-based. de Jong and Walet (2003), Barrera-Esteve et al. (2006), Boogert and de Jong (2008) adjust the Least Square Monte Carlo simulation (LSMC) method for American options to value storage. Ludkovski and Carmona (2009) further propose a Bivariate Least Squares Monte Carlo scheme. The major drawback of simulation-based approaches is their slow computation speed. Analogous to stochastic dynamic programming, an optimization technique called stochastic dual dynamic programming is discussed in Bringedal (2003).

In this chapter, we develop a generalized Gaussian quadrature (GGQ) scheme to solve for the dynamically optimal spot-trading strategy. This quadrature method has the same flexibility in incorporating operational constraints as simulation-based approaches while being more computationally efficient. The quadrature method is first applied to American options pricing in Sullivan (2000). Because the abscissas constructed are non-recombining, Chebyshev polynomials are used to approximate value functions. Andricopoullos et al. (2000) improve it by proposing a quadrature method with recombining abscissas for options valuation under Black-Scholes setting. Our GGQ method is an extension that can be applied to more generalize underlying processes, especially mean-reverting processes that are more suitable for natural gas price modeling. Furthermore, Gauss-Legendre quadrature, rather than trapezium rule or Simpson's rule, is used to improve computational efficiency. It also is the first time such a quadrature method is applied to the complex problem of natural gas storage valuation.

The other important category of trading strategies is forward or futures-based. The natural gas forward market exhibits significant seasonality due to demand variation. Prices are low in the summer and high in the winter. These price spreads are extracted by trading

multiple forward or futures contracts. Two major valuation approaches are widely used in practice. One is viewing gas storage as a series of calendar spread options, as is discussed in Eydeland and Wolyniec (2003). The other is the static or rolling intrinsic forward trading approach described in Blanco et al. (2002) and Gray and Khandelwal (2004).

Each category of trading strategies has its own advantages. Spot price has larger volatility and mean-reversion than forward price, while forward trading has much lower risk exposure than spot trading. Because natural gas can be traded at spot and forward markets simultaneously, it will be ideal to integrate spot and forward trading. Due to the distinct characteristics of these two kinds of trading strategies and the complexity of storage valuation, it is a challenge that has not been fully resolved. Maragos (2002) does optimization with regard to daily information of spot price and forward curve, but only carries out the spot trading. Ronn and Kjaer (2008) impose exogenous restrictions on the operation policy such that the storage is filled during exactly one of the summer months and emptied during exactly one of the winter months. A portion of the gas is acquired by futures contracts and the rest is traded on the spot market. In Li (2007), spot and forward prices are taken into account at the same time. As the dynamic programming problem is solved as an American option, there can be only one exercise of spot and forward trading in the contract lifetime, which will significantly undervalue the storage value. Lai et al. (2008) compute bounds for storage value by an approximate dynamic programming method with Monte Carlo simulation. Trading is restricted to a monthly basis. In addition, to be computationally tractable, spot and forward curves are approximated by information reduction, using a three-dimensional binomial tree.

With the fast and flexible GGQ valuation method for spot trading developed in this chapter, we are able to propose a hybrid trading strategy that integrates spot trading into

various forward trading strategies used in practice. This hybrid trading strategy significantly improves the storage valuation by accounting for both the inter-month and intra-month operational flexibilities and price variations. It captures more value than forward-base strategies and has better risk control than spot trading strategies.

This chapter is organized as follows. Section 4.2 introduces the model setup for storage valuation under spot-trading strategies, develops the generalized Gaussian Quadrature scheme, and presents a summary and comparison with existing methods. Based on this GGQ method, we proceed to propose a hybrid trading strategy in Section 4.3 that incorporates both spot and forward trading. A multi-factor model for spot and forward prices is described and calibrated. Several numerical examples are given in Section 4.4. Section 4.5 concludes this chapter.

4.2 Generalized Gaussian Quadrature method for spot trading

Here is an example of a storage contract.

- Term: $4/1/2010 - 3/30/2011$
- Basis: Henry Hub
- Maximum capacity: 4 Bcf = 10^6 million of British thermal unit (MMBtu)
- Initial inventory level: 2 Bcf
- Maximum injection rate: 40,000 MMBtu/day
- Maximum withdrawal rate: 80,000 MMBtu/day
- Injection fuel loss rate: 0.1% and no withdrawal fuel loss.
- Injection/withdrawal fee: \$0.02/MMBtu

We value the storage contract from the perspective of the holder. First, we consider trading only in the spot market. At each operation time point, the storage holder first observes the market spot price, for example Gas Daily price, and then determines the optimal

operation strategy: store, inject, or withdraw. If the strategy is to inject, natural gas is purchased in the spot market and injected into the storage facility. If the strategy is to withdraw, natural gas is withdrawn and sold in the spot market. All these operations are subject to volumetric constraints and physical operational constraints such as maximum injection and withdrawal rates, fuel losses, and various costs. Since the payoff is linear in the injection and withdrawal rates, the optimal strategy is of a "bang-bang" type (Øksendal and Sulem 2005)[1]. In other words, it is always optimal to inject or withdraw at maximum speeds. In light of the volumetric constraints, when the inventory level is so high that there is not enough room for full injection, the maximum amount feasible will be injected. Likewise, when the inventory level is too low for full withdrawal, the maximum amount feasible will be withdrawn. At the expiration of the contract, a pre-specified payoff function will be applied to the final inventory left in the storage. Sometimes a final inventory level at expiration is required, and a penalty will be imposed if inventory is below that requirement.

[1]The Generalized Gaussian Quadrature method proposed in this chapter can also be applied to solve non "bang-bang" type problems.

4.2.1 Model setup

Before developing our model for valuing the storage contracts, we introduce the following notations:

t : Index for time.

T : Contract length.

r : Constant risk adjusted discount rate.

$S(t)$: Current spot price of natural gas ($/MMBtu).

$I(t)$: Current inventory level (Bcf).

$I_{\max}$: Capacity limit of the facility.

$I_{\min}$: Minimum required inventory level.

I_{final} : Required final inventory level at expiration.

$i \in \{1, 2, 3\}$: Three operating regimes: storage, injection, and withdrawal.

$a_2(I(t))$: Injection rate (Bcf/year). A positive constant or a function of inventory level.

$a_3(I(t))$: Withdrawal rate (Bcf/year). A positive constant or a function of inventory level.

$L_i(I(t))$: Fuel loss rate (in percentage).

c_i : Injection and withdrawal charges ($/MMBtu).

$M_i(S(t), I(t))$: Various cost rate, including operational and maintenance cost, storage cost etc.

$g(i, S(t), I(t))$: Payoff rate in regime i at time t.

$f(S(T), I(T))$: Final payoff at the end of the contract. Can be zero or a penalty function.

$\pi(t, S(t), I(t)) \in \{1, 2, 3\}$: Optimal operating strategy; enoted as $\pi(t)$ for simplicity.

Let $V(t, S(t), I(t))$ be the storage contract value at t. The objective is to find the optimal operating strategy $\pi(t)$ at each time t such that the expected value of the accumulated payoff

is maximized.

$$V(0,S(0),I(0)) = \max_{\pi} \mathbb{E}\Big[\int_0^T e^{-ru} g(\pi(u),S(u),I(u))du\Big] \tag{4.2.1}$$

$$s.t. \quad I_{\min} \le I(t) \le I_{\max},\ t \in [0,T] \tag{4.2.2}$$

With the payoff rate in each operation regime being:

$$\begin{cases} g(1,S(t),I(t)) = -M_1(S(t),I(t)), \text{ Store} \\ g(2,S(t),I(t)) = -S(t)a_2(I(t))[1+L_2(I(t))] - c_2 a_2(I(t)) - M_2(S(t),I(t)), \text{ Inject} \\ g(3,S(t),I(t)) = S(t)a_3(I(t))[1-L_3(I(t))] - c_3 a_3(I(t)) - M_3(S(t),I(t)), \text{ Withdraw} \end{cases} \tag{4.2.3}$$

In reality, trading and switching of operations only occur at certain time points. We assume that it occurs at time $t_n = n\Delta t$ ($\Delta t = \frac{T}{N}, n = 0,1,\ldots,N$). N is chosen so that the trading frequency is daily. The impact of different trading frequencies will be shown in Example 1 in Section 4.4. The following dynamic program gives storage contract value:

$$V(T,S(T),I(T)) = f(S(T),I(T)) \tag{4.2.4}$$

$$V(t_n,S(t_n),I(t_n)) = \max_{\pi(t_n)} \left\{ g(\pi(t_n),S(t_n),I(t_n))\Delta t + \mathbb{E}[e^{-r\Delta t} V(t_{n+1},S(t_{n+1}),I(t_{n+1}))\big|\mathcal{F}(t_n)] \right\} \tag{4.2.5}$$

$\mathcal{F}(t)$ is the information filtration at time t. Inventory level is updated as follows:

$$I(t_{n+1}) = \begin{cases} I(t_n), \text{ Store} \\ I(t_n) + \min\{a_2(I(t_n))\Delta t, I_{\max} - I(t_n)\}, \text{ Inject} \\ I(t_n) - \min\{a_3(I(t_n))\Delta t, I(t_n) - I_{\min}\}, \text{ Withdraw} \end{cases} \tag{4.2.6}$$

Starting from $V(T,S(T),I(T))$ given, this dynamic programming problem is solved backward. $V(0,S(0),I(0))$ computed is the value of the storage contract. For simplicity, bid and ask spreads are ignored in this chapter, but this model can easily include them.

4.2.2 Generalized Gaussian quadrature method

As $I(t_{n+1})$ depends on $I(t_n)$ and the operations strategy at time t_n, we build up a grid for inventory level and compute storage value at each grid point. Now the major difficulty in

solving dynamic problem (4.2.5) is how to efficiently compute the conditional expectation:

$$\mathbb{E}\Big[e^{-r\Delta t}V(t_{n+1}, S(t_{n+1}), I(t_{n+1}))\Big|\mathcal{F}(t_n)\Big] \tag{4.2.7}$$

We use gaussian quadrature to approximate the conditional expectation when the conditional transition density of the spot price is known analytically. Let $p(y, t_{n+1}; x, t_n)$ be conditional transition density of the underlying price $S(t)$ going from x at time t_n to y at time t_{n+1}. Various choices of abscissas and weights could be taken depending on the function property, such as the trapezium rule or Simpson's rule. In this chapter, we use Gauss-Legendre polynomials. The conditional expectation (4.2.7) is approximated as:

$$\begin{aligned}
&\mathbb{E}\Big[e^{-r\Delta t}V(t_{n+1}, S(t_{n+1}), I(t_{n+1}))\Big|S(t_n) = x\Big] \\
&= \int_{-\infty}^{\infty} e^{-r\Delta t}p(y, t_{n+1}; x, t_n)V(t_{n+1}, y, I(t_{n+1}))dy \\
&\approx \int_{l_{n+1}}^{u_{n+1}} e^{-r\Delta t}p(y, t_{n+1}; x, t_n)V(t_{n+1}, y, I(t_{n+1}))dy \\
&\approx \sum_{k=1}^{K} w_k e^{-r\Delta t}p(y_k, t_{n+1}; x, t_n)V(t_{n+1}, y_k, I(t_{n+1}))
\end{aligned} \tag{4.2.8}$$

where

$$\begin{aligned}
&l_{n+1}, u_{n+1} \text{ are appropriate lower and upper bounds of } y \text{ at time } t_{n+1}, \\
&w_k = \tfrac{u_{n+1}-l_{n+1}}{2} w_k^{GL}, \\
&y_k = \tfrac{u_{n+1}-l_{n+1}}{2} y_k^{GL} + \tfrac{l_{n+1}+u_{n+1}}{2}, \\
&w_k^{GL}, y_k^{GL} \text{ are Gauss-Legendre abscissas and weights.}
\end{aligned} \tag{4.2.9}$$

As the quadrature is taken with respect to $y = S(t_{n+1})$, the same set of abscissas are used for different values of $x = S(t_n)$. Thus this quadrature method is equivalent to a recombining tree. So no need to do interpolations as in Sullivan (2000). Figure (4.2.1) illustrates the abscissa positioning. This property greatly improves the computation efficiency.

Generalized Gaussian Quadrature method could be applied when spot price is characterized as any one factor stochastic processes that have analytical conditional transition densities or conditional characteristic functions. Some examples are given in the appendix, including mean-reverting process, constant elasticity of variance process, inverse of square-root model and some Levy processes. In this chapter, we focus on mean-reverting processes, as natural gas spot price exhibits apparent mean-reversion property:

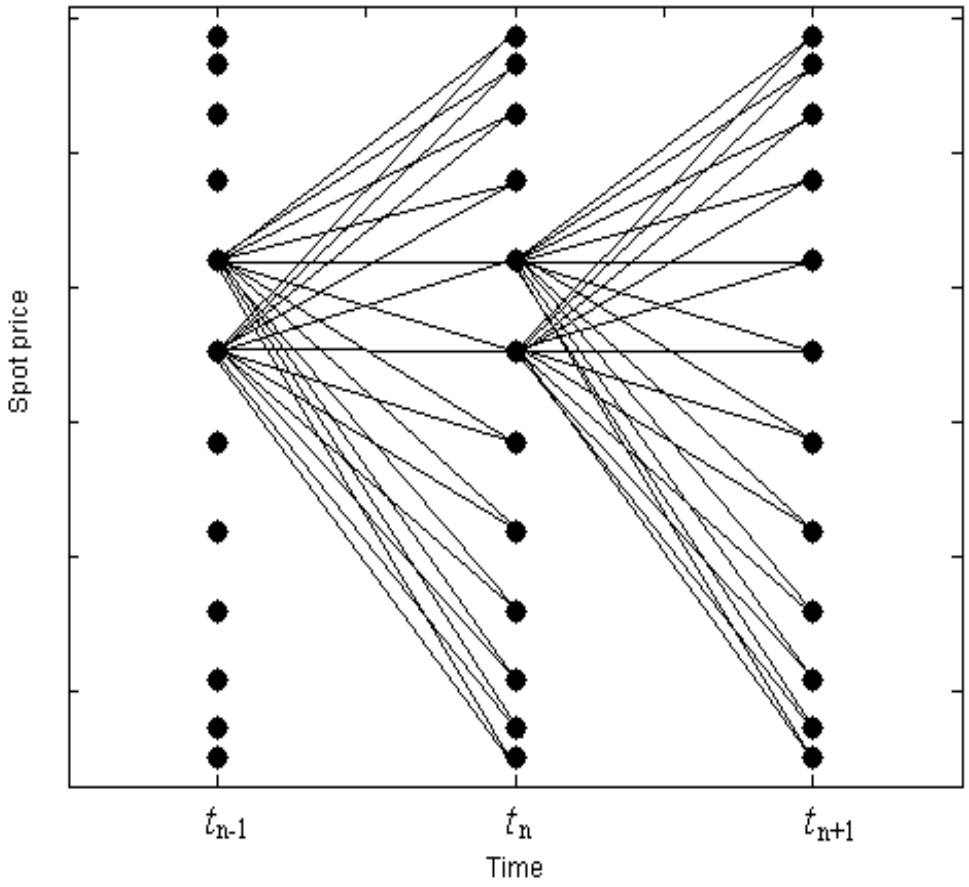

Figure 4.2.1: A schematic demonstration of the quadrature abscissas positioning. For clarity, only four points are linked with their abscissas.

1. When spot follows Ornstein-Uhlenbeck process with time-dependent mean-reverting level:

$$dS(t) = \kappa(\theta(t) - S(t))dt + \sigma dW(t),$$

We have $p(y, t_{n+1}; x, t_n) = \phi\left(y; \mu, \upsilon^2\right)$, with $\phi(y; \mu, \upsilon^2)$ representing normal probability density function with mean μ and variance υ^2:

$$\mu = xe^{-\kappa\Delta t} + \kappa e^{-\kappa t_{n+1}} \int_{t_n}^{t_{n+1}} e^{\kappa u}\theta_u du,$$

$$\upsilon^2 = \frac{\sigma^2}{2\kappa}(1 - e^{-2\kappa\Delta t}).$$

To apply approximation (4.2.8), appropriate numbers G and D are chosen so that

$$\begin{aligned} l_{n+1} &= S(0) + \gamma_{n+1} - D\beta_{n+1}, \\ u_{n+1} &= S(0) + \gamma_{n+1} + D\beta_{n+1}, \\ K &= G\left[\frac{u_{n+1} - l_{n+1}}{2\beta_{n+1}}\right] = GD. \end{aligned} \tag{4.2.10}$$

with

$$\begin{aligned} \gamma_{n+1} &= S(0)e^{-\kappa t_{n+1}} + \kappa e^{-\kappa t_{n+1}} \int_0^{t_{n+1}} e^{\kappa u}\theta_u du, \\ \beta_{n+1}^2 &= \frac{\sigma^2}{2\kappa}(1 - e^{-2\kappa t_{n+1}}). \end{aligned}$$

Numerical experiments suggest that $D = 6$ to 10, $G = 10$ to 20 can already give good results.

2. When spot follows log-Ornstein-Uhlenbeck process:

$$dS(t) = \kappa(\theta(t) - \log S(t))S(t)dt + \sigma S(t)dW(t)$$

Simply take $x = \log(S(t_n)), y = \log(S(t_{n+1}))$, then the result above can be applied.

4.2.3 Generalized Gaussian Quadrature method for natural gas storage valuation

4.2.3.1 Algorithm summary

Here is a summary of the GGQ method for natural gas storage valuation problem (4.2.1).

1. Choose parameters N, M, G, D. Construct a grid for time: $t_n = n\Delta t$ ($\Delta t = \frac{T}{N}, n = 0, 1, \ldots, N$), and a grid for inventory level: $v_m = I_{\min} + m\alpha$ ($\alpha = \frac{I_{\max} - I_{\min}}{M}, m = 0, 1, \ldots, M$).

2. Compute abscissas and weights according to (4.2.9) for each time step t.

3. Initialize contract values at each abscissa and inventory level $V(T, y_k(T), v_m)$ from (4.2.4).

4. Moving backward for $t_n, n = N, N-1, \ldots, 1$:

- At each t_n, for each inventory level $v_m, m = 0, 1, \ldots, M$:

  Now $I(t_n) = v_m$, update $I(t_{n+1})$ for each strategy according to (4.2.6), get $V(t_{n+1}, y_k(t_{n+1}), I(t_{n+1}))$ by interpolating $V(t_{n+1}, y_k(t_{n+1}), v_m), m = 0, 1, \ldots, M$

  - At t_n, with inventory level v_m, for each abscissa $y_k(t_n), k = 0, 1, \ldots, K$:
    - Compute the conditional expectation by (4.2.8), with $x = y_k(t_n), y_k = y_k(t_{n+1})$. Then determine the optimal operation strategy.

$$\pi^*(t_n) = \arg\max_{\pi(t_n)} \Big\{ g(\pi(t_n), y_k(t_n), I(t_n))\Delta t + \mathbb{E}\big[e^{-r\Delta t} V(t_{n+1}, S(t_{n+1}), I(t_{n+1}))\big|\mathcal{F}(t_n)\big] \Big\}$$

    - Update contract value $V(t_n, y_k(t_n), v_m))$ according to $\pi^*(t_n)$.
  - Continue the loop.
- Continue the loop.

  Continue the loop.

5. At $t = 0$, update $I(t_1)$ for each strategy, compute the conditional expectation with $x = S(0), y_k = y_k(t_1)$. Then determine the optimal operation strategy $\pi^*(0)$. Updated $V(0, S(0), I(0))$ is current value of the storage contract.

4.2.3.2 Hedging

Greeks can be derived easily from values by GGQ method. For example, delta, the sensitivity of storage value to the underlying spot price, is given by this second-order finite difference:

$$\Delta = \frac{\partial V}{\partial S(t)} \approx \frac{V(t, S(t) + \varepsilon, I(t)) - V(t, S(t) - \varepsilon, I(t))}{2\varepsilon}$$

with ε being a small number.

4.2.3.3 Ratchet

Usually, injection and withdrawal rates of the storage facility are inventory-level dependent, referred to as ”ratchet” in Gray and Khandelwal (2004). Due to the pressure of the reservoir,

it is harder to inject the higher the inventory lever is, and harder to withdraw the lower the inventory level is. Because the GGQ method has great flexibility in accounting for various operational constraints, these ratchet rates can be easily incorporated into the valuation model with no extra effort. Example 2 in Section 4.4 serves as an illustration.

4.2.3.4 Other existing valuation methods

The most commonly used valuation methods for storage are simulation-based. These approaches first simulate thousands of sample paths of the spot price, then approximate the conditional expectation (4.2.7) in each price path by regressing the storage value at time t_{n+1} against basis functions of the states at t_n. With this approximated expectation, optimal operation strategy $\pi(t)$ can be obtained by comparing the payoffs under three operation strategies. If the approximated expectation is directly put into backwardation of the dynamic programming (4.2.5), the method is called mixed-interpolation Tsitsiklis-van Roy scheme (MITvR) as in Ludkovski and Carmona (2009). If the value of accumulated cash flow in each price path, following the optimal operation strategy, is updated in the backwardation, the method is called Least Square Monte Carlo scheme (LSMC) as in Boogert and de Jong (2008). Ludkovski and Carmona (2009) further propose a scheme called Bivariate Least Squares Monte Carlo (BLSM), which performs bivariate regression against the current spot price and inventory level. Because there is no way to get an actual benchmark for the storage value, we will compare GGQ method with the widely used simulation-based approaches MITvR and LSMC methods in Section 4.4. We do not compare with Ludkovski and Carmona's BLSM method, because at each step it requires heuristics to guess current inventory levels in the algorithm. Compared to these simulation-based approaches, our GGQ method is much more efficient, with computing speed about two orders of magnitude faster.

Compared to another category of valuation approach that translates the Bellman equations into partial differential equations solved by finite difference method, GGQ method is

still much faster and more flexible in incorporating operational constraints and choosing different trading frequencies. We will see in Example 1 in Section 4.4 that various trading frequencies will give different storage values. By GGQ, we can use large time steps and no intermediate steps are needed.

This flexible and fast GGQ method enables further application of spot trading, whereas simulation and PDE approaches can not. A hybrid trading strategy that incorporates both spot and forward trading is discussed in Section 4.3.

4.3 Hybrid trading strategy that incorporates both spot and forward trading

4.3.1 Forward-based trading strategies

Another popular category of trading strategy is forward-based. The two basic strategies are intrinsic method and spread option method. Each of them can be either static or rolled.

In a static intrinsic strategy, the forward curve is observed at the beginning of the storage contract. The holder enters multiple forward positions and makes physical deliveries as the forward contracts expire. Let $F(t, T_i)$ be forward contract price at time t for delivery during $[T_i, T_{i+1})$, n_i be the annualized number of days in the month beginning at T_i. A linear optimization problem is solved to get the optimal forward positions $\mathbf{P}$:

$$V_{\text{forward}}(0) = \max_{\mathbf{P}} \; -\sum_{j=1}^{H} e^{-rT_j} F(0, T_j) h(P_j) \tag{4.3.1}$$

$$s.t. \quad -a_3(I(T_j)) \times n_j \le P_j \le a_2(I(T_j)) \times n_j \tag{4.3.2}$$

$$I_{\min} \le I(0) + \sum_{j=1}^{h} P_j \le I_{\max}, \; h = 1, 2, \ldots, H \tag{4.3.3}$$

$$I(0) + \sum_{j=1}^{H} P_j = I_{\text{final}} \tag{4.3.4}$$

Considering fuel losses,

$$h(P_j) = \begin{cases} P_j[1 + L_2(I(T_j))], \text{ if } P_j \ge 0 \\ P_j[1 - L_3(I(T_j))], \text{ if } P_j < 0 \end{cases} \tag{4.3.5}$$

An example is depicted by blue line in Figure 4.3.1. The storage facility has capacity 4 Bcf. Initial and required final inventory levels are both 2 Bcf. Suppose the optimal forward positions solved in the beginning of April 2006 are injecting 2 Bcf in May, withdrawing 4 Bcf in next February and injecting 2 Bcf in next March. Along the way, the T_i month forward contract expires on the third from the last business day of the month T_{i-1}. Amount of expired forward contract will be equally divided and delivered on each day of the contract month, we call it daily realized forward amount R_i. For example, May 2006 forward contract expires on April 26, 2006. In the month of May, $\frac{2}{31}$ Bcf natural gas will be injected every day.

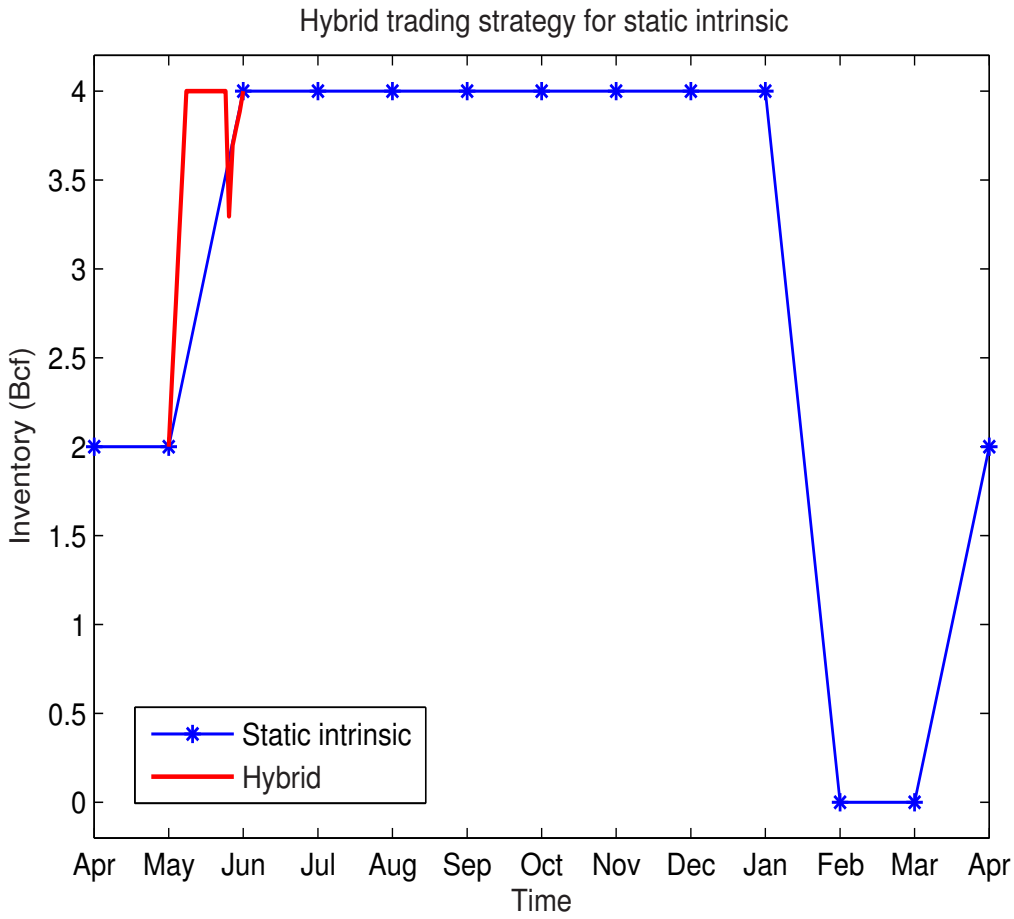

Figure 4.3.1: Example 3: Illustration of hybrid trading strategy for static intrinsic forward trading. Blue line is inventory level by static intrinsic. Red line is inventory level by applying the hybrid trading strategy with static intrinsic forward trading in May

In a rolling intrinsic strategy, optimal forward positions are entered at the beginning of the storage contract. In the next trading day, the forward curve evolves. If the holder finds it more profitable to re-balance, new forward positions are taken. Monte Carlo simulation is used to generate sample paths of forward curve. Storage value is the discounted average of accumulated payoffs.

Spread options approach views storage as a basket of calendar spread options. A linear optimization similar to (4.3.1) is solved with regard to shares of spread options to trade. For calendar spread options that are not so liquidly traded, a dynamic delta hedging is then carried out to replicate the spread option value. This spread options approach can also be rolled.

4.3.2 Hybrid trading strategy for static intrinsic forward trading

We will first look at static intrinsic trading strategy. If the daily realized forward injection is smaller than the maximum injection rate or if the daily realized forward withdrawal is larger than the maximum withdrawal rate, then the operational flexibility of the storage facility is not fully utilized, especially for facilities with high deliverability. The daily variation of spot price is also ignored. The GGQ method enables us to capture these ignored significant extra profits by a hybrid trading strategy.

A hybrid trading strategy for static intrinsic adds intra-month spot trading by solving a one month spot trading problem, with parameters modified by given forward positions **P**.

For $T_i \le t < T_{i+1}$:

$$R_i = \frac{P_i}{n_i}, \tag{4.3.6}$$

$$\tilde{a}_2(I(t)) = a_2(I(t)) - R_i, \text{ if } R_i > 0 \tag{4.3.7}$$

$$\tilde{a}_3(I(t)) = a_3(I(t)) + R_i, \text{ if } R_i < 0 \tag{4.3.8}$$

$$\tilde{I}(0) = I(T_i) = I(0) + \sum_{j=1}^{i-1} P_j \tag{4.3.9}$$

$$\tilde{I}_{\text{final}} = I(0) + \sum_{j=1}^{i} P_j \tag{4.3.10}$$

$$f\left(S\left(T_{i+1}\right), I(T_{i+1})\right) = -2S\left(T_{i+1}\right)|I(T_{i+1}) - \tilde{I}_{\text{final}}| \tag{4.3.11}$$

The penalty function (4.3.11) is used to ensure that end of month inventory level matches the scheduled inventory level of the original static intrinsic forward trading.

For $0 < t < T_1$, only update

$$\tilde{I}_{\text{final}} = I(0) \tag{4.3.12}$$

$$f\left(S\left(T_1\right), I(T_1)\right) = -2S\left(T_1\right)|I(T_1) - \tilde{I}_{\text{final}}| \tag{4.3.13}$$

Here is summary for this hybrid trading strategy:

1. At the beginning of the contract, use Q forward prices to solve problem (4.3.1). Get $V_{\text{forward}}(0)$ and the optimal forward positions $\mathbf{P}$.

2. For each month, including the current month, solve one month spot trading problem as in Section 4.2.3.1 with updated parameters by (4.3.6) to (4.3.13).

3. Storage value equals $V_{\text{forward}}(0)$ plus the sum of $Q+1$ discounted spot trading profits.

For the example in Figure 4.3.1, red line in May illustrates the inventory level determined by physical delivery of the expired May forward contract as well as spot trading in that month.

4.3.3 Hybrid trading strategy for rolling intrinsic forward trading

A hybrid trading strategy for rolling intrinsic is more complicated as sample paths of spot and forward curves are simulated. Along each price path, forward positions are rolled. At the same time, when the T_i forward contract expires, optimal operation strategy π_i^* is solved from the one month spot trading problem with updated parameters by (4.3.6) to (4.3.11). During the month $T_i \leq t < T_{i+1}$, spot trading is carried out according to π_i^*. To avoid repeated calculation, π_i^* only needs to be calculated once for sample paths with the same R_i and $\tilde{I}_{\text{final}}$. Let $T_0 = 0$, the algorithm is summarized as follows:

1. At the beginning of the contract, use Q forward contract prices to solve problem (4.3.1). Get $V_{\text{forward}}(0)$ and the optimal forward positions $\mathbf{P}$.

2. With $\mathbf{P}$ given, solve a one month spot trading problems as in Section 4.2.3.1 with updated parameter in (4.3.12) and (4.3.13). Get the optimal operation strategy π_0^*.

3. Simulate sample paths of spot and forward curves.

4. For $i = 1, 2, \ldots, Q$:

    - For each price path:

        - At each trading day $t = T_{i-1}, T_{i-1} + 1, ...,$ before the T_i forward contract expires, re-balance forward positions $P(T_i), P(T_{i+1}), \ldots, P(T_Q)$ if the new forward revenue plus the re-balance cost is higher than the old revenue. At the same time, trade in the spot market and operate the storage facility according to π_{i-1}^*. Accumulate payoffs from rolling forward positions as well as spot trading.

        - When the T_i forward contract expires, with the latest forward positions, check if the optimal operation strategy π_i^* has been solved for the pair $(R_i, \tilde{I}_{\text{final}})$ in this month. If not, solve one month spot trading problem with updated parameters by (4.3.6) to (4.3.11). Get π_i^*.

- Continue the loop.

Continue the loop.

5. In the last month, for each price path, at each trading day $t = T_Q, T_Q + 1, ..., T$, carry out spot trading according to π_Q^*.

6. Storage value is $V_{\text{forward}}(0)$ plus average of the discounted cumulative payoffs.

In this algorithm, the one month spot trading problem may need to be solved hundreds of times. GGQ method's fast speed and high flexibility are key to the implementation of such a hybrid strategy.

This hybrid trading strategy can also be applied to both static and rolling basket of spread options approaches in a similar way when dynamic delta hedging is used to replicate spread options values.

A numerical example is given in Section 4.4.2. Compared with forward trading strategies, a hybrid trading strategy can significantly increase profits. Compared with a spot-only trading strategy, a hybrid trading strategy has much smaller risk exposure, as the majority of the hybrid strategy value is locked in by forward trading. Furthermore, the proportion of intra-month spot trading in the hybrid strategy can be adjusted to satisfy different risk management requirements.

4.3.4 Spot and forward price model

We model spot and forward prices by twelve deterministic seasonal functions $f_i(t)$ and twelve mean-reverting processes:

$$dX_i(t) = \kappa(\theta_i - X_i(t))dt + \sigma_i dW_i(t) \tag{4.3.14}$$

$$dW_i(t)dW_j(t) = \rho_{ij}dt,\ i, j = 1, 2, \ldots, 12 \tag{4.3.15}$$

For $T_i \leq t < T_{i+1}$, spot price is determined by that month's seasonal factor as well as a log-OU stochastic factor:

$$S(t) = f_i(t) \exp\{X_i(t)\}$$

Forward price satisfies the no arbitrage condition $F(t,T) = \mathbb{E}[S_T|\mathcal{F}(t)]$, thus

$$F(t,T_i) = f_i(T_i)\exp\left\{X_i(t)e^{-\kappa(T_i-t)} + \theta_i(1-e^{-\kappa(T_i-t)}) + \frac{\sigma_i^2(1-e^{-2\kappa(T_i-t)})}{4\kappa}\right\}$$

We calibrate this model to historical data from Bloomberg. We get 7 business days' data from 4/3/2006. For each day, we obtain spot price, future prices for the following 36 months, volatilities for options on the following month's futures contract on Henry Hub natural gas. The parameters shown in Table 4.3.1 are taken as average of the 7 sets of calibrated results.

4.4 Numerical Results

All methods are implemented in MATLAB 7.0 on an IBM Thinkpad T21 with 3.80 GHz Intel Pentium(R) 4 CPU and 1G RAM. We consider the storage contract below, with spot price model, maximum injection and withdrawal rates specified in each example. D is taken to be 6.

- Duration: $T = 1$ year. We assume there are 252 business days in a year.
- Risk adjusted discount rate: $r = 6\%$.
- Maximum inventory level: $I_{\max} = 4$ Bcf, minimum inventory level: $I_{\min} = 0$ Bcf.
- Initial inventory level: $I(0) = 2$ Bcf.
- Final payoff: $f(S(T), I(T)) = 0$.
- Fuel cost rates for storage, injection and withdrawal: $\mathbf{L} = [0, 1\%, 0]$.
- Storage, injection and withdrawal fees: $\mathbf{c} = [0, 0.02, 0.02]$ \$/MMBtu.
- No other costs.

Table 4.3.1: Example 3: Calibrated parameters of multi-factor model for spot and forward prices

Parameter	Jan	Feb	Mar	Apr	May	Jun	Jul	Aug	Sep	Oct	Nov	Dec
Seasonal factor f	1.1437	1.1408	1.1395	0.9446	0.9363	0.9186	0.9218	0.9236	0.9251	0.9326	1.0160	1.0907
Long-term log level η	2.2164	2.2161	2.2069	2.1892	2.2151	2.2114	2.2259	2.2334	2.2363	2.2368	2.2259	2.2198
Volatility σ	0.4605	0.4643	0.3086	0.2193	0.4837	0.7615	0.5771	0.4650	0.4019	0.3680	0.4148	0.4409
Initial value $X(0)$	2.4737	2.7707	3.2821	5.8590	1.9343	1.9002	1.8621	1.8083	1.7386	1.6701	1.8868	2.1362
Mean-reverting rate κ						3.8992						

Table 4.4.1: Example 1: comparison of storage values
This table reports the prices ($\$10^6$) and computing time (second) for various methods. 252 time steps and 200 grid points for inventory levels are used. For GGQ method, $G = 18$. MITvR and LSMC methods use 6 basis functions and the same 10,000 sample paths of spot prices.

Method	Mean	Std. Err.	Time
GGQ	10.9464	—	10.99
MITvR	10.9461	0.0003	1063.21
LSMC	10.9592	0.015	1167.11

4.4.1 Spot-trading only

Example 1: As a first example, we consider spot price following a log Ornstein-Uhlenbeck process as in Carmona and Ludkovski (2005):

$$d\log S(t) = 17.1(\log 3 - \log S(t))dt + 1.33dW(t), \quad S(0) = 3 \tag{4.4.1}$$

Injection and withdrawal rates are constants:

$$a_2 = 0.04 * 252 \text{ Bcf/year.} \quad a_3 = 0.08 * 252 \text{ Bcf/year.}$$

Table 4.4.1 compares the prices and computing time for our GGQ method, MITvR method as in Ludkovski and Carmona (2009), and LSMC method, as in Boogert and de Jong (2008). Results show that our GGQ method is much more efficient than simulation-based approaches. It is in the same level of accuracy and about two orders of magnitude faster. A one year storage contract with daily spot trading can be solved by the GGQ method in about 11 seconds.

Here we do not compare with Ludkovski and Carmona's BLSM method and finite difference method. The speeds of these two methods reported in their paper are about 70% and 140% of the MITvR method, respectively. They are still much slower than our method.

Figure 4.4.1 shows the optimal operation strategies when the contract is three months to expiration. The optimal strategies computed by the GGQ, MITvR, and LSMC methods

Table 4.4.2: Example 1: Statistics of out of sample testing relative errors
This table reports the distribution of relative errors of out of sample testing values v.s. value computed by GGQ method. 10,000 sample paths of spot prices are generated.

Mean	Standard deviation
-0.0003	0.1380

are consistent with one another and match the intuition ”buy at low prices and sell at high prices.”

To further assess the accuracy of GGQ valuation. 10,000 sample paths of spot prices are generated according to (4.4.1). Along each path, the storage facility is operated according to the optimal operation strategies π computed by the GGQ method. The discounted accumulated payoff is the out-of-sample value. We compare these out-of-sample valuation results to the value computed by GGQ. A relative difference is defined as (out of sample value - GGQ value)/(GGQ value). Table 4.4.2 and Figure 4.4.2 show the distribution of these relative errors, the average of which is less than 0.03%.

Sensitivity of the GGQ method with regard to storage characteristics and spot model parameters is analyzed. Table 4.4.3 reports effects of variations in G, trading frequency, storage contract maturity, maximum capacity, injection and withdrawal rates, initial spot price, volatility, and mean-reverting rate for spot price process.

Example 2: In this example we use an Ornstein-Uhlenbeck process with seasonally-adjusted mean-reverting level for spot price. It’s modified from the model in Chen and Forsyth (2007).

$$dS(t) = 4\,(6 + \sin(4\pi t) - S(t))\,dt + 0.5dW(t), \quad S(0) = 6 \tag{4.4.2}$$

The storage facility has inventory level dependent injection and withdrawal rates, similar to the ones given in Gray and Khandelwal (2004). As shown in Figure 4.4.3, maximum

Table 4.4.3: Example 1: Sensitivity analysis by GGQ with $G = 18$

Panel A: Effect of G

G	10	14	18	20
Value	10.9459	10.9463	10.9464	10.9464

Panel B: Effect of Trading frequency

Frequency	Monthly	Weekly	Daily	Twice a day
Value	2.8540	6.9020	10.9464	13.9009

Panel C: Effect of maturity T (Daily trading)

T	0.5	1	2	3
Value	7.1671	10.9464	21.9013	34.3049

Panel D: Effect of maximum capacity $I_{\max}$

$I_{\max}$	2	4	6	8
Value	9.9913	10.9464	11.0429	11.0720

Panel E: Effect of injection rate a_2

a_2	0.02*252	0.04*252	0.08*252	0.16*252
Value	9.8551	10.9464	12.0605	12.9570

Panel F: Effect of withdrawal rate a_3

a_3	0.04*252	0.08*252	0.16*252	0.32*252
Value	9.3265	10.9464	12.2880	13.1731

Panel G: Effect of initial spot price $S(0)$

$S(0)$	2	3	4	5
Value	5.0400	10.0800	20.1600	40.3200

Panel H: Effect of volatility σ

σ	0.3	0.6	0.9	1.33
Value	6.5997	7.7753	9.0335	10.9464

Panel I: Effect of mean reverting rate κ

κ	2	7	12	17.1
Value	11.1749	11.5046	11.2956	10.9464

Table 4.4.4: Example 2: comparison of storage values
This table reports the prices ($\$10^6$) and computing time (second) for various methods. 252 time steps and 400 grid points for inventory levels are used. For GGQ method, $G = 16$. MITvR and LSMC methods use 6 basis functions and the same 10,000 sample paths of spot price.

Method	Mean	Std. Err.	Time
GGQ	11.8907	–	18.82
MITvR	11.8884	0.0002	1041.17
LSMC	11.9111	0.0018	1172.36

Table 4.4.5: Example 2: Effect of "ratchet"
This table reports the effect of "ratchet" rates on the storage value. Valued by GGQ method with 252 time steps, 400 inventory grid points and $G = 16$.

Injection rate a_2	Withdrawal rate a_3	Storage value
Inventory dependent rates as in Example 2		11.8907
3.65	3.65	12.2435

injection and withdrawal rates are represented by stepwise functions of percentage of inventory level $x = I(t)/I_{\max}$:

$$a_2(I(t)) = \begin{cases} 6.5x + 0.73, & 0 \le x < 45\% \\ 3.65, & 45\% \le x < 85\% \\ 4.38, & 85\% \le x < 100\% \end{cases}$$

$$a_3(I(t)) = \begin{cases} 3.65, & 0 \le x < 45\% \\ 3.77 - 0.26x, & 45\% \le x < 100\% \end{cases}$$

Table 4.4.4 Compares the prices and computing time for GGQ method, MITvR and LSMC methods.

As shown in Table 4.4.5, if we take maximum injection and withdrawal rates as constant 3.65, this simplification will lead to apparent mispricing of the storage value. Thus, our method's ability to incorporate "ratchet" rates is very important.

Table 4.4.6: Example 3: storage values under different trading strategies
For rolling intrinsic method, 10,000 sample paths of spot and forward prices are generated. Spot trading in hybrid strategy is implemented by GGQ method with 252 time steps, 200 inventory grid points and $G = 30, D = 10$.

	Static intrinsic	Rolling intrinsic
Without hybrid strategy	6.8699	13.5639
With hybrid strategy	8.9778	15.7884
Relative increment of profit	30.7%	16.4%

4.4.2 Hybrid trading strategy

Example 3: We use the multi-factor model for spot and future prices proposed in Section 4.3. We assume for simplicity that there are 21 days in each month, forward contracts expire one day before the delivery month, no fuel losses, no injection and withdrawal fees. Maximum injection and withdrawal rates are taken to be constants:

$$a_2 = 0.3 * 252 \text{ Bcf/year}, \quad a_3 = 0.6 * 252 \text{ Bcf/year}.$$

When applied for real-world problems, more realistic weekday, weekend schedules, forward contract expiration dates, ratchet rates and bid-ask spreads can be easily included. Final inventory I_{final} is required to be 2 Bcf, with penalty function

$$f(S(T), I(T)) = -2S(T)|I(T) - I_{\text{final}}|.$$

A hybrid trading strategy can significantly increase profits. As shown in Table 4.4.6, a relative increment of 30.7% is achieved when the hybrid strategy is applied to static intrinsic forward trading. Even for the rolling intrinsic forward trading strategy, we can improve the profit by 16.4% by following the hybrid strategy. Compared with a spot-only-trading strategy, a hybrid trading strategy has much smaller risk exposure. About 76.5% and 85.9% of the hybrid strategy values are locked-in by forward trading respectively.

4.5 Conclusion

Under a market-based valuation framework for natural gas storage with realistic operational characteristics, we model the operational process as a multi-stage stochastic optimization problem. The GGQ method is developed to solve for the dynamically optimal spot-trading strategy. Numerical examples show that the computational efficiency of this method exceeds existing Monte Carlo approaches in about two orders of magnitude while keeping the same accuracy and flexibility in incorporating operational constraints. Furthermore, with this fast and flexible quadrature scheme, we propose to value a gas storage based on a novel hybrid trading strategy that successfully incorporates both spot and forward trading. This hybrid strategy creates more profit because it maximizes the use of the storage deliverability and simultaneously captures both the variance of spot price and seasonal spreads of forward prices. In addition, risk exposure can be controlled and adjusted according to different risk preferences.

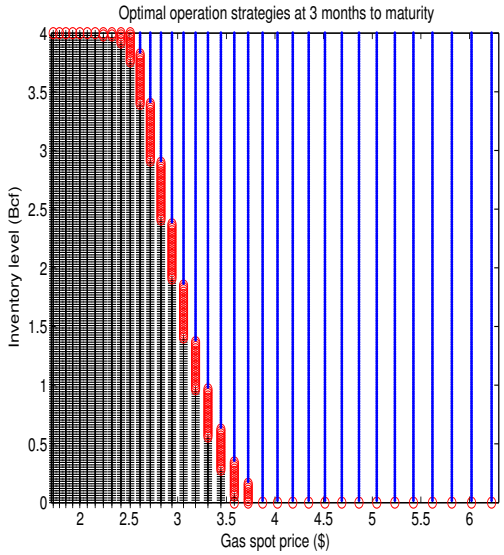

(a) By GGQ method

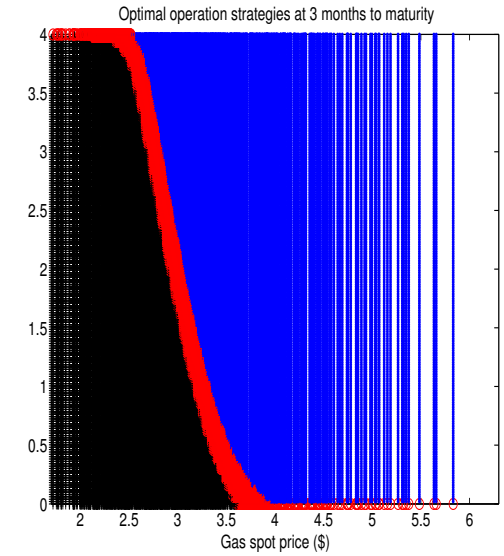

(b) By MITvR method

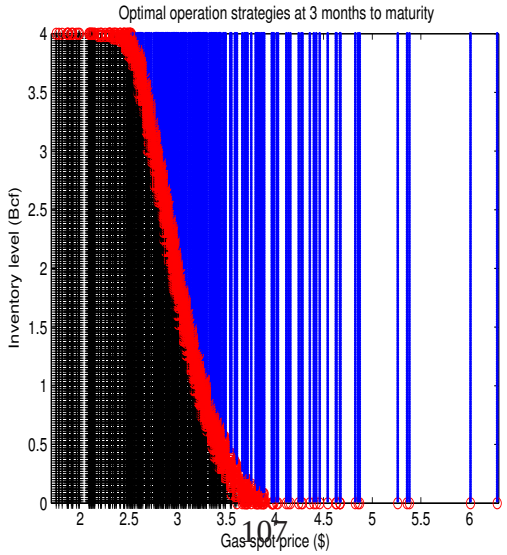

(c) By LSMC method

Figure 4.4.1: Example 1: Optimal operation strategies at 3 months to expiration. For each $(S(t), I(t))$ pair, black represents injection, red represents storage and blue represents withdrawal).

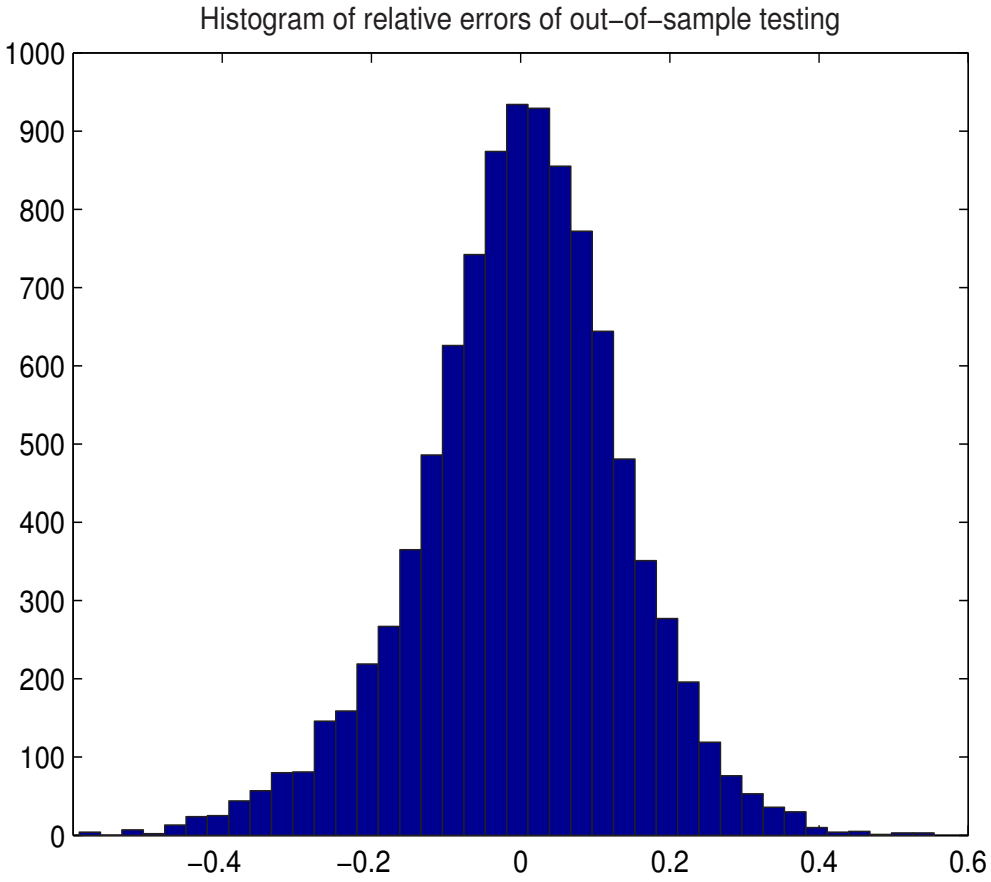

Figure 4.4.2: Example 1: Histogram of out of sample testing relative errors

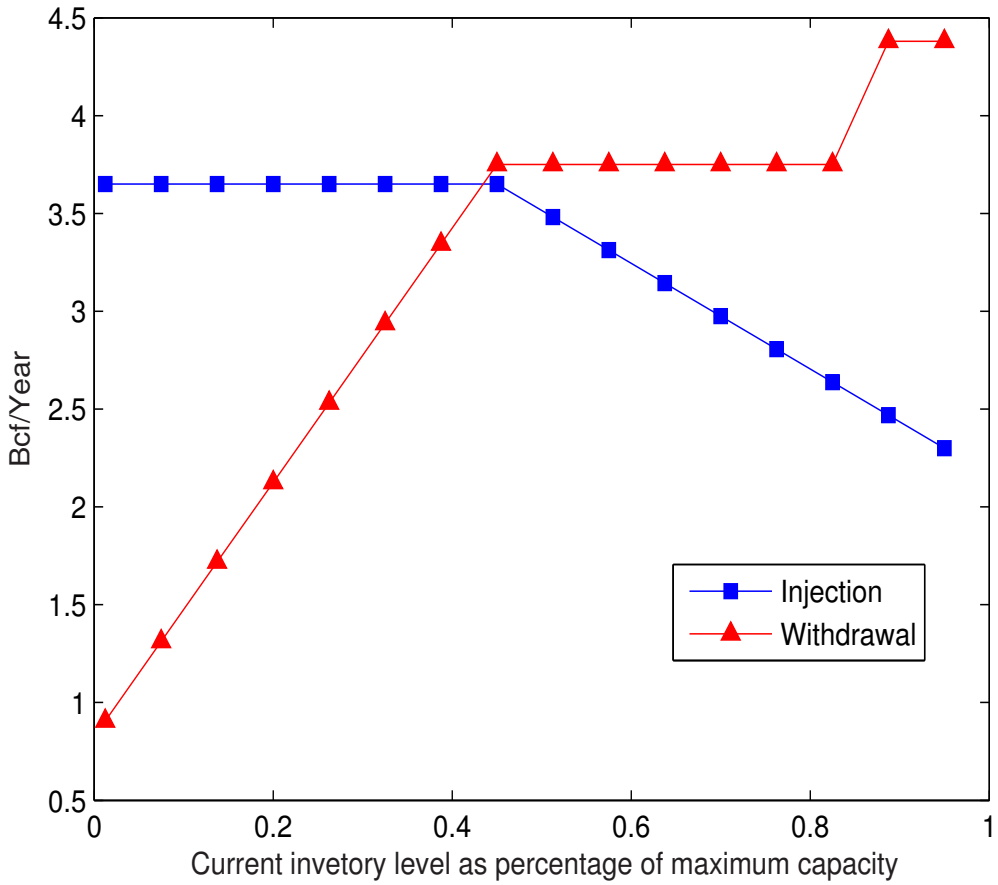

Figure 4.4.3: Example 2: Inventory level dependent injection and withdrawal rates.

CHAPTER V

CONTINUOUS-TIME OPTIMAL STOPPING FORMULATION FOR POWER PLANT VALUATION

5.1 Introduction

In today's competitive power market, efficient market-based valuation of power- generation assets is crucial. However, doing so has proven challenging, as power plant operation is subject to various physical constraints, as well as to the uncertain market prices of electricity and fuel. The traditional approach to power plant valuation, the discounted cash flow approach, overlooks the value of operational flexibility. Specifically, it ignores the fact that the owners of power plants have the right but not the obligation to either initiate or cease operations when the market prices of electricity and fuel change. This right is analogous to the right of exercising financial options. Based on recognition of this right, more and more real-options-based models have been proposed for use in power plant valuation, including Deng, Johnson and Sogomonian (1998) and Deng (2005)'s spread option-base valuation. The real-options-based approach provides more accurate valuation results than the traditional discounted cash-flow approach by taking into account the option value of operational flexibility.

However, most applications of financial-options theory to power-plant valuation assume that there are no operational constraints, and because these constraints actually have great effects on the market value of power plant, ignoring them leads to overvaluation. To take operational characteristics into account, Deng and Oren (2003) propose a stochastic dynamic programming model using discrete-time price lattices. Tseng and Barz (2002) develop a model that adapted least squares Monte Carlo simulation (LSMC) to power plant valuation. Such simulation approaches have great flexibility in incorporating operational

constraints but face the drawback of slow computation speed. Hamadène and Jeanblanc (2005) addressed the valuation problem within the Backward Stochastic Differential Equation (BSDE) framework. Porchet et al. (2009) further relate a coupled system of reflected BSDE to a system of variational inequalities.

In most of the power plant valuation literature, operational characteristics of the power plant are usually modeled by discrete variables. In this chapter we explore a continuous-time formulation for a power plant valuation in infinite time horizon. We propose a real-options-based model for power plant to account for the embedded operational flexibility. To make the problem tractable, power plant operations are restricted to be subject to threshold policies. Yet the model is sophisticated enough to incorporate two major operational constraints: the start-up and shut-down costs. To solve the power plant valuation problem, many researchers model the uncertain electricity price and fuel price as two separated stochastic processes and discretize the continuous stochastic processes to apply numerical methods, such as lattice method and Monte Carlo simulation. Because in our model the power plant value is considered in infinite time horizon, the long- term co-integration relationship that exists between electricity and fuel prices is important. Therefore, it is more reasonable to model directly the stochastic spark spread between electricity and fuel prices. Spark spread is a critical measure in power plant valuation. It is defined as the spread between electricity price and fuel price multiplied by heat rate, which measures the efficiency of the power plant. We model the spark spread directly by a continuous-time Ornstein-Uhlenbeck process that captures the mean-reverting feature of a commodity spread, as illustrated in Dempster et al. (2008). Instead of discretizing the stochastic process, we preserve continuity of the stochastic spark spread process and work directly with the value function. Under this model setup, closed-form of the value function under threshold policy is obtained by property of the first hitting time of stochastic process and optional sampling theorem. The corresponding optimal operational strategy can then be solved.

The chapter is organized as follows. Section 5.2 introduces the model setup for power

plant valuation under threshold policy. In the model, we directly model spark spread as a mean-reverting process. A solution to the valuation problem is given in Section 5.3 by deriving an explicit expression for the value function. Finally, Section 5.5 concludes the chapter.

5.2 Model setup

We first introduce the following standard notation. Let Ω be the space of all continuous functions $\omega : [0, \infty) \to \mathbb{R}$. For $t \geq 0$, let $X_t : \Omega \to \mathbb{R}$ be the coordinate projection map $X_t(\omega) = \omega(t)$. Then $X = (X_t, t \geq 0)$ is the canonical process on Ω. Let $\mathcal{F} = \sigma(X_t, t \geq 0)$ denote the smallest σ-field such that X_t is $\mathcal{F}$-measurable for each $t \geq 0$, and similarly let $\mathcal{F}_t = \sigma(X_s, 0 \leq s \leq t)$ for $t \geq 0$. When we mention adapted processes and stopping times hereafter, the underlying filtration is understood to be $\{\mathcal{F}_t, t \geq 0\}$. Suppose under risk neutral measure, the spark spread process follows:

$$\mathrm{d}X_t = \kappa(\theta - X_t)\mathrm{d}t + \sigma \mathrm{d}W_t \tag{5.2.1}$$

with $X_0 = x$, and κ is mean-reversion coefficient, θ is the risk-adjusted long-term mean, σ is the instantaneous volatility and W_t is standard Brownian motion. For simplicity, here we assume these parameters are constants, while a model with time-dependent parameters can be dealt with similarly. Appropriate parameters for spark spread prices can be obtained through calibration to market data as illustrated in Dempster et al. (2008).

We consider a power plant valuation problem in infinite time horizon. To make the problem tractable, we restrict the operation strategy set to be threshold policies $\{(L, U)\}$ and assume there is no ramp-up or down time. That means the power plant is turned on immediately when the spark spread reaches an upper bound U, and q megawatts of electricity is generated, with q a constant between minimum and maximum generation capacities. The power plant is turned off when the spread reaches a lower bound L. If the spread at time $t = 0$ is higher than or equal to U, the power plant will be turned on immediately. Each time the power plant is turned on or shut down, a start-up cost C^u

or shut-down cost C^d will incur. If these start-up and shut-down costs are ignored, it is obvious that the optimal threshold policy will be turning on the plant whenever the spark spread is positive and turning off the plant when the spread is negative. However, this overly simplified assumption will lead to an unrealistic description of the power plant and overvaluation. Therefore, in this chapter we consider non-zero C^u and C^d. They can be constants, functions of the number of re-starts, functions of the boiler temperature (Tseng and Barz (2002)) or other contract specified functions. Here we keep C^u and C^d as general functions of (L, U). Under non-zero start-up and shut-down costs, the optimal operation strategy (L, U) can not be easily seen. An optimization problem of maximizing the expected value of the discounted cash flow over lifetime under different threshold policies (L, U) needs to be solved.

Define:

$$\tau_1 : \text{The first time the spread hits } U = \begin{cases} \inf\{t \geq 0 : X_t = U\} & : \quad U > x \\ 0 & : \quad U \leq x \end{cases}$$

ζ_1 : The first time the spread hits L after $\tau_1 = \inf\{t \geq \tau_1 : X_t = L\}$.

τ_n : The first time the spread hits U after $\zeta_{n-1} = \inf\{t \geq \zeta_{n-1} : X_t = U\}$.

ζ_n : The first time the spread hits L after $\tau_n = \inf\{t \geq \tau_n : X_t = L\}$, for $n = 2, 3, \ldots$

The continuous-time optimal stopping formulation of the power plant value is:

$$\max_{L \leq U} V(x, L, U) = \mathbb{E}_x \left[\sum_{n=1}^{\infty} q \int_{\tau_n}^{\zeta_n} e^{-rt} X_t \, dt - C^u \sum_{n=1}^{\infty} e^{-r\tau_n} - C^d \sum_{n=1}^{\infty} e^{-r\zeta_n} \right] \tag{5.2.2}$$

5.3 Valuation

To solve the optimal operation strategy problem(5.2.2), we first construct a martingale:

$$\begin{aligned} Y_t &= \int_0^t e^{-rs} X_s \, ds - \int_0^t e^{-rs} \mathbb{E}[X_s] \, ds \\ &= \int_0^t e^{-rs} X_s \, ds + \frac{(x - \theta)}{r + \kappa} \left(1 - \mathbb{E}_x[e^{-(r+\kappa)t}]\right) + \frac{\theta}{r} \left(1 - \mathbb{E}_x[e^{-rt}]\right) \end{aligned}$$

By Optional Sampling Theorem, for a stopping time τ, and $m = 1, 2, \ldots$

$$\mathbb{E}_x [Y_{\tau \wedge m}] = \mathbb{E}_x [Y_0] = 0$$

As proved in Appendix C.2, we have

$$\mathbb{E}_x \left[\int_{\tau_n \wedge m}^{\zeta_n \wedge m} e^{-rt} X_t \, dt \right] = \mathbb{E}_x \left[\int_0^{\zeta_n \wedge m} e^{-rt} X_t \, dt \right] - \mathbb{E}_x \left[\int_0^{\tau_n \wedge m} e^{-rt} X_t \, dt \right] \tag{5.3.1}$$

$$\lim_{m \to \infty} \mathbb{E}_x \left[\int_0^{\tau \wedge m} e^{-rt} X_t \, dt \right] = \mathbb{E}_x \left[\lim_{m \to \infty} \int_0^{\tau \wedge m} e^{-rt} X_t \, dt \right] = \mathbb{E}_x \left[\int_0^{\tau} e^{-rt} X_t \, dt \right] \tag{5.3.2}$$

$$\mathbb{E}_x \left[\sum_{n=1}^{\infty} q \int_{\tau_n}^{\zeta_n} e^{-rt} X_t \, dt \right] = q \mathbb{E}_x \left[\sum_{n=1}^{\infty} \int_{\tau_n}^{\zeta_n} e^{-rt} X_t \, dt \right] = q \sum_{n=1}^{\infty} \mathbb{E}_x \left[\int_{\tau_n}^{\zeta_n} e^{-rt} X_t \, dt \right] \tag{5.3.3}$$

The discounted expected revenue (5.2.2) becomes:

$$\begin{aligned} V(x, L, U) = \textstyle\sum_{n=1}^{\infty} \Big\{ & \tfrac{q(x-\theta)}{r+\kappa} \mathbb{E}_x[e^{-(r+\kappa)\tau_n}] - \tfrac{q(x-\theta)}{r+\kappa} \mathbb{E}_x[e^{-(r+\kappa)\zeta_n}] \\ & - \left(C^u - \tfrac{q\theta}{r}\right) \mathbb{E}_x[e^{-r\tau_n}] - \left(C^d + \tfrac{q\theta}{r}\right) \mathbb{E}_x[e^{-r\zeta_n}] \Big\} \end{aligned} \tag{5.3.4}$$

In the case of $U \leq x$, the power plant is turned on at time 0, so $\tau_1 = 0$. $\mathbb{E}_x[e^{-\lambda \tau_n}]$ and $E_x[e^{-\lambda \zeta_n}]$ can be calculated explicitly. We have the following proposition:

Proposition 5.3.1. *When spark spread follows Ornstein-Uhlenbeck process (5.2.1), the value of a power plant operated according to a threshold policy* (L, U) *is given by:*

1. *When* $U > x$

$$\begin{aligned} V(x, L, U) = & \tfrac{q(x-\theta)}{r+\kappa} \delta_{r+\kappa} \left\{ \mathbb{E}_x[e^{-(r+\kappa)\tau_1}] - \mathbb{E}_x[e^{-(r+\kappa)\zeta_1}] \right\} \\ & - \delta_r \left\{ (C^u - \tfrac{q\theta}{r}) \mathbb{E}_x[e^{-r\tau_1}] + (C^d + \tfrac{q\theta}{r}) \mathbb{E}_x[e^{-r\zeta_1}] \right\} \end{aligned} \tag{5.3.5}$$

With $D_{-\nu}(x), \nu > 0$ being the parabolic cylinder function, and for $\lambda = r$ or $r + \kappa$:

$$\gamma = \sigma / \sqrt{2\theta}$$

$$\mathbb{E}_x[e^{-\lambda\tau_1}] = \frac{D_{-\lambda/\kappa}(-\frac{x-\theta}{\gamma})}{D_{-\lambda/\kappa}(-\frac{U-\theta}{\gamma})} e^{\frac{(x-\theta)^2-(U-\theta)^2}{4\gamma^2}}$$

$$\mathbb{E}_x[e^{-\lambda\zeta_1}] = \frac{D_{-\lambda/\kappa}(-\frac{x-\theta}{\gamma})\, D_{-\lambda/\kappa}(\frac{U-\theta}{\gamma})}{D_{-\lambda/\kappa}(-\frac{U-\theta}{\gamma})\, D_{-\lambda/\kappa}(\frac{L-\theta}{\gamma})} e^{\frac{(x-\theta)^2-(L-\theta)^2}{4\gamma^2}}$$

$$\delta_\lambda = \frac{1}{1 - \frac{D_{-\lambda/\kappa}(-\frac{L-\theta}{\gamma})\, D_{-\lambda/\kappa}(\frac{U-\theta}{\gamma})}{D_{-\lambda/\kappa}(-\frac{U-\theta}{\gamma})\, D_{-\lambda/\kappa}(\frac{L-\theta}{\gamma})}}$$

2. *When $U \le x$*

$$\begin{aligned} V(x, L, U) = \tfrac{q(x-\theta)}{r+\kappa} - (C^u - \tfrac{q\theta}{r}) + \tfrac{q(x-\theta)}{r+\kappa}\delta_{r+\kappa}\left\{\mathbb{E}_x[e^{-(r+\kappa)\tau_2}] - \mathbb{E}_x[e^{-(r+\kappa)\zeta_1}]\right\} \\ -\delta_r\left\{(C^u - \tfrac{q\theta}{r})\mathbb{E}_x[e^{-r\tau_2}] + (C^d + \tfrac{q\theta}{r})\mathbb{E}_x[e^{-r\zeta_1}]\right\} \end{aligned} \tag{5.3.6}$$

For $\lambda = r$ or $r + \kappa$, δ_λ is as above and

$$\mathbb{E}_x[e^{-\lambda\tau_2}] = \frac{D_{-\lambda/\kappa}(\frac{x-\theta}{\gamma})\, D_{-\lambda/\kappa}(-\frac{L-\theta}{\gamma})}{D_{-\lambda/\kappa}(-\frac{U-\theta}{\gamma})\, D_{\lambda/\kappa}(\frac{L-\theta}{\gamma})} e^{\frac{(x-\theta)^2-(U-\theta)^2}{4\gamma^2}}$$

$$\mathbb{E}_x[e^{-\lambda\zeta_1}] = \frac{D_{-\lambda/\kappa}(\frac{x-\theta}{\gamma})}{D_{-\lambda/\kappa}(\frac{L-\theta}{\gamma})} e^{\frac{(x-\theta)^2-(L-\theta)^2}{4\gamma^2}}$$

Proofs are given in Appendix C.1.

5.4 Discussion

The closed-form expression given in Proposition 5.3.1 for the value function can give us some insights into the power plant valuation problem. For example, in practice one often needs to decide the optimal threshold policy, or compute the power plant value for a given operation policy, or analyze the sensitivity of the plant value with respect to various model parameters. These will be quite difficult to achieve in other numerical approaches. But with the closed-form value formula of the power plant, solving these problems will involve only simple arithmetic computation.

Optimal threshold policy

The optimal threshold policy (L^*, U^*) is given by solving the constrained optimization problem numerically:

$$\max V(x, L, U)$$

$$s.t. \quad L - U \leq 0$$

This problem can be easily solved by any optimization software or by Karush Kuhn Tucker conditions:

$$\begin{cases} \frac{\partial(-V)}{\partial U} - \mu = 0 \\ \frac{\partial(-V)}{\partial L} + \mu = 0 \\ L - U \leq 0 \\ \mu(L - U) = 0 \\ \mu \geq 0 \end{cases} \tag{5.4.1}$$

Value under given threshold policy

The value of a power plant operated under a given threshold policy (L, U) is given explicitly in Proposition 5.3.1. This closed-from expression can serve as a valuable tool for real-time decision making.

Sensitivity analysis

Sensitivities of power plant value with respect to a model parameter can be obtained by differentiating the closed-form formulation in Proposition 5.3.1.

For instance: suppose start-up cost is a function of a parameter α. Given the definitions in Proposition 5.3.1, sensitivity of power plant value with respect to α is given by:

1. When $U > x$

$$\frac{\partial V(x, L, U)}{\partial \alpha} = -\delta_r \frac{\partial C^u}{\partial \alpha} \mathbb{E}_x[e^{-r\tau_1}] \tag{5.4.2}$$

2. When $U \leq x$

$$\frac{\partial V(x, L, U)}{\partial \alpha} = -\frac{\partial C^u}{\partial \alpha} - \delta_r \frac{\partial C^u}{\partial \alpha} \mathbb{E}_x[e^{-r\tau_2}] \tag{5.4.3}$$

Similarly, sensitivities of power plant value with respect to parameters of shut-down cost and parameters of spark spread price process can be calculated by pure algebraic manipulation. As an example, sensitivity of power plant value with respect to risk-adjusted long-term mean θ is given in Appendix C.3.

Furthermore, sensitivity of the optimal threshold policy with respect to a model parameter can be obtained by finite difference method. First, the optimal threshold policy for the original valuation problem is solved as in Section 5.4. Then a slightly different model with a small change in the parameter under study is solved. Sensitivity can then be derived.

5.5 Conclusion

In this chapter we develop a continuous-time formulation for power plant valuation in infinite time horizon. We propose a real-option-based model for a power plant to account for the embedded operational flexibility. This model incorporates the start-up and shutdown costs as two major operational constraints. Under this continuous valuation model, spark spread is modeled directly as a continuous stochastic process to take account of the long-term co-integration relationship between electricity and fuel prices. Instead of discretizing the stochastic process, we preserve continuity of the stochastic spark spread process and work directly with the value function. Under this model setup, closed form of value function under threshold policy is obtained by property of first hitting time of stochastic process and optional sampling theorem. The corresponding optimal operational strategy can then be solved. Compared with other numerical methods, this continuous-time model reduces computational complexity while at the same time incorporating major operation characteristics. It enables fast computation of a power plant value that approximates the real market value and sensitivity analysis of the asset value with respect to cost parameters of a power plant and the distribution parameters of spark spread.

CHAPTER VI

CONCLUSIONS AND FUTURE WORK

6.1 Summary of Conclusions

This thesis investigates three different approaches to real options valuation and contributes to aspects of modeling realism and computational efficiency. The contributions are illustrated through two important applications of real options in energy markets: natural gas storage and power plant valuation.

Because spread options are widely used in basic real options valuation techniques, the first part of the thesis addresses the problem of spread option pricing and hedging. We first develop a new closed-form approximation for pricing spread options. It is helpful for designing and analyzing real options that are decomposed as a series spread options or with embedded spread-option-like features. Numerical analysis demonstrates that our method is extremely fast as well as more accurate than existing analytical approximations. Closed-form approximations of Greeks are also derived to provide a valuable tool in financial applications such as dynamic hedging and Value-at-Risk calculations. As a byproduct, we also obtain lower and upper bounds for digital spread options by analyzing the exercise boundary and the price sensitivities of spread options.

We then generalize the above results for spread options on an arbitrary number of assets. Two new closed-form approximations for pricing are developed and proven to be very robust, fast, and accurate in numerical experiments. Because our methods enable the accurate pricing of a bulk volume of spread options on multiple assets with different contract specifications in real time, it offers traders a potential edge in financial markets. We also extend our results to hybrid spread-basket options. In addition, the Greeks of spread options can be efficiently approximated by our methods, especially the second order boundary

approximation.

Third, we develop a generalized Gaussian quadrature method to solve for the multi-stage stochastic problem in natural gas storage valuation. Under a market-based valuation framework with realistic operational characteristics, the GGQ method can efficiently give the dynamically optimal spot-trading strategy in speed about two orders of magnitude faster than Monte Carlo approach while keeping the same accuracy and flexibility in incorporating operational constraints. Furthermore, we are able to propose a novel hybrid trading strategy that successfully incorporates both spot and forward trading with this fast and flexible quadrature scheme.

Fourth, we investigate the power plant valuation problem as another important application of real options. We develop a continuous-time formulation for power plant valuation in infinite time horizon. A real-options-based model for a power plant is proposed to account for the embedded operational flexibility. This model incorporates the start-up and shut-down costs as two major operational constraints and models spark spread directly. We preserve continuity of the stochastic spark spread process and work directly with the value function. Closed-form of value function under threshold policy is obtained. The corresponding optimal operational strategy and sensitivity analysis of the asset value with respect to cost parameters of a power plant and the distribution parameters of spark spread can then be solved. This continuous-time formulation enables fast computation of a power plant value that approximates the real market value and sensitivities of the power plant value to various model parameters.

6.2 Future work

One can take several directions to extend and improve the results in this thesis:

For two-asset spread option pricing and hedging, first, our approximation is useful even if one wants to incorporate jumps in the price processes of the assets. Carmona and Durrleman (2003b) discuss in detail how the approximated price can be used in such cases.

Second, Li (2008) studies the correction to the exchange option price when the asset returns deviate from the jointly normal distribution using a bivariate Gram-Charlier approximation. His method can be extended to the spread option case if we couple it with our exercise boundary approximation. This will allow the pricing of spread options under arbitrary distributions that are close to jointly-normal. Finally, it is possible to further improve the accuracy of our method. For example, in our spread option approximation, we have set the expansion point to be $y_0 = 0$, that is, we have expanded around the point where the future log price of asset two equals its mean. This is a degree of freedom which we have not utilized. Preliminary numerical analysis suggests that the optimal expansion point y_0 seems to depend on the correlation coefficient ρ. Thus, relaxing y_0 may make our approximation even more accurate, especially when $|\rho|$ is large.

After extending the approximation method to multi-asset spread options pricing and hedging, there are two more directions to improve results. First, in the geometric Brownian motions case, our results can also be easily extended to incorporate jumps in the price processes of the assets. Second, the boundary approximation idea might be useful for pricing other types of more exotic derivatives. Third, it is interesting to consider the effect of non-normality on a multi-asset spread option.

For natural gas storage valuation problem, more numerical experiments can be made for different spot and forward price processes, especially multi-factor models and jump models. Second, the GGQ method can be applied for valuation and decision making not only in the natural gas storage market but also in many other commodity markets, such as the electricity, metal, and oil markets. Third, the hybrid trading strategy also is applicable to other markets in which both spot and forward trading are available.

For power plant valuation problem, modeling the electricity price by a more sophisticated and realistic model, such as jumps process, is a good direction to explore. The result obtained by Novikov (2004) of first passage time of Ornstein-Uhlenbeck processes with a

jump component can be used. For jump processes, the major difficulty lies in the "overshot" problem related to the threshold crossing. Second, we can extend our result to finite time horizon case. The method of Carr (1998) and Chen (2004)will be useful. Third, incorporating more realistic operational constraints, such as nonzero ramp-up and ramp-down time, minimal up or down time will make a more realistic valuation model. These issues are left to future research.

APPENDIX A

SPREAD OPTIONS PRICING AND HEDGING

Proof of Proposition 2.2.1:

The random variables X and Y are jointly normally distributed. Denote this density $n(x, y; \rho)$. The conditional density of X given $Y = y$ is $n(x; \rho y, 1-\rho^2)$, i.e., a normal density with mean ρy and variance $1 - \rho^2$. Thus, we can now compute the price of the digital spread option as follows:

$$\Pi^{\mathrm{D}} = e^{-rT} \int_{-\infty}^{\infty} \int_{-\infty}^{\infty} 1_{x \geq \underline{x}(y)} n(x, y; \rho) \mathrm{d}x \mathrm{d}y = e^{-rT} \int_{-\infty}^{\infty} n(y) \mathrm{d}y \int_{\underline{x}}^{\infty} n(x; \rho y, 1-\rho^2) \mathrm{d}x \quad \text{(A.0.1)}$$

$$= e^{-rT} \int_{-\infty}^{\infty} n(y) N(A(y)) \mathrm{d}y. \quad \text{(A.0.2)}$$

Similarly, the spread option price can be computed as

$$\Pi = e^{-rT} \int_{-\infty}^{\infty} \int_{-\infty}^{\infty} (e^{\nu_1 x + \mu_1} - e^{\nu_2 y + \mu_2} - K)^+ n(x, y; \rho) \mathrm{d}x \mathrm{d}y \quad \text{(A.0.3)}$$

$$= e^{-rT} \int_{-\infty}^{\infty} n(y) \mathrm{d}y \int_{\underline{x}}^{\infty} (e^{\nu_1 x + \mu_1} - e^{\nu_2 y + \mu_2} - K)\, n(x; \rho y, 1-\rho^2) \mathrm{d}x. \quad \text{(A.0.4)}$$

By virtue of the identity

$$\int_{x_0}^{\infty} e^{tx} n(x; \mu, \sigma^2) \mathrm{d}x = e^{\mu t + \sigma^2 t^2/2} N\left(\frac{\mu - x_0}{\sigma} + \sigma t\right), \quad \text{(A.0.5)}$$

the inner integral can be performed to yield

$$\Pi = e^{-rT} \int_{-\infty}^{\infty} n(y) e^{\rho y \nu_1 + (1-\rho^2)\nu_1^2/2 + \mu_1} N\left(A(y) + \sqrt{1-\rho^2}\nu_1\right) \mathrm{d}y \quad \text{(A.0.6)}$$

$$- e^{-rT} \int_{-\infty}^{\infty} n(y) e^{\nu_2 y + \mu_2} N(A(y))\, \mathrm{d}y \quad \text{(A.0.7)}$$

$$- e^{-rT} \int_{-\infty}^{\infty} n(y) K N(A(y))\, \mathrm{d}y. \quad \text{(A.0.8)}$$

It is very useful to perform a change of variable to the above equation to obtain

$$\Pi = e^{\nu_1^2/2+\mu_1-rT}\int_{-\infty}^{\infty} n(y)N\Big(A(y+\rho\nu_1) + \sqrt{1-\rho^2}\nu_1\Big)\mathrm{d}y \tag{A.0.9}$$

$$- e^{\nu_2^2/2+\mu_2-rT}\int_{-\infty}^{\infty} n(y)N\Big(A(y+\nu_2)\Big)\mathrm{d}y. \tag{A.0.10}$$

$$- Ke^{-rT}\int_{-\infty}^{\infty} n(y)N(A(y))\mathrm{d}y \tag{A.0.11}$$

$$\equiv e^{\nu_1^2/2+\mu_1-rT}\,\mathbf{I}_1 - e^{\nu_2^2/2+\mu_2-rT}\,\mathbf{I}_2 - Ke^{-rT}\,\mathbf{I}_3. \tag{A.0.12}$$

Mathematically, this is similar to a change of numeraire.

Proof of Proposition 2.2.2:

Define

$$F(a) \equiv \int_{-\infty}^{\infty} N(a+y)n(y)\mathrm{d}y, \quad G(b) \equiv \int_{-\infty}^{\infty} N(a+by)n(y)\mathrm{d}y. \tag{A.0.13}$$

Notice that

$$F(0) = \int_{-\infty}^{\infty} N(y)n(y)\mathrm{d}y = \int_{-\infty}^{\infty} N(y)\mathrm{d}N(y) = \frac{1}{2}, \tag{A.0.14}$$

and

$$F'(a) = \int_{-\infty}^{\infty} n(a+y)n(y)\mathrm{d}y = \frac{1}{2\sqrt{\pi}}\exp\left(-\frac{a^2}{4}\right) = \frac{1}{\sqrt{2}}\,n\left(\frac{a}{\sqrt{2}}\right). \tag{A.0.15}$$

Thus,

$$F(a) = F(0) + \int_0^a F'(a)\mathrm{d}a = N\left(\frac{a}{\sqrt{2}}\right). \tag{A.0.16}$$

We can compute

$$G(1) = F(a) = N\left(\frac{a}{\sqrt{2}}\right), \quad \text{and} \quad G'(b) = -\frac{ab}{(1+b^2)^{3/2}}n\left(\frac{a}{\sqrt{1+b^2}}\right). \tag{A.0.17}$$

Thus

$$\int_{-\infty}^{\infty} N(a+by)n(y)\mathrm{d}y = G(b) = G(1) + \int_1^b G'(b)\mathrm{d}b = N\left(\frac{a}{\sqrt{1+b^2}}\right). \tag{A.0.18}$$

The first integral in the lemma now follows immediately:

$$\int_{-\infty}^{\infty} N(a+by)n(y;\mu,\sigma^2)\mathrm{d}y = \int_{-\infty}^{\infty} N(a+b\mu+b\sigma z)n(z)\mathrm{d}z = N\left(\frac{a+b\mu}{\sqrt{1+b^2\sigma^2}}\right). \quad \text{(A.0.19)}$$

To prove the Margrabe formula, notice that when $K = 0$, we have

$$\underline{x}(y) = \frac{\nu_2 y + \mu_2 - \mu_1}{\nu_1}, \quad A(y) = \frac{\mu_1 - \mu_2}{\nu_1\sqrt{1-\rho^2}} + \frac{(\rho\nu_1 - \nu_2)}{\nu_1\sqrt{1-\rho^2}}y \equiv a + by. \quad \text{(A.0.20)}$$

By Proposition 3.1.1, we need to compute $\mathbf{I}_1$ and $\mathbf{I}_2$. Since the conditional moneyness $A(y)$ is linear, we can use equation (2.2.19). For example, to compute $\mathbf{I}_2$, we have

$$\mathbf{I}_2 = \int_{-\infty}^{\infty} N(A(y+\nu_2))n(y)\mathrm{d}y = \int_{-\infty}^{\infty} N(A(y))\, n(y;-\nu_2,1)\mathrm{d}y \quad \text{(A.0.21)}$$

$$= \int_{-\infty}^{\infty} N(a+by)\, n(y;-\nu_2,1)\mathrm{d}y = N\left(\frac{a-b\nu_2}{\sqrt{1+b^2}}\right) = N\left(\frac{\mu_1-\mu_2-(\nu_2^2-\rho\nu_1\nu_2)}{\sqrt{\nu_1^2+\nu_2^2-2\rho\nu_1\nu_2}}\right). \quad \text{(A.0.22)}$$

Similarly for $\mathbf{I}_1$.

Proof of Proposition 2.2.3:

This proposition follows from pure algebraic manipulation. In particular, we need to examine the first and second-order derivatives of $\underline{x}(y)$, $A(y)$ and $N(A(y))$ with respect to y.

Proof of Proposition 2.3.1:

This proposition follows immediately from equation (2.3.5) and Proposition 2.2.1.

Proof of Proposition 2.3.2:

With $B(y)$ defined in the text, we have

$$\mathbf{I}_3 = \int_{-\infty}^{\infty} n(y)N(A(y))\mathrm{d}y = \int_{-\infty}^{\infty} n(y)N(B(y))\mathrm{d}y + \int_{-\infty}^{\infty} n(y)(N(A(y)) - N(B(y)))\mathrm{d}y \tag{A.0.23}$$

$$\geq \int_{-\infty}^{\infty} n(y)N(B(y))\mathrm{d}y - \int_{-\infty}^{\infty} n(y)(N(A(y)) - N(B(y)))^{+}\mathrm{d}y \tag{A.0.24}$$

$$= N\Big(\frac{P}{\sqrt{1+Q^2}}\Big) - \int_{-\infty}^{y_l} n(y)(N(A(y)) - N(B(y)))\mathrm{d}y - \int_{y_r}^{\infty} n(y)(N(A(y)) - N(B(y)))\mathrm{d}y. \tag{A.0.25}$$

The upper bound is approximated by replacing $N(B(y))$ with 1. When $\rho \leq 0$ or $\rho \geq \nu_2/\nu_1$, we can use Proposition 2.2.3 to tighten up the bound.

Proof of Proposition 2.4.1:

We will consider the last term for the spread option first.

$$\mathbf{I}_3 = \int_{-\infty}^{\infty} n(y)N(A(y))\mathrm{d}y \approx \int_{-\infty}^{\infty} n(y)N(C^3 + D^3y + \epsilon y^2)\mathrm{d}y. \tag{A.0.26}$$

This integral can not be performed. However, if the curvature ϵ is small around the expansion point $y = y_0$, then we can expand the above integral around $\epsilon = 0$. Since,

$$\frac{\mathrm{d}N(C^3 + D^3y + \epsilon y^2)}{\mathrm{d}\epsilon} = n(C^3 + D^3y + \epsilon y^2)y^2, \tag{A.0.27}$$

$$\frac{\mathrm{d}^2N(C^3 + D^3y + \epsilon y^2)}{\mathrm{d}\epsilon^2} = -(C^3 + D^3y + \epsilon y^2)n(C^3 + D^3y + \epsilon y^2)y^4, \tag{A.0.28}$$

we have

$$\mathbf{I}_3 \approx \mathbf{J}_0 + \mathbf{J}_1\epsilon + \frac{1}{2}\mathbf{J}_2\epsilon^2, \tag{A.0.29}$$

where

$$\mathbf{J}_0 = \int_{-\infty}^{\infty} n(y)N(C^3 + D^3y)\mathrm{d}y, \tag{A.0.30}$$

$$\mathbf{J}_1 = \int_{-\infty}^{\infty} n(y)n(C^3 + D^3y)y^2\mathrm{d}y, \tag{A.0.31}$$

$$\mathbf{J}_2 = -\int_{-\infty}^{\infty} n(y)(C^3 + D^3y)n(C^3 + D^3y)y^4\mathrm{d}y, \tag{A.0.32}$$

The $\mathbf{J}_i$'s can be computed to give the expressions in the proposition. In particular, $\mathbf{J}_0$ can be computed using Proposition 2.2.2. The integrals $\mathbf{I}_1$ and $\mathbf{I}_2$ can be treated similarly. However, in Proposition 2.2.1, the expansion points for $\mathbf{I}_1$ and $\mathbf{I}_2$ are chosen to be $y_0 - \rho\nu_1$ and $y_0 - \nu_2$, respectively. This amounts to using the same expansion point y_0 for all three terms in equation (A.0.4).

Proof of Proposition 2.4.2:

The first four statements can be proven by differentiating either equations (A.0.6) to (A.0.8) or the expression for Π in Proposition 2.2.1. The algebra is tedious and omitted here. Statement 5 and 6 are shown in Carmona and Durrleman (2003a).

Proof of Proposition 2.4.3:

Notice that in the geometric Brownian motions cases, we have equation (2.2.5) for the μ_i's. The first statement follows from directly differentiating the expression of Π in Proposition 2.2.1. Notice that by definition, when $x = \underline{x}(y)$, we have $e^{\sigma_1\sqrt{T}x+\mu_1} - e^{\sigma_2\sqrt{T}y+\mu_2} - K = 0$. Statement 2 follows from Proposition 2.4.2 directly. A proof of statement 3 is contained in Carmona and Durrleman (2003a). Finally, statement 4 follows from directly differentiating the expression of Π in Proposition 2.2.1 and simplifying. We will take $\mathcal{V}_2$ as an example. Notice that for the geometric Brownian motions case, equation (A.0.4) becomes

$$\Pi = e^{-rT}\int_{-\infty}^{\infty} n(y)\mathrm{d}y \int_{\underline{x}}^{\infty} \left(e^{\nu_1 x+\mu_1} - S_2 e^{\sigma_2\sqrt{T}y+(r-q-\sigma_2^2/2)T} - K\right) n(x;\rho y, 1-\rho^2)\mathrm{d}x. \quad \text{(A.0.33)}$$

The derivative of Π with respect to σ_2 has two terms: one arising from the dependence of the lower inner integration limit $\underline{x}(y)$ on σ_2 and another arising from the term $e^{\sigma_2\sqrt{T}y+(r-q-\sigma_2^2/2)T}$. Differentiating on the integration limit gives 0 since by definition of the exercise boundary

$$e^{\nu_1\underline{x}(y)+\mu_1} - S_2 e^{\sigma_2\sqrt{T}y+(r-q-\sigma_2^2/2)T} - K = 0. \quad \text{(A.0.34)}$$

Thus,

$$\frac{\partial \Pi}{\partial \sigma_2} = -e^{-rT} \int_{-\infty}^{\infty} n(y)\sqrt{T}(y - \sigma_2\sqrt{T})\mathrm{d}y \int_{\underline{x}}^{\infty} S_2 e^{\sigma_2\sqrt{T}y + (r-q-\sigma_2^2/2)T}\, n(x; \rho y, 1-\rho^2)\mathrm{d}x \tag{A.0.35}$$

$$= -e^{-rT} \int_{-\infty}^{\infty} n(y)\sqrt{T}(y - \sigma_2\sqrt{T}) S_2 e^{\sigma_2\sqrt{T}y + (r-q-\sigma_2^2/2)T} N(A(y))\mathrm{d}y. \tag{A.0.36}$$

Completing the square like we did in the proof of Proposition 2.2.1 now gives

$$\frac{\partial \Pi}{\partial \sigma_2} = -S_2\sqrt{T} \int_{-\infty}^{\infty} n(y; \sigma_2\sqrt{T}, 1)(y - \sigma_2\sqrt{T}) N(A(y))\mathrm{d}y. \tag{A.0.37}$$

Finally, a change of variable gives the final expression for $\mathcal{V}_2$ in the proposition

$$\frac{\partial \Pi}{\partial \sigma_2} = -S_2\sqrt{T} \int_{-\infty}^{\infty} n(y) y N(A(y + \sigma_2\sqrt{T}))\mathrm{d}y. \tag{A.0.38}$$

The expression for $\mathcal{V}_1$ is more complicated because differentiating Π in equation (A.0.33) with respect to σ_1 will give

$$\frac{\partial \Pi}{\partial \sigma_1} = e^{-rT} \int_{-\infty}^{\infty} n(y)\mathrm{d}y \int_{\underline{x}}^{\infty} \sqrt{T}(x - \nu_1) e^{\nu_1 x + \mu_1} n(x; \rho y, 1-\rho^2)\mathrm{d}x \tag{A.0.39}$$

and the factor $x - \nu_1$ contributes to the inner integration. If we now let $z \equiv (x - \rho y)/\sqrt{1-\rho^2}$, then we have

$$\frac{\partial \Pi}{\partial \sigma_1} = \sqrt{T} e^{-rT} \int_{-\infty}^{\infty} n(y) e^{\rho\nu_1 y + \mu_1}\mathrm{d}y \int_{-A(y)}^{\infty} (\sqrt{1-\rho^2}z + \rho y - \nu_1) e^{\sqrt{1-\rho^2}\nu_1 z} n(z)\mathrm{d}z. \tag{A.0.40}$$

By virtue of equation (A.0.5),

$$\int_{-A(y)}^{\infty} e^{\sqrt{1-\rho^2}\nu_1 z} n(z)\mathrm{d}z = e^{\nu_1^2(1-\rho^2)/2} N\left(A(y) + \nu_1\sqrt{1-\rho^2}\right). \tag{A.0.41}$$

Integration by parts using $n'(z) = -zn(z)$ gives

$$\int_{-A(y)}^{\infty} z e^{\sqrt{1-\rho^2}\nu_1 z} n(z)\mathrm{d}z = e^{\nu_1(\underline{x}(y) - \rho y)} n(A(y)) + \nu_1\sqrt{1-\rho^2} e^{\nu_1^2(1-\rho^2)/2} N\left(A(y) + \nu_1\sqrt{1-\rho^2}\right). \tag{A.0.42}$$

Substituting the last two equations into (A.0.40), simplifying, and performing a last change of variable $w = y - \rho\nu_1$ gives the expression for $\mathcal{V}_1$ in the proposition.

For the signs of vegas, notice that $\mathcal{V}_1$ is positive whenever

$$\rho \int_{-\infty}^{\infty} n(y) y N(A(y+\rho\nu_1) + \sqrt{1-\rho^2}\nu_1)\mathrm{d}y$$
$$= \rho \int_{0}^{\infty} n(y) y \Big(N(A(y+\rho\nu_1) + \sqrt{1-\rho^2}\nu_1) - N(A(-y+\rho\nu_1) + \sqrt{1-\rho^2}\nu_1) \Big) \mathrm{d}y \quad \text{(A.0.43)}$$

is positive. By Proposition 2.2.3, $\rho N(A(y+\rho\nu_1) + \sqrt{1-\rho^2}\nu_1)$ is an increasing function when $\rho \leq 0$ or when $\rho \geq \sigma_2/\sigma_1$. From the above equation, $\mathcal{V}_1 \geq 0$ when $\rho \leq 0$ or when $\rho \geq \sigma_2/\sigma_1$. Similarly,

$$\mathcal{V}_2 \equiv \frac{\partial \Pi}{\partial \sigma_2} = -S_2\sqrt{T}\int_{-\infty}^{\infty} n(y) y N(A(y+\nu_2))\mathrm{d}y \quad \text{(A.0.44)}$$
$$= -S_2\sqrt{T}\int_{0}^{\infty} n(y) y \Big(N(A(y+\nu_2)) - N(A(-y+\nu_2)) \Big) \mathrm{d}y. \quad \text{(A.0.45)}$$

This integral is positive when $\rho \geq 0$ and negative when $\rho \geq \sigma_2/\sigma_1$. Alternatively, one could apply Chebyshev's algebraic inequality on equation (A.0.44). See, for example, Chapter IX of Mitrinovic, Pecaric and Fink (1992).

Proof of Proposition 2.4.4:

Statement 1 follows from Proposition 2.4.3. For statement 2, we will only derive the approximation for Γ_{11} since the other gamma's are similar. We have

$$\Gamma_{11} \equiv \frac{\partial^2 \Pi}{\partial S_1^2} = \frac{\partial \Delta_1}{\partial S_1} = \frac{\partial}{\partial S_1}\int_{-\infty}^{\infty} n(y) N(A(y+\rho\nu_1) + \sqrt{1-\rho^2}\nu_1)\mathrm{d}y \quad \text{(A.0.46)}$$
$$\approx \frac{\partial}{\partial S_1}\int_{-\infty}^{\infty} n(y) N(C^1 + D^1 y + \epsilon y^2)\mathrm{d}y \quad \text{(A.0.47)}$$
$$\approx \int_{-\infty}^{\infty} n(y) n(C^1 + D^1 y + E' y^2)(C^1_{S_1} + D^1_{S_1} y + \epsilon_{S_1} y^2)\mathrm{d}y \quad \text{(A.0.48)}$$
$$\approx \int_{-\infty}^{\infty} n(y) n(C^1 + D^1 y)(C^1_{S_1} + D^1_{S_1} y + \epsilon_{S_1} y^2)\mathrm{d}y = \Phi(C^1, D^1, C^1_{S_1}, D^1_{S_1}, \epsilon_{S_1}), \quad \text{(A.0.49)}$$

where the function Φ can be computed analytically to give the expression in the proposition. The Greek $\mathcal{V}_1$ can be computed similarly. The approximation for $\mathcal{V}_2$ is developed similarly using the last statement in Proposition 2.4.3.

Proof of Proposition 2.5.1:

This proposition follows from brute-force calculation. We also verified the statements using both Mathematica and MATLAB. We sketch the proof below. Let $Z = (B - \mu_B)/\sigma_B$ be the standardized random variable of B. Then the Gram-Charlier density for Z is given by

$$f_Z^{\mathrm{GC}}(z) = n(z)\left(1 + \frac{\gamma_B}{3!}h_3(z) + \frac{\kappa_B}{4!}h_4(z)\right), \tag{A.0.50}$$

where $h_3(\cdot)$ and $h_4(\cdot)$ are Hermite polynomials of order 3 and 4, respectively. The option price under this Gram-Charlier density can be computed by direct integration to give equation (2.5.5). Finally, the following fact is useful in the computation of γ_B and κ_B. Let X and Y be jointly normal with means μ_X and μ_Y, variances σ_X^2 and σ_Y^2, and correlation coefficient ρ. For any real numbers t and s, the joint moment generating function is given by

$$\mathbb{E}[e^{tX+sY}] = \exp\left(t\mu_X + s\mu_Y + \frac{1}{2}t^2\sigma_X^2 + \frac{1}{2}s^2\sigma_Y^2 + \rho st\sigma_X\sigma_Y\right). \tag{A.0.51}$$

Proof of Proposition 3.1.1:

The conditional density of X given $Y = \mathbf{y}$ is $\phi(x; \mu_{x|\mathbf{y}}, \Sigma_{x|\mathbf{y}})$. By formula for the determinants for partitioned matrix, we have $\Sigma_{x|\mathbf{y}} \neq 0$ since

$$\det \boldsymbol{\Sigma} = \det(\boldsymbol{\Sigma}_{11} - \boldsymbol{\Sigma}_{\mathbf{10}}\boldsymbol{\Sigma}'_{\mathbf{10}}) = (\det(\boldsymbol{\Sigma}_{11}))^{-1}\Sigma_{x|\mathbf{y}} \neq 0.$$

Thus, we can compute the price of the spread option as follows:

$$\begin{aligned}\Pi &= e^{-rT}\int_{\mathbb{R}^N}\int_{\mathbb{R}}\left(e^{\nu_0 x+\mu_0} - \sum_{k=1}^{N} e^{\nu_k y_k+\mu_k} - K\right)^+ \phi(\{x, \mathbf{y}\}; \mathbf{0}, \boldsymbol{\Sigma})\mathrm{d}x\mathrm{d}\mathbf{y} \\ &= e^{-rT}\int_{\mathbb{R}^N}\phi(\mathbf{y}; \mathbf{0}, \boldsymbol{\Sigma}_{\mathbf{11}})\mathrm{d}\mathbf{y}\int_{\underline{x}(\mathbf{y})}^{\infty}\left(e^{\nu_0 x+\mu_0} - \sum_{k=1}^{N} e^{\nu_k y_k+\mu_k} - K\right)\phi(x; \mu_{x|\mathbf{y}}, \Sigma_{x|\mathbf{y}})\mathrm{d}x.\end{aligned}$$

By virtue of the identity

$$\int_{x_0}^{\infty} e^{tx}n(x; \mu, \sigma^2)\mathrm{d}x = e^{\mu t+\sigma^2 t^2/2}\Phi\left(\frac{\mu - x_0}{\sigma} + \sigma t\right), \tag{A.0.52}$$

the inner integral can be performed to yield

$$\begin{aligned}\Pi = \; & e^{\frac{1}{2}\nu_0^2\Sigma_{x|\mathbf{y}}+\mu_0-rT}\int_{\mathbb{R}^N} e^{\nu_0\mu_{x|\mathbf{y}}}\,\phi(\mathbf{y};\mathbf{0},\boldsymbol{\Sigma_{11}})\,\Phi\Big(A(\mathbf{y})+\nu_0\sqrt{\Sigma_{x|\mathbf{y}}}\Big)\mathrm{d}\mathbf{y}\\ & -\sum_{k=1}^{N} e^{-rT}\int_{\mathbb{R}^N} e^{\nu_k y_k+\mu_k}\,\phi(\mathbf{y};\mathbf{0},\boldsymbol{\Sigma_{11}})\,\Phi\Big(A(\mathbf{y})\Big)\mathrm{d}\mathbf{y}\\ & -Ke^{-rT}\int_{\mathbb{R}^N}\phi(\mathbf{y};\mathbf{0},\boldsymbol{\Sigma_{11}})\,\Phi\Big(A(\mathbf{y})\Big)\mathrm{d}\mathbf{y}. \qquad \text{(A.0.53)}\end{aligned}$$

Completing the square after a change of variable $\mathbf{z} = \mathbf{y} - \nu_0\boldsymbol{\Sigma_{10}}$ gives

$$\begin{aligned}& e^{\frac{1}{2}\nu_0^2\Sigma_{x|\mathbf{y}}+\mu_0-rT}\int_{\mathbb{R}^N} e^{\nu_0\mu_{x|\mathbf{y}}}\,\phi(\mathbf{y};\mathbf{0},\boldsymbol{\Sigma_{11}})\,\Phi\Big(A(\mathbf{y})+\nu_0\sqrt{\Sigma_{x|\mathbf{y}}}\Big)\mathrm{d}\mathbf{y}\\ &= e^{-rT+\mu_0+\frac{1}{2}\nu_0^2}\int_{\mathbb{R}^N}\phi(\mathbf{z};\mathbf{0},\boldsymbol{\Sigma_{11}})\Phi\Big(A(\mathbf{z}+\nu_0\boldsymbol{\Sigma_{10}})+\nu_0\sqrt{\Sigma_{x|\mathbf{y}}}\Big)\mathrm{d}\mathbf{z}.\end{aligned}$$

Similarly, a change of variable $\mathbf{z} = \mathbf{y} - \nu_k\boldsymbol{\Sigma_{11}}\mathbf{e_k}$, for $k = 1, 2, \cdots, N$, gives

$$\begin{aligned}& e^{-rT}\int_{\mathbb{R}^N} e^{\nu_k y_k+\mu_k}\,\phi(\mathbf{y};\mathbf{0},\boldsymbol{\Sigma_{11}})\,\Phi\Big(A(\mathbf{y})\Big)\mathrm{d}\mathbf{y}\\ &= e^{-rT+\mu_k+\frac{1}{2}\nu_k^2}\int_{\mathbb{R}^N}\phi(\mathbf{z};\mathbf{0},\boldsymbol{\Sigma_{11}})\Phi\Big(A(\mathbf{z}+\nu_k\boldsymbol{\Sigma_{11}}\mathbf{e_k})\Big)\mathrm{d}\mathbf{z}.\end{aligned}$$

Collecting terms, we get the expressions in Proposition 3.1.1.

Proof of Proposition 3.2.1:

Consider a spread option on two assets with final payoff $(S_0(T) - L(T) - K)^+$, where $\log S_0(T)$ and $\log L(T)$ are jointly normal with means μ_0, μ_a, variances ν_0^2, ν_a^2, and correlation ρ_a. Then the two-asset Kirk approximation for the spread option price is given by

$$e^{\mu_0+\frac{1}{2}\nu_0^2-rT}\Phi(d_1) - (e^{\mu_a+\frac{1}{2}\nu_a^2-rT} + Ke^{-rT})\Phi(d_2),$$

where

$$d_1 = \frac{1}{\nu_K}\log\Big(\frac{e^{\mu_0+\frac{1}{2}\nu_0^2-rT}}{e^{\mu_a+\frac{1}{2}\nu_a^2-rT}+Ke^{-rT}}\Big)+\frac{1}{2}\nu_K, \quad d_2 = d_1-\nu_K,$$

with

$$\nu_K = \sqrt{\nu_0^2+m^2\nu_a^2-2m\rho_a\nu_0\nu_a} \quad \text{and} \quad m = \frac{e^{\mu_a+\frac{1}{2}\nu_a^2-rT}}{e^{\mu_a+\frac{1}{2}\nu_a^2-rT}+Ke^{-rT}}.$$

To apply the above result for multi-asset spread options with payoff $(S_0(T) - \sum_{k=1}^N S_N(T) - K)^+$, we let $L(T) = \sum_{k=1}^N S_k(T)$.

A common technique is to approximate the arithmetic average $\sum_{k=1}^N S_k(T)/N$ by the geometric average $\prod_{k=1}^N S_k(T)^{1/N}$.

For ν_a, notice that

$$\begin{aligned}\nu_a^2 &= \mathrm{Var}(\log L(T)) \approx \mathrm{Var}\Big(\log\big(N\prod_{k=1}^N S_k(T)^{1/N}\big)\Big)\\ &= \mathrm{Var}\Big(\frac{1}{N}\sum_{k=1}^N \log S_k(T)\Big) = \frac{1}{N^2}\sum_{i=1}^N\sum_{j=1}^N \rho_{i,j}\nu_i\nu_j.\end{aligned}$$

For ρ_a, notice that

$$\begin{aligned}\rho_a &= \frac{1}{\nu_0\nu_a}\mathrm{Cov}(\log S_0(T), \log L(T)) \approx \frac{1}{\nu_0\nu_a}\mathrm{Cov}\Big(\log S_0(T), \log\prod_{k=1}^N S_k(T)^{\frac{1}{N}}\Big)\\ &= \frac{1}{\nu_0\nu_a}\mathrm{Cov}\Big(\log S_0(T), \frac{1}{N}\sum_{k=1}^N \log S_k(T)\Big) = \frac{1}{N\nu_a}\sum_{k=1}^N \rho_{0,k}\nu_k.\end{aligned}$$

To compute μ_a, notice that since $\log L(T)$ is approximated normally distributed with mean μ_a and variance ν_a^2, we have $\mathbb{E}\, e^{\log L(T)} \approx e^{\mu_a + \nu_a^2/2}$. Thus,

$$\mu_a \approx \log \mathbb{E}\, e^{\log L(T)} - \frac{1}{2}\nu_a^2 = \log \mathbb{E}\sum_{k=1}^N S_k(T) - \frac{1}{2}\nu_a^2 = \log\Big(\sum_{k=1}^N e^{\mu_k + \frac{\nu_k^2}{2}}\Big) - \frac{1}{2}\nu_a^2.$$

The final step of the proof involves simplifying the expressions for m and m_0 using the expression for μ_a.

Proof of Proposition 3.2.2:

This proposition follows directly from Taylor expanding the exercise boundary (3.1.9) to second order in $\mathbf{y}$ around $\mathbf{y} = \mathbf{0}$:

$$\begin{aligned}(\nabla \underline{x}|_{\mathbf{0}})_k &= \frac{\partial \underline{x}}{\partial y_k}\bigg|_{\mathbf{0}} = \frac{e^{\mu_k}\nu_k}{\nu_0(R+K)}, \quad k = 1, 2, \cdots, N\\ (\nabla^2 \underline{x}|_{\mathbf{0}})_{i,j} &= \frac{\partial^2 \underline{x}}{\partial y_i \partial y_j}\bigg|_{\mathbf{0}} = -\frac{\nu_i\nu_j e^{\mu_i+\mu_j}}{\nu_0(R+K)^2} + \delta_{i,j}\frac{\nu_j^2 e^{\mu_j}}{\nu_0(R+K)}, \quad i, j = 1, 2, \cdots, N.\end{aligned}$$

Proof of Proposition 3.2.3:

From Proposition 3.1.1, we have

$$\Pi = e^{-rT+\mu_0+\frac{1}{2}\nu_0^2}\,\mathbf{I}_0 - \sum_{k=1}^{N} e^{-rT+\mu_k+\frac{1}{2}\nu_k^2}\,\mathbf{I}_k - Ke^{-rT}\,\mathbf{I}_{N+1}.$$

First, by Proposition 3.2.2, $A(\mathbf{y}) \approx c + \mathbf{d}'\mathbf{y} + \mathbf{y}'\mathbf{E}\mathbf{y}$. Next, we treat $\mathbf{y}'\mathbf{E}\mathbf{y}$ as an independent quantity from $c + \mathbf{d}'\mathbf{y}$ and expand $\Phi(A(\mathbf{y})) \approx \Phi(c + \mathbf{d}'\mathbf{y} + \mathbf{y}'\mathbf{E}\mathbf{y})$ to second order in $\mathbf{y}'\mathbf{E}\mathbf{y}$ around

$$\mathbf{y}'\mathbf{E}\mathbf{y} = \epsilon = \int_{\mathbb{R}^N} \phi(\mathbf{y}; \mathbf{0}, \mathbf{\Sigma_{11}})\mathbf{y}'\mathbf{E}\mathbf{y}\mathrm{d}\mathbf{y} = tr(\mathbf{F}).$$

Since

$$\left.\frac{\mathrm{d}\Phi(c + \mathbf{d}'\mathbf{y} + \mathbf{y}'\mathbf{E}\mathbf{y})}{\mathrm{d}\mathbf{y}'\mathbf{E}\mathbf{y}}\right|_{\mathbf{y}'\mathbf{E}\mathbf{y}=\epsilon} = \phi(c + \epsilon + \mathbf{d}'\mathbf{y}),$$
$$\left.\frac{\mathrm{d}^2\Phi(c + \mathbf{d}'\mathbf{y} + \mathbf{y}'\mathbf{E}\mathbf{y})}{\mathrm{d}(\mathbf{y}'\mathbf{E}\mathbf{y})^2}\right|_{\mathbf{y}'\mathbf{E}\mathbf{y}=\epsilon} = -(c + \epsilon + \mathbf{d}'\mathbf{y})\,\phi(c + \epsilon + \mathbf{d}'\mathbf{y}),$$

we have

$$\begin{aligned}
\mathbf{I}_{N+1} &= \int_{\mathbb{R}^N} \phi(\mathbf{y}; \mathbf{0}, \mathbf{\Sigma_{11}})\Phi(A(\mathbf{y}))\mathrm{d}\mathbf{y} && \text{(A.0.54)}\\
&\approx \int_{\mathbb{R}^N} \phi(\mathbf{y}; \mathbf{0}, \mathbf{\Sigma_{11}})\Phi(c + \mathbf{d}'\mathbf{y} + \mathbf{y}'\mathbf{E}\mathbf{y})\mathrm{d}\mathbf{y} && \text{(A.0.55)}\\
&\approx \int_{\mathbb{R}^N} \phi(\mathbf{y}; \mathbf{0}, \mathbf{\Sigma_{11}})\Big[\Phi(c + \epsilon + \mathbf{d}'\mathbf{y}) + \phi(c + \epsilon + \mathbf{d}'\mathbf{y})(\mathbf{y}'\mathbf{E}\mathbf{y} - \epsilon) && \text{(A.0.56)}\\
&\quad - \frac{1}{2}(c + \epsilon + \mathbf{d}'\mathbf{y})\,\phi(c + \epsilon + \mathbf{d}'\mathbf{y})(\mathbf{y}'\mathbf{E}\mathbf{y} - \epsilon)^2\Big]\mathrm{d}\mathbf{y} && \text{(A.0.57)}\\
&\equiv \mathbf{J}^0_{N+1} + \mathbf{J}^1_{N+1} - \frac{1}{2}\mathbf{J}^2_{N+1}, && \text{(A.0.58)}
\end{aligned}$$

where

$$\begin{aligned}
\mathbf{J}^0_{N+1} &= \int_{\mathbb{R}^N} \phi(\mathbf{y}; \mathbf{0}, \mathbf{\Sigma_{11}})\Phi(c + \epsilon + \mathbf{d}'\mathbf{y})\mathrm{d}\mathbf{y},\\
\mathbf{J}^1_{N+1} &= \int_{\mathbb{R}^N} \phi(\mathbf{y}; \mathbf{0}, \mathbf{\Sigma_{11}})\,\phi(c + \epsilon + \mathbf{d}'\mathbf{y})\,(\mathbf{y}'\mathbf{E}\mathbf{y} - \epsilon)\mathrm{d}\mathbf{y},\\
\mathbf{J}^2_{N+1} &= \int_{\mathbb{R}^N} \phi(\mathbf{y}; \mathbf{0}, \mathbf{\Sigma_{11}})(c + \epsilon + \mathbf{d}'\mathbf{y})\,\phi(c + \epsilon + \mathbf{d}'\mathbf{y})(\mathbf{y}'\mathbf{E}\mathbf{y} - \epsilon)^2\mathrm{d}\mathbf{y}.
\end{aligned}$$

For $\mathbf{J}^0_{N+1}$, a change of variable $w = \mathbf{d}'\mathbf{y}$ gives

$$\mathbf{J}^0_{N+1} = \int_{\mathbb{R}} \phi(w; 0, \mathbf{d}'\boldsymbol{\Sigma}_{\mathbf{11}}\mathbf{d})\Phi(c + \epsilon + w)\mathrm{d}w. \tag{A.0.59}$$

The following result in Li (2007) is very useful and we refer readers to Li (2007) for a proof:

$$\int_{-\infty}^{\infty} \Phi(a + by)\phi(y; \mu, \sigma^2)\,\mathrm{d}y = \Phi\Big(\frac{a + b\mu}{\sqrt{1 + b^2\sigma^2}}\Big).$$

With the help of the above identity, the integral in (A.0.59) can be performed to give

$$\mathbf{J}^0_{N+1} = \Phi\Big(\frac{c + \epsilon}{\sqrt{1 + \mathbf{d}'\boldsymbol{\Sigma}_{\mathbf{11}}\mathbf{d}}}\Big) = \Phi\Big(\frac{c_{N+1}}{\sqrt{1 + \mathbf{d}'_{N+1}\mathbf{d}_{N+1}}}\Big) = \mathbf{J}^0(c_{N+1}, \mathbf{d}_{N+1}). \tag{A.0.60}$$

For $\mathbf{J}^1_{N+1}$, a change of variable $\mathbf{z} = \boldsymbol{\Sigma}_{\mathbf{11}}^{-\frac{1}{2}}\mathbf{y}$ gives

$$\mathbf{J}^1_{N+1} = \int_{\mathbb{R}^N} \phi(\mathbf{z}; \mathbf{0}, \mathbf{I})\ \phi(c + \epsilon + \mathbf{d}'_{N+1}\mathbf{z})\ (\mathbf{z}'\mathbf{F}\mathbf{z} - \epsilon)\mathrm{d}\mathbf{z} \tag{A.0.61}$$

$$= \int_{\mathbb{R}^N} \phi(\mathbf{z}; \mathbf{0}, \mathbf{I})\ \phi(c + \epsilon + \mathbf{d}'_{N+1}\mathbf{z})\ (\mathbf{z}'\mathbf{F}\mathbf{z})\mathrm{d}\mathbf{z} - \frac{\epsilon}{\sqrt{1 + \mathbf{d}'_{N+1}\mathbf{d}_{N+1}}}\ \phi\Big(\frac{c_{N+1}}{\sqrt{1 + \mathbf{d}'_{N+1}\mathbf{d}_{N+1}}}\Big). \tag{A.0.62}$$

We now perform a second change of variable $\mathbf{z} = \mathbf{a} + \mathbf{P}\mathbf{w}$, where

$$\mathbf{P} = (\mathbf{I} + \mathbf{d}_{N+1}\mathbf{d}'_{N+1})^{-1/2}, \quad \mathbf{a} = -(c + \epsilon)\mathbf{P}^2\mathbf{d}_{N+1}.$$

This choice of $\mathbf{P}$ and $\mathbf{a}$ gives

$$(c + \epsilon + \mathbf{d}'_{N+1}\mathbf{z})^2 + |\mathbf{z}|^2 = |\mathbf{w}|^2.$$

The determinant of the Jacobian is given by

$$\det\Big|\frac{\mathrm{d}\mathbf{z}}{\mathrm{d}\mathbf{w}}\Big| = \det\mathbf{P} = (1 + \mathbf{d}'_{N+1}\mathbf{d}_{N+1})^{-1/2},$$

where we have used Schur's formula: $\det(\mathbf{I} + \mathbf{d}_{N+1}\mathbf{d}'_{N+1}) = 1 + \mathbf{d}'_{N+1}\mathbf{d}_{N+1}$. Completing the square in equation (A.0.61), we can simplify $\mathbf{J}^1_{N+1}$ to

$$\mathbf{J}^1_{N+1} = \frac{\phi\Big(\frac{c}{\sqrt{1+\mathbf{d}'_{N+1}\mathbf{d}_{N+1}}}\Big)}{\sqrt{1 + \mathbf{d}'_{N+1}\mathbf{d}_{N+1}}}\Big(\int_{\mathbb{R}^N} \phi(\mathbf{w}; \mathbf{0}, \mathbf{I})\ (\mathbf{a} + \mathbf{P}\mathbf{w})'\mathbf{F}(\mathbf{a} + \mathbf{P}\mathbf{w})\mathrm{d}\mathbf{w} - \epsilon\Big).$$

Let $\mathbf{W}$ be a random variable with density $\phi(\mathbf{w}; \mathbf{0}, \mathbf{I})$, then

$$\mathbb{E}[\mathbf{W}_i] = 0, \quad \mathbb{E}[\mathbf{W}_i\mathbf{W}_j] = \delta_{i,j}, \quad \mathbb{E}[\mathbf{W}_i\mathbf{W}_j\mathbf{W}_k] = 0,$$
$$\mathbb{E}[\mathbf{W}_i\mathbf{W}_j\mathbf{W}_k\mathbf{W}_l] = \delta_{i,j}\delta_{k,l} + \delta_{i,k}\delta_{j,l} + \delta_{i,l}\delta_{j,k}, \quad \mathbb{E}[\mathbf{W}_i\mathbf{W}_j\mathbf{W}_k\mathbf{W}_l\mathbf{W}_m] = 0.$$

Thus, with λ given in the text, we have

$$\mathbb{E}(\mathbf{a} + \mathbf{PW})'\mathbf{F}(\mathbf{a} + \mathbf{PW}) - tr(\mathbf{F}) = \lambda = \lambda(c_{N+1}, \mathbf{d}_{N+1}),$$

and

$$\mathbf{J}^1_{N+1} = \frac{\lambda(c_{N+1}, \mathbf{d}_{N+1})}{\sqrt{1 + \mathbf{d}'_{N+1}\mathbf{d}_{N+1}}}\,\phi\Big(\frac{c_{N+1}}{\sqrt{1 + \mathbf{d}'_{N+1}\mathbf{d}_{N+1}}}\Big) = \mathbf{J}^1(c_{N+1}, \mathbf{d}_{N+1}).$$

For $\mathbf{J}^2_{N+1}$, similar changes of variable give

$$\begin{aligned}\mathbf{J}^2_{N+1} = \frac{\phi\Big(\frac{c_{N+1}}{\sqrt{1+\mathbf{d}'_{N+1}\mathbf{d}_{N+1}}}\Big)}{\sqrt{1 + \mathbf{d}'_{N+1}\mathbf{d}_{N+1}}}\Big\{&\epsilon^2\mathbb{E}[c + \epsilon + \mathbf{d}'_{N+1}(\mathbf{a} + \mathbf{PW})] \\ &- 2\epsilon\mathbb{E}[(c + \epsilon + \mathbf{d}'_{N+1}(\mathbf{a} + \mathbf{PW}))((\mathbf{a} + \mathbf{PW})'\mathbf{F}(\mathbf{a} + \mathbf{PW}))] \\ &+ \mathbb{E}[(c + \epsilon + \mathbf{d}'_{N+1}(\mathbf{a} + \mathbf{PW}))((\mathbf{a} + \mathbf{PW})'\mathbf{F}(\mathbf{a} + \mathbf{PW}))^2]\Big\}.\end{aligned}$$

After tedious calculations of the above expectation, we get that $\mathbf{J}^2_{N+1} = \mathbf{J}^2(c_{N+1}, \mathbf{d}_{N+1})$ as in Proposition 3.2.3.

For $\mathbf{I}_0$, notice that

$$\begin{aligned}\mathbf{I}_0 &= \int_{\mathbb{R}^N} \phi(\mathbf{y}; \mathbf{0}, \mathbf{\Sigma_{11}})\Phi\Big(A(\mathbf{y} + \nu_0\mathbf{\Sigma_{10}}) + \nu_0\sqrt{\Sigma_{x|\mathbf{y}}}\Big)\mathrm{d}\mathbf{y} \\ &\approx \int_{\mathbb{R}^N} \phi(\mathbf{y}; \mathbf{0}, \mathbf{\Sigma_{11}})\Phi\Big((c + \epsilon + \nu_0\sqrt{\Sigma_{x|\mathbf{y}}}) + \mathbf{d}'(\mathbf{y} + \nu_0\mathbf{\Sigma_{10}}) + (\mathbf{y} + \nu_0\mathbf{\Sigma_{10}})'\mathbf{E}(\mathbf{y} + \nu_0\mathbf{\Sigma_{10}})\Big)\mathrm{d}\mathbf{y} \\ &= \int_{\mathbb{R}^N} \phi(\mathbf{y}; \mathbf{0}, \mathbf{\Sigma_{11}})\Phi(c_0 + \mathbf{d}'_0\mathbf{y} + \mathbf{y}'\mathbf{E}\mathbf{y})\mathrm{d}\mathbf{y}.\end{aligned}$$

Comparing the last equation with equation (A.0.55), we immediately get without any calculations that

$$\mathbf{I}_0 \approx \mathbf{J}^0(c_0, \mathbf{d_0}) + \mathbf{J}^1(c_0, \mathbf{d_0}) - \frac{1}{2}\mathbf{J}^2(c_0, \mathbf{d_0}).$$

Similarly, we get

$$\begin{aligned}
\mathbf{I}_k &= \int_{\mathbb{R}^N} \phi(\mathbf{y}; \mathbf{0}, \mathbf{\Sigma_{11}}) \Phi\Big(A(\mathbf{y} + \nu_k \mathbf{\Sigma_{11}} \mathbf{e_k})\Big) \mathrm{d}\mathbf{y} \\
&\approx \int_{\mathbb{R}^N} \phi(\mathbf{y}; \mathbf{0}, \mathbf{\Sigma_{11}}) \Phi\Big(c + \epsilon + \mathbf{d}'(\mathbf{y} + \nu_k \mathbf{\Sigma_{11}} \mathbf{e_k}) + (\mathbf{y} + \nu_k \mathbf{\Sigma_{11}} \mathbf{e_k})' \mathbf{E} (\mathbf{y} + \nu_k \mathbf{\Sigma_{11}} \mathbf{e_k})\Big) \mathrm{d}\mathbf{y} \\
&= \int_{\mathbb{R}^N} \phi(\mathbf{y}; \mathbf{0}, \mathbf{\Sigma_{11}}) \Phi(c_k + \mathbf{d_k'} \mathbf{y} + \mathbf{y}' \mathbf{E} \mathbf{y}) \mathrm{d}\mathbf{y} \\
&\approx \mathbf{J}^0(c_k, \mathbf{d_k}) + \mathbf{J}^1(c_k, \mathbf{d_k}) - \frac{1}{2} \mathbf{J}^2(c_k, \mathbf{d_k}).
\end{aligned}$$

Proof of Proposition 3.2.4:

By the definition of $\mathbf{P}$,

$$\mathbf{P}^2 = (\mathbf{I} + \mathbf{v}\mathbf{v}')^{-1} = \mathbf{I} - \psi \mathbf{v}\mathbf{v}',$$

where the last equality follows from the so-called updating formula (see, for example, Greene 2000). To see that $\mathbf{I} - \theta \mathbf{v}\mathbf{v}'$ is the unique square root of $\mathbf{P}^2$, notice that $\mathbf{I} - \theta \mathbf{v}\mathbf{v}'$ is symmetric, and $2\theta - \theta^2 \mathbf{v}'\mathbf{v} = \psi$, so

$$(\mathbf{I} - \theta \mathbf{v}\mathbf{v}')^2 = \mathbf{I} - (2\theta - \theta^2 \mathbf{v}'\mathbf{v}) \mathbf{v}\mathbf{v}' = \mathbf{I} - \psi \mathbf{v}\mathbf{v}'.$$

The other equations now follow from brute-force computations.

Proof of Proposition 3.2.5:

Notice that

$$\Pi = e^{-rT} \int_{\mathbb{R}^N} \phi(\mathbf{y}; \mathbf{0}, \mathbf{\Sigma_{11}}) \mathrm{d}\mathbf{y} \int_{\underline{x}(\mathbf{y})}^{\infty} \Big(e^{\nu_0 x + \mu_0} - \sum_{k=1}^{N} e^{\nu_k y_k + \mu_k} - K\Big) \phi(x; \mu_{x|\mathbf{y}}, \Sigma_{x|\mathbf{y}}) \mathrm{d}x.$$

Thus,

$$\begin{aligned}
\frac{\partial \Pi}{\partial s_0} &= e^{-rT} \frac{\partial \mu_0}{\partial s_0} \int_{\mathbb{R}^N} \phi(\mathbf{y}; \mathbf{0}, \mathbf{\Sigma_{11}}) \mathrm{d}\mathbf{y} \int_{\underline{x}(\mathbf{y})}^{\infty} e^{\nu_0 x + \mu_0} \phi(x; \mu_{x|\mathbf{y}}, \Sigma_{x|\mathbf{y}}) \mathrm{d}x \\
&\quad - e^{-rT} \int_{\mathbb{R}^N} \phi(\mathbf{y}; \mathbf{0}, \mathbf{\Sigma_{11}}) \Big(e^{\nu_0 \underline{x}(\mathbf{y}) + \mu_0} - \sum_{k=1}^{N} e^{\nu_k y_k + \mu_k} - K\Big) \frac{\partial \underline{x}(\mathbf{y})}{\partial s_0} \phi(\underline{x}(\mathbf{y}); \mu_{x|\mathbf{y}}, \Sigma_{x|\mathbf{y}}) \mathrm{d}\mathbf{y} \\
&= \frac{\partial \mu_0}{\partial s_0} \mathbf{S}_0 \mathbf{I}_0.
\end{aligned}$$

The other deltas and kappa can be proven similarly. The two special cases can be obtained by using equations (3.2.28) and (3.2.29).

Implementation of the second-order boundary approximation:

While it is very straightforward to implement the second-order boundary approximation, an efficient implementation which minimizes the computing time requires some effort. Below we comment on some of the details of the actual implementation along with some useful tricks:

1. $\mathbf{\Sigma_{11}^{-1}\Sigma_{10}}$. Matrix inversion is a costly operation and should be avoided. Instead, we use matrix division to find the solution $\mathbf{z}$ of $\mathbf{\Sigma_{10}} = \mathbf{\Sigma_{11}z}$. Because $\mathbf{\Sigma_{11}}$ is positive definite and symmetric, Cholesky factorization is useful in solving the linear system. Alternatively, one could use Gaussian elimination. The quantity $\mathbf{\Sigma_{11}^{-1}\Sigma_{10}}$ is referred to in the computation of $\Sigma_{x|\mathbf{y}}$, $\mathbf{d}$ and many other places.

2. $\mathbf{\Sigma_{11}^{\frac{1}{2}}}$. Notice that since $\mathbf{\Sigma_{11}}$ is positively definite and symmetric, an efficient algorithm to compute its square root is through the similarity transformation $\mathbf{\Sigma_{11}} = \mathbf{Q'\Lambda Q}$, where $\mathbf{Q}$ contains all the eigenvectors of $\mathbf{\Sigma_{11}}$ and $\mathbf{\Lambda}$ is a diagonal matrix containing all the corresponding eigenvalues. Then the square root of $\mathbf{\Sigma_{11}}$ is given by $\mathbf{\Sigma_{11}^{\frac{1}{2}}} = \mathbf{Q'\Lambda^{\frac{1}{2}}Q}$. Efficient algorithm for performing similarity transformation of a positive definite and symmetric matrix exists.

3. $tr(\mathbf{F}^2)$. Once the matrix $\mathbf{F}$ is computed from equation (3.2.19), we can avoid computing $\mathbf{F}^2$ by computing $tr(\mathbf{F}^2)$ as follows:

$$tr(\mathbf{F}^2) = \sum_{i=1}^{N}\sum_{j=1}^{N}[\mathbf{F}_{ij}]^2.$$

The right-hand-side can be computed very efficiently by first taking the element-by-element square of $\mathbf{F}$ and then taking the sum of all the elements. This is computationally more efficient than computing the matrix $\mathbf{F}^2$ because the former involves N^2

multiplications of two real numbers while the latter involves N^3 multiplications.

4. $\mathbf{v}'\mathbf{v}$, $\mathbf{v}'\mathbf{F}\mathbf{v}$ and $\mathbf{v}'\mathbf{F}^2\mathbf{v}$. Define a $(N+2)\times N$ matrix $\mathbf{D}$ as follows

$$\mathbf{D} = (\mathbf{d_0}, \mathbf{d_1}, \cdots, \mathbf{d}_N, \mathbf{d}_{N+1})'.$$

Notice that we need to compute $\mathbf{v}'\mathbf{v}$, $\mathbf{v}'\mathbf{F}\mathbf{v}$ and $\mathbf{v}'\mathbf{F}^2\mathbf{v}$ for $\mathbf{v} = \mathbf{d}_i$ for $i = 0, 1, \cdots, N+1$. It is extremely useful to treat the scalers $\mathbf{v}'\mathbf{v}$, $\mathbf{v}'\mathbf{F}\mathbf{v}$ and $\mathbf{v}'\mathbf{F}^2\mathbf{v}$ as vectors, where the index is for $\mathbf{v}$ ranging from $\mathbf{d_0}$ to $\mathbf{d}_{N+1}$. All the equations below should be interpreted this way.

We use the following identities to compute the vectors $\mathbf{v}'\mathbf{v}$, $\mathbf{v}'\mathbf{F}\mathbf{v}$ and $\mathbf{v}'\mathbf{F}^2\mathbf{v}$:

$$\mathbf{v}'\mathbf{v} = \text{rowsum}(\mathbf{D}^{\cdot 2}), \tag{A.0.63}$$

$$\mathbf{v}'\mathbf{F}\mathbf{v} = \text{diag}(\mathbf{D}\mathbf{F}\mathbf{D}'), \tag{A.0.64}$$

$$\mathbf{v}'\mathbf{F}^2\mathbf{v} = \text{rowsum}((\mathbf{D}\mathbf{F})^{\cdot 2}), \tag{A.0.65}$$

where rowsum is the operator of taking the row sum of a matrix and $\mathbf{A}^{\cdot 2}$ stands for the element-by-element square of a matrix $\mathbf{A}$. Written out component-wise, we have

$$(\mathbf{d}_i)'\mathbf{d}_i = \sum_{j=1}^{N} (\mathbf{D}_{ij})^2, \tag{A.0.66}$$

$$(\mathbf{d}_i)'\mathbf{F}\mathbf{d}_i = (\mathbf{D}\mathbf{F}\mathbf{D}')_{ii}, \tag{A.0.67}$$

$$(\mathbf{d}_i)'\mathbf{F}^2\mathbf{d}_i = \sum_{j=1}^{N} [(\mathbf{D}\mathbf{F})_{ij}]^2. \tag{A.0.68}$$

Equations (A.0.66), (A.0.67) and (A.0.68) can be seen easily by noticing that $\mathbf{F}$ is symmetric.

5. **Vectorization**. It is very important to use vectorization technique in the actual implementation to avoid for-loops in the program and further improve the efficiency. This is especially important when N is large. All the scaler quantities involving $\mathbf{v}$, such as $\psi(\mathbf{v})$, $\theta(\mathbf{v})$, $\mathbf{v}'\mathbf{v}$, $\mathbf{v}'\mathbf{F}\mathbf{v}$, $\mathbf{v}'\mathbf{F}^2\mathbf{v}$, $tr[(\mathbf{P}\mathbf{F}\mathbf{P})^2]$, $\mathbf{v}'\mathbf{P}^2\mathbf{F}\mathbf{P}^2\mathbf{v}$, and $\|\mathbf{P}\mathbf{F}\mathbf{P}^2\mathbf{v}\|^2$ should be treated

as $(N+2)\times 1$ vectors, where the index is on $\mathbf{v}$ ranging from $\mathbf{d_0}$ to $\mathbf{d_{N+1}}$. In particular, this means that we should use equations (A.0.63), (A.0.64) and (A.0.65) instead of (A.0.66), (A.0.67) and (A.0.68). Furthermore, $\lambda(u,\mathbf{v})$, $\mathbf{J}^0(u,\mathbf{v})$, $\mathbf{J}^1(u,\mathbf{v})$ and $\mathbf{J}^2(u,\mathbf{v})$ should be treated as $(N+2)\times 1$ vectors where u ranges from c_0 to c_{N+1} and $\mathbf{v}$ ranges from $\mathbf{d_0}$ to $\mathbf{d_{N+1}}$. Equation (3.2.7) then allows us to treat $\mathbf{I}$ as a $(N+2)\times 1$ vector. In turn, the spread option price in equation (3.2.6) is simply given by

$$\Pi = \mathbf{S}_0\mathbf{I}_0 - \sum_{k=1}^{N} \mathbf{S}_k\mathbf{I}_k - Ke^{-rT}\,\mathbf{I}_{N+1} = \mathbf{S}'\,\mathbf{I}.$$

Despite its seemingly complexity, the second-order boundary approximation is very straightforward to implement and our code in MATLAB is only about 30 lines. The second-order boundary approximation is also extremely fast and the computation of $\mathbf{\Sigma}_{\mathbf{11}}^{\frac{1}{2}}$ is actually where more than half of the computing time is spent. For example, when $N = 50$, the second-order boundary approximation needs less than 3×10^{-3} second to compute the price of one spread option and the computation of $\mathbf{\Sigma}_{\mathbf{11}}^{\frac{1}{2}}$ takes about 1.8×10^{-3} second.

APPENDIX B

GENERALIZED GAUSSIAN QUADRATURE METHOD FOR NATURAL GAS STORAGE VALUATION

B.0.1 Spot price models

Generalized Gaussian quadrature method could be applied to many models that have analytical conditional transition densities. Some examples are listed below.

Example 1: Mean-reverting processes

- Ornstein-Uhlenbeck process:

$$dS(t) = \kappa(\theta(t) - S(t))\,dt + \sigma dW(t),$$
$$p(y, t_{n+1}; x, t_n) = \phi\left(y; xe^{-\kappa\Delta t} + \kappa e^{-\kappa t_{n+1}} \int_{t_n}^{t_{n+1}} e^{\kappa u}\theta_u du, \frac{\sigma^2}{2\kappa}(1 - e^{-2\kappa\Delta t})\right).$$

  $\phi(y; \mu, \sigma^2)$ is normal probability density function with mean μ and variance σ^2.

- Geometric mean-reverting process (Schwartz 1997):

$$dS(t) = \kappa(\theta(t) - \log S(t))\,S(t)dt + \sigma S(t)dW(t)$$

  By taking $X(t) = \log S(t)$, $p(y, t_{n+1}; x, t_n)$ can be easily obtained by the above result.

Example 2: Constant elasticity of variance process (Cox 1975, Emanuel and MacBeth 1982)

$$dS(t) = \mu S(t)dt + \sigma S(t)^{\beta/2}dW(t), \quad \beta \geq 0$$
$$p(y, t_{n+1}; x, t_n) = |2 - \beta|k^{1/(2-\beta)}(zw^{1-2\beta})^{1/(4-2\beta)}e^{-z-w}I_{\frac{1}{|2-\beta|}}(2\sqrt{zw}).$$

with

$$k = \frac{2\mu}{\sigma^2(2-\beta)[e^{\mu(2-\beta)\Delta t} - 1]},$$

$$z = ky^{2-\beta}e^{\mu(2-\beta)\Delta t},$$

$$w = kx^{2-\beta},$$

$I_q(\cdot)$ the modified Bessel function of the first kind of order q.

Special cases of this class of model that are frequently used include:

- Lognormal diffusion model (Black and Scholes 1973):

$$dS(t) = \mu S(t)dt + \sigma S(t)dW(t)$$

- Absolute model (Cox and Ross 1976):

$$dS(t) = \mu S(t)dt + \sigma dW(t)$$

- Square-root model (Cox and Ross 1976):

$$dS(t) = \mu S(t)dt + \sigma \sqrt{S(t)}dW(t)$$

Example 3: Inverse of square-root model (Aït-Sahalia 1999)

$$dS(t) = \left(\kappa(\sigma^2 - \kappa\alpha)S(t)\right)S(t)dt + \sigma S(t)^{3/2}dW(t),$$
$$p(y, t_{n+1}; x, t_n) = \frac{1}{y^2}p^{SR}(\frac{1}{y}, t_{n+1}; \frac{1}{x}, t_n).$$

$p^{SR}(\cdot)$ is the conditional transition density of Square-root model.

Example 4: Levy process

- Geometric Brownian Motion with log-normal Jump (Merton 1976):

$$dX(t) = \mu dt + \sigma dW(t) + \log Y(t)dq(t), \quad X(t) = \log S(t)$$

with $\log Y(t) \sim i.i.d.N(\mu_0, \nu^2)$, $q(t)$ is a Poisson process with rate λ.

The conditional transition density function for $X(t)$ is:

$$p(y, t_{n+1}; x, t_n) = \sum_{n=0}^{\infty} \frac{e^{-\lambda\Delta t}(\lambda\Delta t)^n}{n!} \phi\left(y; x + \mu\Delta t + n\mu_0, \sigma^2\Delta t + n\nu^2\right).$$

- Ornstein-Uhlenbeck process with exponentially decaying jump (Jiang 1998):

$$dX(t) = -\kappa X(t)dt + \sigma dW(t) + \log Y(t)dq(t), \quad X(t) = \log(S(t)/S(0))$$

with $\log Y(t) \sim i.i.d.N(0, e^{-2\kappa t}\nu^2)$, $\kappa > 0$. For $X(t)$:

$$p(y, t_{n+1}; x, t_n) = \sum_{n=0}^{\infty} \frac{e^{-\lambda\frac{1-e^{-\kappa\Delta t}}{\kappa}}(\lambda\frac{1-e^{-\kappa\Delta t}}{\kappa})^n}{n!} \phi\left(y; xe^{-\kappa\Delta t}, \frac{\sigma^2}{2\kappa}(1 - e^{-2\kappa\Delta t}) + ne^{-2\kappa t_{n+1}}\nu^2\right).$$

- Variance Gamma (VG) process (Fusaia and Recchioni 2007):

$$S(t) = S(0)\exp\left\{rt + b(\gamma(t; 1, \nu); \theta, \sigma) + \frac{t}{\nu}\log(1 - \theta\nu - \frac{\sigma^2\nu}{2})\right\}$$

where $\gamma(t; 1, \nu)$ is a gamma process with mean rate 1 and variance rate ν, $b(t; \theta, \sigma)$ is a Brownian motion with drift θ and volatility σ. The conditional transition density function for log return $\log(S(t)/S(0))$ is:

$$p(y, t_{n+1}; x, t_n) = p(y, \Delta t) = \frac{2e^{\theta z/\sigma^2}}{\nu^{\Delta t/\nu}\sqrt{2\pi}\sigma\Gamma(\Delta t/\nu)}\left(\frac{z^2}{2\sigma^2/\nu + \theta^2}\right)^{\frac{\Delta t}{2\nu}-\frac{1}{4}} K_{\frac{\Delta t}{\nu}-\frac{1}{2}}\left(\frac{z\sqrt{2\sigma^2/\nu + \theta^2}}{\sigma^2}\right)$$

with $\Gamma(\cdot)$ the gamma function, $K_q(\cdot)$ the modified Bessel function of the second kind, and

$$z = y - r\Delta t - \frac{\Delta t}{\nu}\ln\left(1 - \theta\nu - \frac{\sigma^2\nu}{2}\right)$$

Example 5: Processes with analytical conditional characteristic functions

If the conditional characteristic function of a process is given analytically, the conditional transition density can be obtained by inverse fourier transform. For example, see Duffie, Pan and Singleton (2000) for affine diffusion (AD) process and affine jump diffusion (AJD) process.

APPENDIX C

CONTINUOUS-TIME OPTIMAL STOPPING FORMULATION FOR POWER PLANT VALUATION

C.1 Calculate $\mathbb{E}_x\left[e^{-\lambda\tau_n}\right]$ *and* $\mathbb{E}_x\left[e^{-\lambda\zeta_n}\right]$

Let $\gamma = \sigma/\sqrt{2\theta}$, $D_{-\nu}(x)$ be the parabolic cylinder function.

$$D_{-\nu}(x) = \frac{1}{\Gamma(\nu)}\exp(-\frac{x^2}{4})\int_0^\infty t^{\nu-1}\exp(-\frac{t^2}{2}-xt)dt$$

From Borodin, Salminen (2002) and Ditlevsen (2004), we know that for $\lambda > 0$, Laplace transform of the stopping times τ_z of O-U process equals:

$$\mathbb{E}_x\left[e^{-\lambda\tau_z}\right] = \begin{cases} \frac{D_{-\lambda/\kappa}(-\frac{x-\theta}{\gamma})}{D_{-\lambda/\kappa}(-\frac{z-\theta}{\gamma})}\, e^{\frac{(x-\theta)^2-(z-\theta)^2}{4\gamma^2}}, & \text{if } x < z \\ \frac{D_{-\lambda/\kappa}(\frac{x-\theta}{\gamma})}{D_{-\lambda/\kappa}(\frac{z-\theta}{\gamma})}\, e^{\frac{(x-\theta)^2-(z-\theta)^2}{4\gamma^2}}, & \text{if } x > z \end{cases} \tag{C.1.1}$$

So we have

C.1.1 When $U > x$

$$\mathbb{E}_x\left[e^{-\lambda\tau_1}\right] = \frac{D_{-\lambda/\kappa}(-\frac{x-\theta}{\gamma})}{D_{-\lambda/\kappa}(-\frac{U-\theta}{\gamma})}\, e^{\frac{(x-\theta)^2-(U-\theta)^2}{4\gamma^2}}$$

$$\mathbb{E}_x\left[e^{-\lambda\zeta_1}\right] = \mathbb{E}_x\left[e^{-\lambda(\zeta_1-\tau_1)}\right]\mathbb{E}_x\left[e^{-\lambda\tau_1}\right] = \frac{D_{-\lambda/\kappa}(-\frac{x-\theta}{\gamma})\, D_{-\lambda/\kappa}(\frac{U-\theta}{\gamma})}{D_{-\lambda/\kappa}(-\frac{U-\theta}{\gamma})\, D_{-\lambda/\kappa}(\frac{L-\theta}{\gamma})}\, e^{\frac{(x-\theta)^2-(L-\theta)^2}{4\gamma^2}}$$

similarly, for $n = 2, 3, \ldots$

$$\mathbb{E}_x\left[e^{-\lambda\tau_n}\right] = \frac{D_{-\lambda/\kappa}(-\frac{x-\theta}{\gamma})\, D_{-\lambda/\kappa}(-\frac{L-\theta}{\gamma})^{n-1}\, D_{-\lambda/\kappa}(\frac{U-\theta}{\gamma})^{n-1}}{D_{-\lambda/\kappa}(-\frac{U-\theta}{\gamma})^n\, D_{-\lambda/\kappa}(\frac{L-\theta}{\gamma})^{n-1}}\, e^{\frac{(x-\theta)^2-(U-\theta)^2}{4\gamma^2}} \tag{C.1.2}$$

$$\mathbb{E}_x\left[e^{-\lambda\zeta_n}\right] = \frac{D_{-\lambda/\kappa}(-\frac{x-\theta}{\gamma})\, D_{-\lambda/\kappa}(-\frac{L-\theta}{\gamma})^{n-1}\, D_{-\lambda/\kappa}(\frac{U-\theta}{\gamma})^{n}}{D_{-\lambda/\kappa}(-\frac{U-\theta}{\gamma})^n\, D_{-\lambda/\kappa}(\frac{L-\theta}{\gamma})^{n}}\, e^{\frac{(x-\theta)^2-(L-\theta)^2}{4\gamma^2}} \tag{C.1.3}$$

C.1.2 When $U \leq x$

$$\tau_1 = 0,\ \mathbb{E}_x\left[e^{-\lambda\tau_1}\right] = 1$$

$$\mathbb{E}_x\left[e^{-\lambda\zeta_1}\right] = \frac{D_{-\lambda/\kappa}(\frac{x-\theta}{\gamma})}{D_{-\lambda/\kappa}(\frac{L-\theta}{\gamma})}\, e^{\frac{(x-\theta)^2-(L-\theta)^2}{4\gamma^2}}$$

for $n = 2, 3, \ldots$

$$\mathbb{E}_x\left[e^{-\lambda\tau_n}\right] = \frac{D_{-\lambda/\kappa}(\frac{x-\theta}{\gamma}) D_{-\lambda/\kappa}(-\frac{L-\theta}{\gamma})^{n-1}\, D_{-\lambda/\kappa}(\frac{U-\theta}{\gamma})^{n-2}}{D_{-\lambda/\kappa}(-\frac{U-\theta}{\gamma})^{n-1}\, D_{-\lambda/\kappa}(\frac{L-\theta}{\gamma})^{n-1}}\, e^{\frac{(x-\theta)^2-(U-\theta)^2}{4\gamma^2}} \tag{C.1.4}$$

$$\mathbb{E}_x\left[e^{-\lambda\zeta_n}\right] = \frac{D_{-\lambda/\kappa}(\frac{x-\theta}{\gamma})\, D_{-\lambda/\kappa}(-\frac{L-\theta}{\gamma})^{n-1}\, D_{-\lambda/\kappa}(\frac{U-\theta}{\gamma})^{n-1}}{D_{-\lambda/\kappa}(-\frac{U-\theta}{\gamma})^{n-1}\, D_{-\lambda/\kappa}(\frac{L-\theta}{\gamma})^{n}}\, e^{\frac{(x-\theta)^2-(L-\theta)^2}{4\gamma^2}} \tag{C.1.5}$$

C.2 Justifications for Section 5.3

Justify the separation of integral interval (5.3.1)

By simple algebra, we can prove that

$$\mathbb{E}_x\left[\int_0^\infty e^{-rt} X_t\, dt\right] < \infty \tag{C.2.1}$$

For $\forall\ n, m$ we have

$$\mathbb{E}_x\left[\int_0^{\zeta_n\wedge m} e^{-rt} X_t\, dt\right] \leq \mathbb{E}_x\left[\int_0^\infty e^{-rt} X_t\, dt\right] < \infty$$

$$\mathbb{E}_x\left[\int_0^{\tau_n\wedge m} e^{-rt} X_t\, dt\right] \leq \mathbb{E}_x\left[\int_0^\infty e^{-rt} X_t\, dt\right] < \infty$$

Thus equation (5.3.1) is justified.

Justify the exchanges of expectation and limit (5.3.2)

We know for $\forall\ n, m$,

$$\left|\int_{\tau_n\wedge m}^{\zeta_n\wedge m} e^{-rt} X_t\, dt\right| \leq \int_0^\infty e^{-rt} X_t\, dt < \infty$$

and equation (C.2.1) holds. By Dominated Convergence Theorem, equation (5.3.2) is justified.

Justify the exchanges of expectation and infinite sum (5.3.3)

We have the following lemma from Ash (1972):

Lemma C.2.1. *Let $f_1, f_2, \ldots$ be Borel measurable functions on $(\Omega, \mathcal{F}, \mu)$. If*

$$\int_\Omega \left(\sum_{n=1}^{\infty} |f_n| \right) d\mu < \infty$$

then $\sum_{n=1}^{\infty} f_n$ converges a.e. to a finite valued function, and

$$\int_\Omega \left(\sum_{n=1}^{\infty} f_n \right) d\mu = \sum_{n=1}^{\infty} \int_\Omega f_n d\mu.$$

Because

$$\mathbb{E}_x \left[\sum_{n=1}^{\infty} \int_{\tau_n}^{\zeta_n} e^{-rt} X_t \, dt \right] \leq \mathbb{E}_x \left[\int_0^{\infty} e^{-rt} X_t \, dt \right] < \infty$$

$$\mathbb{E}_x \left[\sum_{n=1}^{\infty} e^{-r\tau_n} \right] < \infty$$

$$\mathbb{E}_x \left[\sum_{n=1}^{\infty} e^{-r\zeta_n} \right] < \infty$$

Thus equation (5.3.3) is justified.

C.3 Sensitivity of power plant value with respect to θ

When $U > x$, given the definitions in Proposition 5.3.1, we have

$$\begin{aligned}
\frac{\partial V(x,L,U)}{\partial \theta} = & -\frac{q}{r+\kappa}\delta_{r+\kappa}\left\{\mathbb{E}_x[e^{-(r+\kappa)\tau_1}] - \mathbb{E}_x[e^{-(r+\kappa)\zeta_1}]\right\} + \frac{q(x-\theta)}{r+\kappa}\left\{\mathbb{E}_x[e^{-(r+\kappa)\tau_1}] - \mathbb{E}_x[e^{-(r+\kappa)\zeta_1}]\right\} F_{r+\kappa} \\
& + \frac{q(x-\theta)}{r+\kappa}\delta_{r+\kappa}\left\{\frac{D_{-(r+\kappa)/\kappa}(-\frac{x-\theta}{\gamma})}{D_{-(r+\kappa)/\kappa}(-\frac{U-\theta}{\gamma})} e^{\frac{(x-\theta)^2-(U-\theta)^2}{4\gamma^2}} \left(\frac{2(U-x)\theta}{\sigma^2} + \frac{x^2-U^2}{2\sigma^2}\right) + e^{\frac{(x-\theta)^2-(U-\theta)^2}{4\gamma^2}} G_{r+\kappa} \right. \\
& \left. - \frac{D_{-(r+\kappa)/\kappa}(-\frac{x-\theta}{\gamma}) D_{-(r+\kappa)/\kappa}(\frac{U-\theta}{\gamma})}{D_{-(r+\kappa)/\kappa}(-\frac{U-\theta}{\gamma}) D_{-(r+\kappa)/\kappa}(\frac{L-\theta}{\gamma})} e^{\frac{(x-\theta)^2-(L-\theta)^2}{4\gamma^2}} \left(\frac{2(L-x)\theta}{\sigma^2} + \frac{x^2-L^2}{2\sigma^2}\right) - e^{\frac{(x-\theta)^2-(L-\theta)^2}{4\gamma^2}} H_{r+\kappa} \right\} + \frac{\delta_r q}{r}\mathbb{E}_x[e^{-r\tau_1}] \\
& - \frac{\delta_r q}{r}\mathbb{E}_x[e^{-r\zeta_1}] - \delta_r(C^u - \frac{q\theta}{r}) \left\{ \frac{D_{-r/\kappa}(-\frac{x-\theta}{\gamma})}{D_{-r/\kappa}(-\frac{U-\theta}{\gamma})} e^{\frac{(x-\theta)^2-(U-\theta)^2}{4\gamma^2}} \left(\frac{2(U-x)\theta}{\sigma^2} + \frac{x^2-U^2}{2\sigma^2}\right) + e^{\frac{(x-\theta)^2-(U-\theta)^2}{4\gamma^2}} G_r \right\} \\
& - \delta_r(C^d + \frac{q\theta}{r}) \left\{ -\frac{D_{-r/\kappa}(-\frac{x-\theta}{\gamma}) D_{-r/\kappa}(\frac{U-\theta}{\gamma})}{D_{r/\kappa}(-\frac{U-\theta}{\gamma}) D_{-r/\kappa}(\frac{L-\theta}{\gamma})} e^{\frac{(x-\theta)^2-(L-\theta)^2}{4\gamma^2}} \left(\frac{2(L-x)\theta}{\sigma^2} + \frac{x^2-L^2}{2\sigma^2}\right) - e^{\frac{(x-\theta)^2-(L-\theta)^2}{4\gamma^2}} H_r \right\}
\end{aligned} \tag{C.3.1}$$

With $\lambda = r + \kappa$ or r:

$$F_\lambda = \frac{D_{-\lambda/\kappa}(-\frac{U-\theta}{\gamma})\, D_{-\lambda/\kappa}(\frac{L-\theta}{\gamma}) \left\{ D'_{-\lambda/\kappa}(-\frac{U-\theta}{\gamma})\, D'_{-\lambda/\kappa}(\frac{L-\theta}{\gamma}) - D'_{-\lambda/\kappa}(-\frac{L-\theta}{\gamma})\, D'_{-\lambda/\kappa}(\frac{U-\theta}{\gamma}) \right\}}{\gamma^2 \left(D_{-\lambda/\kappa}(-\frac{U-\theta}{\gamma})\, D_{-\lambda/\kappa}(\frac{L-\theta}{\gamma}) - D_{-\lambda/\kappa}(-\frac{L-\theta}{\gamma})\, D_{-\lambda/\kappa}(\frac{U-\theta}{\gamma}) \right)^2}$$

$$- \frac{D'_{-\lambda/\kappa}(-\frac{U-\theta}{\gamma})\, D'_{-\lambda/\kappa}(\frac{L-\theta}{\gamma}) \left\{ D_{-\lambda/\kappa}(-\frac{U-\theta}{\gamma})\, D_{-\lambda/\kappa}(\frac{L-\theta}{\gamma}) - D_{-\lambda/\kappa}(-\frac{L-\theta}{\gamma})\, D_{-\lambda/\kappa}(\frac{U-\theta}{\gamma}) \right\}}{\gamma^2 \left(D_{-\lambda/\kappa}(-\frac{U-\theta}{\gamma})\, D_{-\lambda/\kappa}(\frac{L-\theta}{\gamma}) - D_{-\lambda/\kappa}(-\frac{L-\theta}{\gamma})\, D_{-\lambda/\kappa}(\frac{U-\theta}{\gamma}) \right)^2}$$

$$G_\lambda = \frac{D'_{-\lambda/\kappa}(-\frac{x-\theta}{\gamma}) D_{-\lambda/\kappa}(-\frac{U-\theta}{\gamma}) + D_{-\lambda/\kappa}(-\frac{x-\theta}{\gamma}) D'_{-\lambda/\kappa}(-\frac{U-\theta}{\gamma})}{\gamma D_{-\lambda/\kappa}(-\frac{U-\theta}{\gamma})^2}$$

$$H_\lambda = \frac{D_{-\lambda/\kappa}(-\frac{x-\theta}{\gamma}) D_{\lambda/\kappa}(\frac{U-\theta}{\gamma}) D'_{-\lambda/\kappa}(-\frac{U-\theta}{\gamma}) D'_{\lambda/\kappa}(\frac{L-\theta}{\gamma}) - D'_{-\lambda/\kappa}(-\frac{x-\theta}{\gamma}) D'_{\lambda/\kappa}(\frac{U-\theta}{\gamma}) D_{-\lambda/\kappa}(-\frac{U-\theta}{\gamma}) D_{\lambda/\kappa}(\frac{L-\theta}{\gamma})}{\gamma^2 \left(D_{-\lambda/\kappa}(-\frac{U-\theta}{\gamma}) D_{-\lambda/\kappa}(\frac{L-\theta}{\gamma}) \right)^2}$$

Result for $U \leq x$ can be derived in a similar way.

REFERENCES

Ahn, H., A. Danilova and G. Swindle "Storing arb." *Wilmott 1*, (2002).

Aït-Sahalia, Y. "Transition Densities for Interest Rate and other Nonlinear Diffusions." *The Journal of Finance*, LIV(4)(1999), 1361-1394.

Albizzati, M-O., and H. Geman. "Interest rate risk management and valuation of the surrender option in life insurance policies." *Journal of Risk and Insurance*, 61, No. 4 (1994), 616-637.

Andricopoulos, A. D., M. Widdicks, P. W. Duck and D. P. Newton. "Universal option valuation using quadrature methods." *Journal of Financial Economics*, 67(2003), 447-471.

Arak, M., P. Fisher, L. Goodman, and R. Daryanani. "The municipal-treasury futures spread." *Journal of Futures Markets*, 7 (1987), 355-371.

Ash, R. B. "Measure, Integration and Functional Analysis." Academic Press Inc.,U.S.(1972), 52.

Barrera-Esteve C. et al. "Numerical methods for the pricing of swing options: A stochastic control approach." *Methodology And Computing In Applied Probability*, 8(2006), 517-540.

Bjerksund, M. J. "The price of convenience and the valuation of commodity contingent claims." in D. Lund and B. Øksendal, Eds: *Stochastic Models and Option Values*, North Holland (1991).

Black, F., and M. Scholes. "The pricing of options and corporate liabilities." *Journal of Political Economy*, 81 (1973), 637-659.

Blanco, C. and P. Stefiszyn. "Valuation Natural Gas Storage Using Seasonal Principal Component Analysis." *Commodities Now*, (2002).

Boogert, A. and C. de Jong. "Gas storage valuation using a monte carlo method." *The Journal of Derivatives*, 15(2008), 81-98.

Borodin, A. N. and P. Salminen. "Handbook of Brownian Motion-Facts and Formulae." Birkhäuser Verlag, Basel-Boston-Berlin(2002), 622.

Bringedal, B. "Valuation of Gas Storage: A Real Options Approach." Master's Thesis, The Norwegian University of Science and Technology, (2003).

Broadie, M., and J. Detemple. "American option valuation: New bounds, approximations, and a comparison of existing methods." *Review of Financial Studies*, 9, No. 4 (1996), 1211-12250.

Carmona, R., and V. Durrleman. "Pricing and hedging spread options." *SIAM Review*, 45, No. 4 (2003a), 627-685.

Carmona. "Pricing and hedging spread options in a lognormal model." Working paper, 2003b.

Carmona, R.,M. Ludkovski. "Gas storage and supply guarantees: an optimal switching approach." Submitted to Management Science, (2005).

Carmona, R. and V. Durrleman. "Generalizing the Black-Scholes formula to multivariate contingent claims." *Journal of Computational Finance*, 9, No. 2 (2006), 43-67.

Carmona, R., M. Ludkovski. "Valuation of energy storage: an optimal switching approach." *Quantitative Finance*, 08 October (2009).

Carr, P. "Randomization and the American Put." *The Review of Financial Studies*, 11, No. 3 (1998), 597-626.

Chen, R-R., and S-K. Yeh. “Analytical upper bounds for American option prices.” *Journal of Financial and Quantitative Analysis*, 37, No. 1 (2002), 117-136.

Chen, X. and D. S. Levi. “Coordinating Inventory Control and Pricing Strategies with Random Demand and Fixed Ordering Cost: The Finite Horizon Case.” *Operations research*, 52, No. 6 (2004), 887-896.

Chen, Z. L., P. A. Forsyth. “A Semi-Lagrangian Approach for Natural Gas Storage Valuation and Optimal Operation.” *SIAM J. Scientific Computing*, 30(2007), 339-368.

Chung, S-L., and H-C. Chang. “Generalized analytical upper bounds for American option prices.” *Journal of Financial and Quantitative Analysis*, 42, No. 1 (March 2007), 209-228.

Chung S. L., K. Ko and M. B. Sharkleton. “Toward option values of near machine precision using Gaussian Quadrature.” National Taiwan University, Taiwan, (2005).

Cox, J. C. “Notes on option pricing I: Constant elasticity of variance diffusions.” Working paper, Stanford University, 1975. (Reprinted in *Journal of Portfolio Management*, 22(1996), 15-17.

Cox, J. C., and S. A. Ross. “The valuation of options for alternative stochastic processes.”*J. Financial Econom*, 3(1976), 145-166.

de Jong, C. and K. Walet. “To store or not to store.” ” *Energy Power Risk Management*, October 2003.

Dempster, M., and S. Hong. “Pricing spread options with the Fast Foruier Transform.” First World Congress of the Bachelier Finance Society, Paris, 2000.

Dempster, M., E Medova and K Tang “Long term spread option valuation and hedging.” *Journal of Banking and Finance*, 32 (2008), 2530-2540.

Deng, S. J. “Valuation of investment and opportunity-to- invest in power generation assets with spikes in electricity price.” *Managerial Finance*, 31, No. 6 (2005), 95-115.

Deng, S. J. “Financial methods in competitive electricity markets.” Ph.D. thesis, University of California, Berkeley, CA, (1999).

Deng, S.J., B. Johnson, and A. Sogomonian. “Exotic electricity options and the valuation of electricity generation and transmission assets.” *Decision Support Systems*, 30, No. 3 (2001), 383-392.

Deng, S.J., M. Li, and J. Zhou. “Multi-asset spread option pricing and hedging.” Working paper, 2008.

Deng, S. J. and S. S. Oren. “Incorporating Operational Characteristics and Startup Costs in Option-Based Valuation of Power Generation Capacity.” *Probability in the Engineering and Informational Sciences*, 17 (2003), 155-181.

Dias, M. A. G. “Valuation of Exploration and Production Assets: an Overview of Real Options Models.” *Journal of Petroleum Science and Engineering*, 44 (2004), 93-114.

Dilevsen, S. “A result on the first-passage time of an Ornstein-Uhlenbeck process.” (2004).

Dixit, A. and R. Pindyck. “Investment under Uncertainty.” Princeton University Press, (1994).

Duffie, D., J. Pan and K. Singleton. “Transform analysis and asset pricing for affine jump-diffusions.” *Econometrica*, 68(6)(2000), 1343-1376.

Easterwood, J.C., and A.J. Senchack Jr. “Arbitrage opportunities with T-Bills/T-Bonds combinations.” *Journal of Futures Markets.* 6 (1986), 433-442.

Emanuel, D. C. and J. D. MacBeth. “Further results on the constant elasticity of variance call option pricing model.” *J. Financial and Quant. Anal*, 17(1982), 533-554.

Eydeland, A., and K. Wolyniec. *Energy and Power Risk Management: New Developments in Modeling, Pricing and hedging*. John Wiley & Sons, New York, 2003.

Fusaia, G., M. C. Recchioni. "Analysis of quadrature methods for pricing discrete barrier options." *Journal of Economic Dynamics and Control*, 31(2007), 826-860.

Geman, H., N. E. Karoui, and J. C. Rochet. "Changes of numeraire, changes of probability measure and option pricing." *Journal of Applied Probability*, 32 (1995), 443-458.

Ghiuvea, C. S., J. P. Lehoczky, and D. Seppi. "Pricing swing and other generalized American options." Working Paper, Carnegie Mellon University, (2003).

Gibson, R. and E. S. Schwartz. "Stochastic convenience yield and the pricing of oil contingent claims." *Journal of Finance*, 45(1990), 959-976.

Girma, P.B., and A.S. Paulson, "Seasonality in petroleum futures spreads." *Journal of Futures Markets*, 18 (1998), 581-598.

Girma, P.B. "Risk arbitrage opportunities in petroleum futures spreads." *Journal of Futures Markets*, 18 (1999), 931-955.

Gray, J. and P. Khandelwal. "Towards a Realistic Gas Storage Model." *Commodities Now*, June(2007), 1-4.

Greene, W. H. *Econometric Analysis*, Prentice Hall, New Jersey (2000).

Grinblatt, M., and S. Titman. "Adverse risk incentives and the design of performance-based contracts." *Management Science*, 35, No. 7 (July 1989), 807-822.

Hamadène, S., and M. Jeanblanc. "On the starting and stopping problem: Application in reversible investments." *Mathematics of Operations Research*, 32, No. 1, (2007), 182-192.

Henderson, V., D. Hobson, W.T. Shaw, and R. Wojakowski. "Bounds for in-progress floatingstrike Asian options using symmetry." *Annals of Operations Research*, 151, No. 1 (April 2007), 81-98.

Insley, M. C. "On the option to invest in pollution control under a regime of tradable emissions allowances." *Canadian Journal of Economics*, 36, No. 4, (2003), 860-883.

Insley, M.C. and T.S. Wirjanto. "Contrasting Two Approaches in Real Options Valuation: Contingent Claims versus Dynamic Programming", Working paper, University of Waterloo, (2006).

Jaillet, P., E. Ronn, and S. Tompaidis. "Valuation of commodity-based swing options." *Management Science*,50(2004), 909-921.

Jamshidian, F. and M. Fein. "Closed-form solutions for oil futures and European options in the Gibson-Schwartz model: A comment." unpublished paper, Financial Strategies Group, Merrill Lynch Capital Markets, New York (1990).

Jarrow, R., and A. Rudd. "Approximate option valuation for arbitrary stochastic processes." *Journal of Financial Economics*, 10 (1982), 347-369.

Jiang, G. J. "Jump-Diffusion Model of Exchange Rate Dynamics: Estimation via Indirect Inference" working paper, University of Groningen, The Netherlands, (1998).

Johnson, S.A., and Y.S. Tian. "Indexed executive stock options." *Journal of Financial Economics*, 57 (2000), 35-64.

Johnson, R.L., C.R. Zulauf, S.H. Irwin and M.E. Gerlow. "The soy-bean complex spread: An examination of Market Efficiency from the viewpoint of a production process." *Journal of Futures Markets*, 11 (1991), 25-37.

Jones, F.J. “Spreads: Tails, turtles and all that.” *Journal of Futures Markets*, 11 (1991), 565-596.

Karatzas, I., S. E. Shreve, J. H. Ewing. “Brownian Motion and Stochastic Calculus.” Springer Science and Business Media, Inc. (1991), 196.

Kirk, E. “Correlations in the energy markets, in managing energy price risk.” Risk Publications and Enron, 1995.

Kluge, T. “Pricing options in electricity markets.” Preprint (2004).

Li, M. “The impact of return nonnormality on exchange options.” *Journal of Futures Markets*, 28(9)(2008), 845-870.

Li, M., S. J. Deng, and J. Zhou. “Closed-form approximations for spread option prices and Greeks.” *Journal of Derivatives*, 15 (2008), 58-80.

Li, M., S. J. Deng, and J. Zhou. “Multi-asset spread option pricing and hedging.” *Quantitative Finance*, 10(3) (2010), 305-324.

Ludkovski, M, R. Carmona. “Valuation of energy storage: an optimal switching approach.” *Quantitative Finance*, 08 October (2009).

Lo, A. “Semiparametric upper bounds for option prices and expected payoffs.” *Journal of Financial Economics* 19 (1987), 373-388.

Manoliu, M. “Storage options valuation using multilevel trees and calendar spreads.” *International Journal of Theoretical and Applied Finance*, 7(2004), 425-464.

Maragos, S. “Valuation of the Operational Flexibility of Natural Gas Storage Reservoirs.” E. Ronn, ed. Real Options and Energy Management. Risk Books, London, UK, 431-456.

Margrabe, W. “The value of an option to exchange one asset for another.” *Journal of Finance*, 33 (1978), 177-186.

Mbafeno, A. “Co-movement term structure and the valuation of energy spread options.” In M. Dempster and S. Pliska, eds., *Mathematics of Derivative Securities*. Cambridge University Press, Cambridge, UK, 1997.

McDonald, R. L., and D. R. Siegel. “Investment and the valuation of firms when there is an option to shut down.” *International Economic Review*, 26, No. 2 (June 1985), 331-349.

Merton, R. C. “Option pricing when underlying stock returns are discontinuous.” *J. of Financial Economics*, 3(1976), 125-144.

Mitrinovic, D.S., J. Pecaric, and A.M. Fink. *Classical and New Inequalities in Analysis*. Springer, New York, 1992.

Nielsen, J.A., and K. Sandmann. “Pricing bounds on Asian options.” *Journal of Financial and Quantitive Analysis*, 38, No. 2. (2003), 449-473.

Nilsson, O. and D. Sjelvgren. “Hydro unit start-up costs and their impact on the short term scheduling strategies of Swedish power producers.” *IEEE Transactions on Power Systems*, 12, No. 1 (1997), 38-44.

Novikov, A. “Martingales and first-passage times for Ornstein-Uhlenbeck processes with a jump component.” *Theory Probab. Appl*, 8, No. 2 (2004), 288-303.

Obersteiner, M et al. “Biomass Energy, Carbon Removal and Permanent Sequestration? A Real Option for Managing Climate Risk.” Interim report, International Institute for Applied Systems Analysis, Austria, (2002).

Øksendal, B. and A. Sulem. “Applied stochastic control of jump diffusions.” Springer-Verlag, Berlin, (2005).

Parsons, C. “Valuaing commodity storage contracts: A two-factor tree approach.” Preprint WTM Energy Software LLC, (2005).

Pearson, N. “An efficient approach for pricing spread options.” *Journal of Derivatives*, (Fall 1995), 76-91.

Perrakis, S., and P.J. Ryan. “Option pricing bounds in discrete time.” *Journal of Finance*, 39 (1984), 519-525.

Poitras, G. “Spread options, exchange options, and arithmetic Brownian motion.” *Journal of Futures Markets*, 18 (1998), 487-517.

Porchet, A.,N. Touzi, and X. Warin. “Valuation of power plants by utility indifference and numerical computation.” *Mathematical Methods of Operations Research*, 70(2009), 1432-2994.

Press, W. H., B. P. Flannery, S. A. Teukolsky, and W. T. Vetterling. *Numerical recipes in C: The art of scientific computing*, Cambridge University Press: Cambridge (1992).

Ronn, E. I. and M. Kjaer. “Valuation of a Natural Gas Storage Facility.” *Journal of Energy Markets*, forthcoming, 2008.

Routledge, S., D. J. Seppi, and C. S. Spatt. “The “Spark Spread”: An Equilibrium Model of Cross-Commodity Price Relationship in Electricity.” Working Paper. Carnegie Mellon University, (2001).

Schwartz, E. S., and L. Trigeorgis. “Real Options and Investment under Uncertainty: Classical Readings and Recent Contributions.” The MIT Press, 2004.

Shevlin, T. “The valuation of R&D firms with R&D limited parterships.” *The Accounting Review*, 66, No. 1 (Jan. 1991), 1-21.

Shimko, D. “Options on future spreads: Hedging, Speculating, and Valuation.” *Journal of Futures Markets*, 14, No. 2 (1997), 183-213.

Sullivan, M. A. “Valuing American put options using Gaussian quadrature.” *Review of Financial Studies*, 13(2000), 75-94.

Thompson, M., M. Davison and H. Rasmussen. “Natural gas storage valuation and optimization: A real options approach.” Tech. rep., University of Western Ontario (2003).

Tseng, C. and G. Barz. “Short-term generation asset valuation.” *Proceedings of the 32nd Hawaii International Conference on System Sciences*, (1999).

Tseng, C. and G. Barz. “Short-term generation asset valuation: a real options approach.” *Operations Research*, 50, No. 2 (2002), 297-310.

Weston, T. “Applying Stochastic Dynamic Programming to the Valuation of Gas Storage and Generation Assets.” E. Ronn, ed. Real Options and Energy Management. Risk Books, London, UK, 183-216.

Wilcox, D. “Energy futures and options: Spread options in energy markets.” Goldman Sachs & Co., New York, 1990.

Wood, A. J. and B. F. Wollenberg. “Power generation operation and control.” John Wiley & Sons, Inc. (1996), 137.

Zhang, P. G. *Exotic options: a guide to second generation options*. World Scientific, Singapore; New Jersey (1997), 489-499.